2017

Pre-Mt. Simon Seismic Sequences Below West-Central Indiana: Local Interpretation and Regional Significance

Andrew Michael Parent
Wright State University

PRE-MT. SIMON SEISMIC SEQUENCES BELOW WEST-CENTRAL INDIANA: LOCAL INTERPRETATION AND REGIONAL SIGNIFICANCE

A thesis submitted in partial fulfillment of the requirements for the degree of
Master of Science

By

ANDREW MICHAEL PARENT
B.S. Salem State University, 2015

2017
Wright State University

WRIGHT STATE UNIVERSITY
GRADUATE SCHOOL

April 14, 2017

I HEREBY RECOMMEND THAT THE THESIS PREPARED UNDER MY SUPERVISION BY Andrew Michael Parent ENTITLED Pre-Mt. Simon Seismic Sequences Below West-Central Indiana: Local Interpretation and Regional Significance BE ACCEPTED IN PARTIAL FULFILLMENT OF THE REQUIREMENTS FOR THE DEGREE OF Master of Science.

____
Ernest Hauser, Ph.D.
Thesis Director

____
David F. Dominic, Ph.D.
Chair, Department of Earth & Environmental Sciences

Committee on
Final Examination

____
Ernest C. Hauser, Ph.D.

____
Doyle R. Watts, Ph.D.

____
David F. Dominic, Ph.D.

____
Robert E. W. Fyffe, Ph.D.
Vice President for Research and
Dean of the Graduate School

ABSTRACT

Parent, Andrew Michael, M.S., Department of Earth and Environmental Sciences, Wright State University, 2017. Pre-Mt. Simon Seismic Sequences Below West-Central Indiana: Local Interpretation and Regional Significance

Constraining the composition, structure, and origin of basement provinces, deep assemblages of Precambrian rocks, is largely dependent on deep boreholes and geophysical techniques. This is especially true for the eastern U.S. midcontinent. Here, I employ regional 2-D seismic reflection, Bouguer gravity, and aeromagnetic data to interpret the upper crust below west-central Indiana. Seismic reflection data were donated to Wright State University in 2015. Geopotential data are available through the USGS and affiliates. These geophysical data, together, are analyzed in a regional geologic context.

Three distinct seismic stratigraphic sequences are observed on 2-D sections. The first, uppermost sequence, typified by continuous, high-amplitude, stratified reflections is constrained by boreholes and previous seismic investigations as the Paleozoic sedimentary sequence that masks the midcontinent basement. The Cambrian Mt. Simon Sandstone constitutes the base of this unit, which is underlain by the second, poorly reflective, westward-thinning sequence. Weak internal reflections create an apparent angular unconformity with the base of the Mt. Simon and appear concordant with reflections of the basal seismic package. This unit, termed the Wilbur sequence, compares well with the seismic character of the Middle Run Formation of western Ohio and Kentucky. A third, well-reflective sequence is observed at the base of the record. Stratal geometries, such as onlap and stratigraphic terminations, are locally observable on regional east-west profiles. A positive Bouguer anomaly appears associated with the apparent structural closure of this sequence, herein termed the Quincy, below northeast Owen County. Geophysical signatures of the Quincy suggest a depositional origin, composed of low-magnetic igneous rocks (rhyolites) sourced from midcontinent volcanic centers and clastic sediments from collapsed calderas.

These data facilitate two alternative hypotheses. The pattern seen in west-central Indiana (Wilbur over Quincy) may correlate with that seen below southwest Ohio (Middle Run over reflective basement). This would suggest that the Middle Run was deposited over a larger regional area than early syn-rift models suggested, fortifying recent interpretations that the Middle Run represents the foreland basin sedimentary package generated by the Grenville Orogeny. It is possible, conversely, that both Wilbur and Quincy sequences are sedimentary and/or volcanic units associated with the Eastern Granite-Rhyolite Province and pre-date the Middle Run entirely. Both models suggest contrasting yet significant tectonic settings of the pre-Mt. Simon U.S. midcontinent.

TABLE OF CONTENTS

LIST OF FIGURES

LIST OF TABLES

LIST OF ACRONYMS

CDP – common depth point

CGFS – Cottage Grove Fault System

COCORP – Consortium of Continental Reflection Profiling

ECRB – East Continent Rift Basin

FAFS – Fluorspar Area Fault System

F-K – frequency-wavenumber

GFTZ – Grenville Front Tectonic Zone

GLIMPSE – Great Lakes International Multi-disciplinary Program on Crustal Evolution

HRAM – high resolution aeromagnetic

IGS – Indiana Geological Survey

MCFZ – Mt. Carmel Fault Zone

MCR – Midcontinent Rift

mGal – milligal

NAD83 – North American Datum 1983

NMO – normal moveout

nT – nanotesla

PACES – Pan-American Center for Earth and Environmental Studies

RCG – Rough Creek Graben

RMS – root-mean-squared (velocity)

RR – Reelfoot Rift

SGRP – Southern Granite-Rhyolite Province

SHRIMP – sensitive high resolution ion microprobe

TWT – two-way (travel) time

T-X – time-offset

USGS – United State Geological Survey

UTEP – University of Texas at El Paso

WSU – Wright State University

WVFS – Wabash Valley Fault Sytstem

ACKNOWLEDGMENTS

This research would not have been possible without Bryan Pope of CountryMark, Inc. and Rachel Walker of Mundell & Assoc. (formerly of CountryMark) for the donation of the seismic reflection data. I would also like to thank Schlumberger (*Petrel*), IHS (*Kingdom*), Neauralog, IGS, UTEP, and USGS for their respective contributions to the project. I would like to thank Dr. Doyle Watts for his warm reception to WSU and continuous advice throughout my time transitioning to and being in Dayton. The constant insight and mentoring from Dr. Ernest Hauser were paramount in the completion of this thesis. Many thanks to Dr. Hauser for his leadership through this work while passing on his passion for attacking geologic problems with geophysical tools.

Thank you to the Dept. of Earth & Environmental Sciences at WSU for their unwavering support. To Andrea Peterson and Suzanne Semones, thank you for your consistency and tireless effort in supporting student activities. To Dave Peterman, thank you for your guidance and wisdom throughout coursework and research. To Ryan Shell, for always supplying a laugh and providing an ear and eye. To EES 9000, for always providing a rewarding “class” and the rest of the faculty, classmates and colleagues who created such a comfortable work environment.

I would also like to thank Dr. Peter Sablock, formerly of Salem State University, for his suggestion of WSU during the application process and his support and encouragement through my time in the geosciences. Thank you to the faculty and former classmates at Salem State for, as I continuously say, everything. A million thanks to (the other) Rachel Walker for her undying love and loyalty. Lastly, and most importantly, I would like to thank my family for always believing in me and motivating me to improve every day.

1. INTRODUCTION

1.1 Overview

Precambrian lithospheric structure and distribution are heavily confined to analysis through geophysical methods. Studying the basement, traditionally thought of as the crystalline portion of the crust that serves as the foundation for overlying sedimentary rocks, is limited at the surface and requires indirect methods, such as geophysics, to better understand the geology (Rudman et al., 1965; Heigold and Kolata, 1993). Ideally, deep drilling ventures could recover basement rocks for direct analysis but this is not always feasible. Utilizing multiple geophysical tools allows for basement properties to be inferred while correlating data with previously published interpretations to better constrain models. Not only is basement lithology a key component in understanding Earth history, but crustal genesis and evolution may provide ties to analyzing deeper time and adding insight to past global tectonism. Since much of the focus in basin analysis is confined to Phanerozoic strata, Precambrian basement rocks often go un-interpreted and ignored (Carter et al., 1996). This leaves a substantial amount of information out of the geologic fabric.

1.2 Purpose

Here, I utilize four two-dimensional seismic reflection profiles and associated potential field data to characterize the basement below west-central

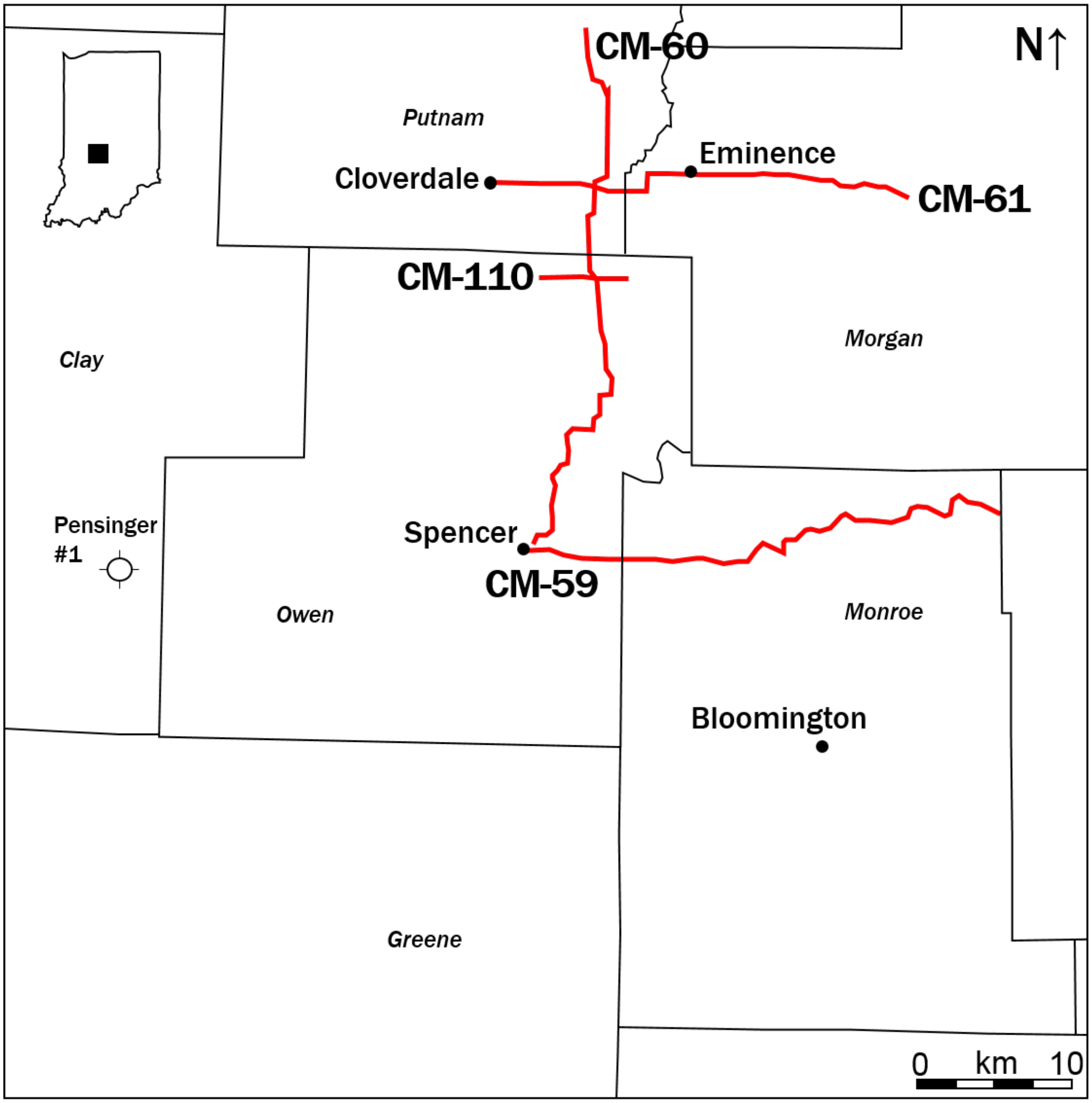

Figure 1 - Locus map of seismic coverage with respect to counties of west-central Indiana. Seismic lines are represented at shot transects along roadways. Pensinger #1 is marked by a dry hole to the west in Clay County.

Indiana (Figure 1). These data were first introduced by Walker (2015). The area is situated along the eastern margin of the Illinois Basin, a prominent intracratonic basin of the United States (Kolata, 1991b). Therefore, my findings may be applicable to similar settings in future basin analysis. Reactivation of structure and paleotopography of the Precambrian surface may have had profound effects on overlying Phanerozoic depositional systems (Rudman et al., 1965; Sexton et al., 1986; Lucius and von Frese, 1988; Drahovzal et al., 1992; Heigold and Kolata, 1993; Furer, 1996; Bear et al., 1997; Drahovzal, 1997; Stark, 1997a; Stark 1997b; Thomas, 2005). The structural and stratigraphic styles of Phanerozoic sedimentary sequences may play a role in dictating the migration and occurrence of hydrocarbons, which have been produced from Illinois Basin strata for over a century (Macke, 1995). Basement tectonics, therefore, may be analyzed through our geophysical interpretations and the associated overlying structural expression may be placed into a framework of petroleum geology.

In a broad sense, I seek to interpret the true composition and structure of the basement, incorporating both crystalline Precambrian unit(s) and associated sedimentary formations. The pre-Mt. Simon Middle Run formation was reported to be a red lithic arenite overlying basement in the neighboring Appalachian Basin (Shrake et al., 1990; Shrake, 1991; Shrake et al., 1991; Drahovzal et al., 1992). The Middle Run overlies both the Eastern Granite-Rhyolite Province (EGRP) and underlies rocks of the Grenville Province and the Cambrian Mt. Simon Sandstone. Recently, Freiburg (2015) discovered a similar unit under Illinois, the proposed Argenta Formation. This unit, however, is only loosely defined as pre-Mt. Simon and has not been assigned to a chronostratigraphic unit. Correlation of these seismic reflection data and similar published works, along with both lithologic and geophysical well log data, allow me to deduce the occurrence, if any, of a lateral equivalent to the Middle Run in the Precambrian Illinois Basin.

The eastern U.S. midcontinent basement is widely interpreted as rocks of the EGRP (Bickford et al., 1981; Denison et al., 1984; Lidiak, 1993; Van Schmus, 1996; Bickford et al., 2015) amongst a mosaic of distinct terranes (Figure 2). What is unclear, however, is how its composition varies across its inferred extent. Pratt et al. (1989) revealed the proposed seismic signature of the EGRP through correlation of deep reflection data with well recovery reports. The geophysical suggestions reported may not be indicative of the true nature of the geology, or a product of only a portion of the EGRP. I hope to add insight into the true lithologic properties of the EGRP under west-central Indiana utilizing a similar yet scaled-back approach as McBride et al. (2016).

Employing a full array of geophysical methods, including 2-D seismic reflection, reduced-to-pole gravity, aeromagnetics, and well log data, I seek to better interpret the origin, composition, and structure of the Precambrian crust along the eastern margin of the Illinois Basin. Moreover, I approach this research as a useful tool to apply to similar basins worldwide in the context of both geologic insight and resource exploration. This thesis should serve not only as a valuable catalyst in increasing Precambrian research in both academia and industry, but an insightful suggestion that basement genesis and tectonics play a vital role in basin evolution and should never be ignored.

2. BACKGROUND

2.1 Stratigraphy

2.1.1 Eastern Granite-Rhyolite Province

The EGRP extends northeast to Wisconsin, to the south into Arkansas, and to the west into southern Missouri where they appear truncated by Southern Granite-Rhyolite Prince (SGRP) rocks (Van Schmus et al., 1996; Figure 2). The eastern extent of the EGRP is unknown, extending below the Grenville Front Tectonic Zone (GFTZ). Extrusive components include both rhyolite and dacite with an intrusive suite of epizonal granite. Trachyte has also been reported (Kisvarsanyi, 1980; Lidiak et al., 1993).

Radiometric analyses of exposed rocks of the St. Francois mountains of southwestern Missouri yielded dates between 1.50 and 1.44 Ga (Bickford et al., 2015). A NW-SE trending fault separates the EGRP from the younger SGRP), which is dated at 1.40 to 1.34 Ga; various intrusive suites across the midcontinent have been dated at 1.27 Ga (Bickford et al., 2015). It is thought that each of these assemblages formed from the re-melting of Paleoproterozic crust, as magmatism was triggered to the northeast and continued west in 100 M.y. intervals, in agreement with tectonic rate models that suggest extremely high plate velocities throughout Proterozoic time (Bickford et al., 2015). Geochronologic and petrologic information regarding the EGRP is

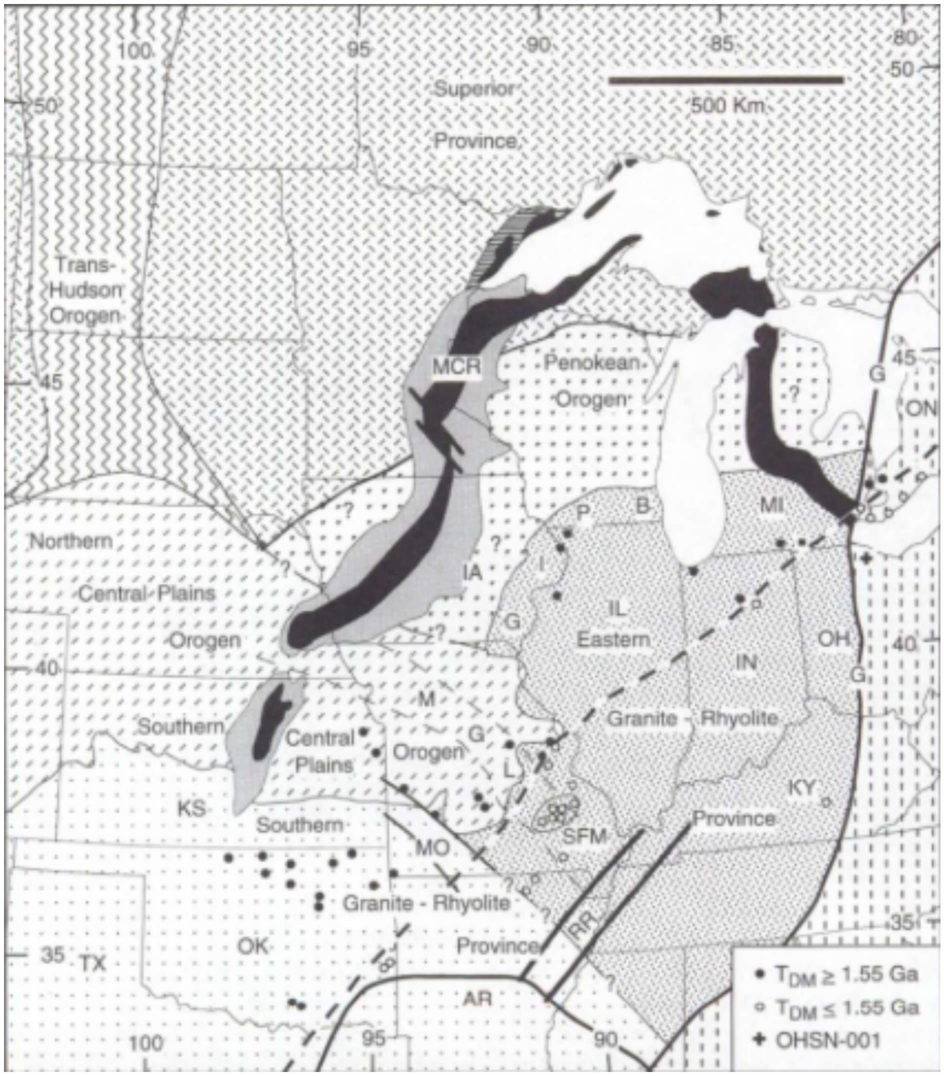

Figure 2 - Distribution of basement provinces underlying the U.S. midcontinent. The northeast-trending dashed line represents eastern limit of juvenile crust derived from >1.55 Ga crust (Van Schmus et al., 1996).

exclusive to the St. Francois mountains and sporadic deep well coverage across the midcontinent, although these wells likely only penetrate the upper region of the basement.

Exposures in the St. Francois mountains provide insight regarding the composition of the EGRP. Silicic volcanics and ash flow tuffs are abundant to the southwest and overlie exposed epizonal granites which have been uplifted due to westward tilting (Sides et al., 1981, Lidiak et al., 1993). The rhyolite and ash flows to the east, coupled with ignimbrites, suggest a caldera setting. Layered flow sequences, gabbro-norites, and tholeiitic olivine diabase dikes exist at depth (Kisvarsanyi, 1980). The various volcanic units comprising the St. Francois locality were highlighted in detail by Sides et al. (1981), and include rhyolites, dacites, volcanic breccias, and andesite.

It is speculated that the St. Francois rocks are anorogenic (A-type) (Kisvarsanyi, 1980; Bickford et al., 1986; Hoffman, 1989; Kolata and Nelson, 1991; Lidiak et al., 1993; Bickford et al., 2015), although Denison et al. (1984) contrast the St. Francois rocks with the volcanics and epizonal granites seen in the Wolf River batholith of Wisconsin, a setting that yielded almost identical age (1.48 Ga). Ring anomalies, both gravitational and magnetic, suggest caldera extrusion and subsequent collapse as the primary emplacement mechanism of A-type granites that post-date midcontinent volcanics. Kisvarsanyi (1980) outlines a chronology of emplacement, sequencing from uplift and fracture development (volcanics) through subsidence to resurgent doming (granites) that results in the reopening of fractures (subsequent mafic-ultramafic intrusions).

Other models have been proposed for the emplacement of the EGRP. Okure (2005) relates complex seismic reflectivity in the mantle to the delamination of the lid and subsequent decompression melting that initiated the emplacement of the province. Delamination, the loss of mantle lithosphere into the asthenosphere due to density and compositional differences (Kay and Kay, 1991; 1993) with respect to the EGRP is discussed further by Bickford et al. (2015). Bedle (2008) discussed the possibility of the EGRP forming due to partial melting of Eoproterozoic crust in a back-arc setting inboard from a convergent plate boundary. Citing a slow-down in S-wave velocity, she argued that the Illinois Basin is underlain by a fossilized subducted slab which, when active, hydrated the lithospheric mantle and produced a zone 7-8 km thick composed of 15% metabasalt and 85% peridotite. Hoffman (1989) previously argued against the subduction model, suggesting that lithologies of the EGRP are too dissimilar from the dacitic ignimbrites that typify Andean rocks that are derived from low-angle subduction, although these units are present in small numbers in the St. Francois as reported by Kisvarsanyi (1980). Still, Hoffman (1989) argued that potassic and silicic rocks are far too abundant to be subduction-related. Instead, he argues for emplacement due to episodic large-scale mantle upwelling. Upwelling was of the same pulsatory nature as eustatic shifts and magnetic reversals, and all three may be due to fluctuations in heat transfer across the core-mantle boundary.

2.1.2 Pre-Mt. Simon sedimentary record

Red, lithic, homogenous sandstone has been reported in multiple deep wells that penetrate the Mt. Simon in Ohio (Shrake et al., 1990; Shrake, 1991; Shrake et al., 1991; Drahovzal et al., 1992; Harris, 1992). Shrake et al. (1990, 1991) and Drahovzal et al. (1992) discuss this unit, the Middle Run Formation, in the context of a rift-related sedimentary unit above the variable basement in the Appalachian Basin and below the Cambrian Mt. Simon. Lithic grains within the Middle Run are likely derived from recycled orogens, most likely the adjacent EGRP and Grenville Province which were well-exposed during Precambrian time (Shrake et al., 1991; Santos et al., 2002). Moecher et al. (2017) revealed the likely contribution of Middle Run grains from the SGRP using detrital zircon U-Pb dates. The distribution of the Middle Run suggested by Santos et al. (2002) does not include west-central Indiana. This exclusion may be due to well information that is insufficient for correlation across not only a vast distance but a separate basin, though the Middle Run basin proposed by Santos et al. (2002) encroaches into the Illinois Basin proper. Sargent (1993) contrasts numerous Middle Run occurrences from deep wells in Indiana with its absence in Illinois. A post-Middle Run, pre-Mt. Simon unit is discussed by Furer (1996).

Drahovzal et al. (1992) and Wolfe et al. (1993) discussed the presence of basalts interlayering the Middle Run clastic component. The presence of volcanics, due to extension and crustal thinning, is not uncommon in rift fill sediments (Drahovzal et al., 1992; Drahovzal, 1997; Prothero, 2004). The Indiana Farm Bureau No. 1 Brown well, drilled in Lawrence County, Indiana, recovered basalt at its base underlying the Mt. Simon (Dawson, 1960). Lawrence County is located just south of Monroe County, which is transected by one of the seismic reflection profiles used herein. The driller's log does not explicitly report the presence of a pre-Mt. Simon sedimentary unit but does note the shift to a high velocity and petrologically distinct unit, associated with the Mt. Simon, at 6,350 ft. (Dawson, 1960). The occurrence of "granite wash" in core below southern Indiana is inferred as pre-Mt. Simon in age and in some places, such as the Grayville graben, comprises ~3 km of the sedimentary record (Sexton et al., 1986). The lithic component of the Lawrence County pre-Mt. Simon clastic unit suggests the occurrence of the Middle Run or a lateral equivalent, quite possibly the Argenta (Freiburg, 2015), below the south-central Illinois Basin.

A similar deep well was completed in 1989 with a focus on clarifying pre-Mt. Simon geology in southwestern Ohio. The well, ODGS 2627, recovered 1,910 ft. of red lithic arenite with siltstone and lithic clasts, officially termed the Middle Run (Shrake et al., 1990; Shrake, 1991) and was identified on an associated 2-D seismic reflection profile, ODNR-1-88 (Figure 3). The Middle Run has been discussed as a regional Grenvillian foreland basin sedimentary unit (Hauser, 1993; Hauser, 1996; Dean and Baranoski, 2002a; Dean and Baranoski 2002b; Baranoski et al., 2009; Peterman, 2016; Moecher et al., 2017) though Drahovzal et al. (1992) argue that interbedded basalts give rise to the interpretation of the East Continent Rift Basin (ECRB). Drahovzal et al. (1992) and Hauser (1996) illustrated a possible relationship between Middle Run found below Ohio and Kentucky with the unknown extent of the Midcontinent Rift

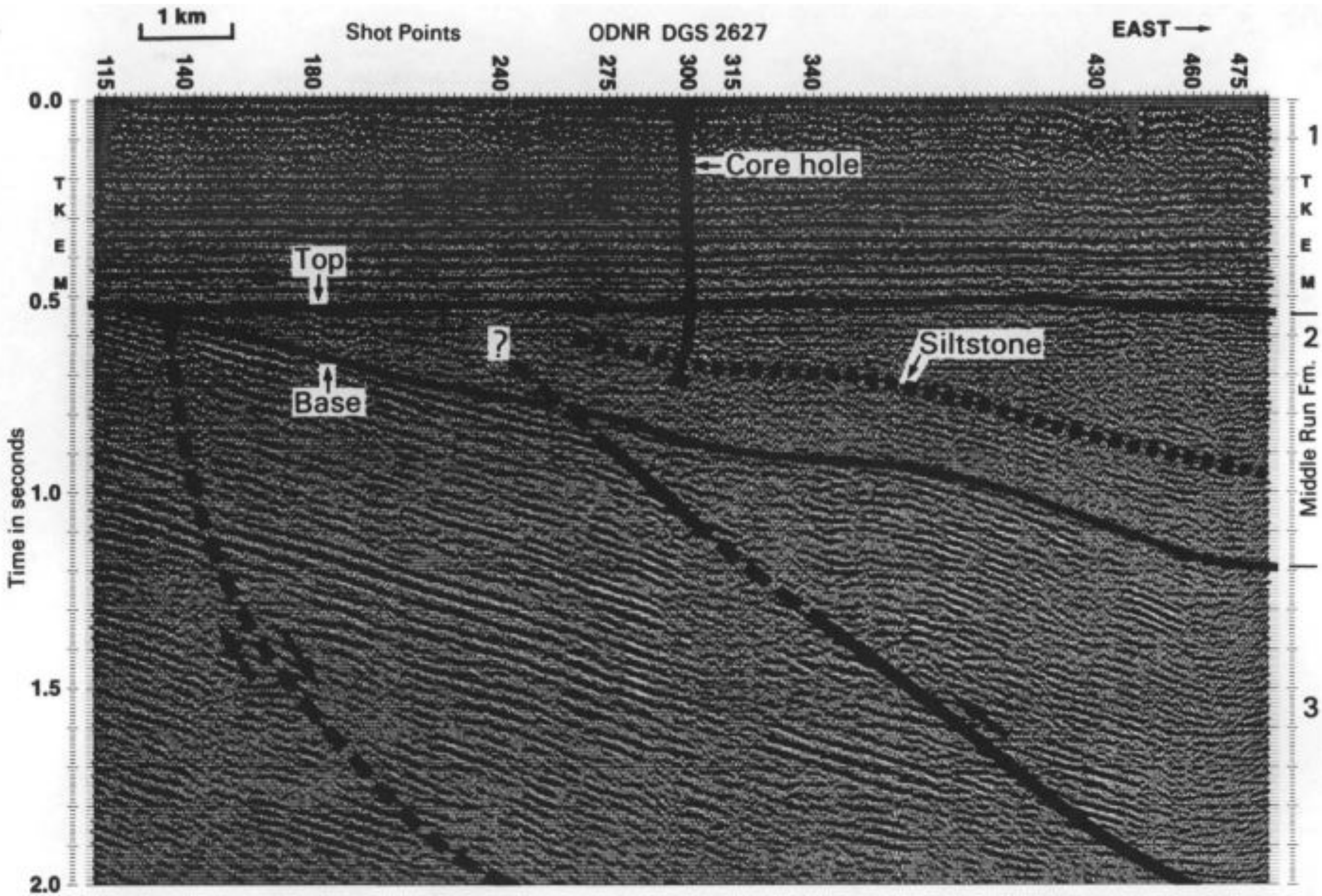

Figure 3 - ODNR-1-88 seismic profile across the Middle Run type section. Middle Run (sequence boundaries marked "Top" and "Base") is characterized by weak, discontinous reflections which appear parallel with the underlying reflective sequence. T = Trenton top, K = Knox top, E = Eau Claire top, and M = Mt. Simon top (Shrake, 1991).

(MCR), suggesting that these Precambrian sediments may have been deposited within the MCR before being truncated by the GFTZ. Rb-Sr dating of detrital zircons in the Middle Run yield pre-MCR dates and reveal ages close to lower radiometric values in the EGRP (Hauser, 1993). Santos et al. (2002) followed up the interpretations by Drahoval et al. (1992) and Hauser (1993) by employing sensitive high resolution ion microprobe (SHRIMP) zircon dating on detrital Middle Run grains. This study concluded that the bulk, all but one, of grains sampled were derived from the Grenville orogen. Drahovzal et al. (1992) and Stark (1997a) reported no observable metamorphic (Grenville-derived) lithics in Middle Run sediments. Harris (1992) and Peterman (2016) pointed out that Grenville-related deformation post-dates Middle Run in seismic reflection data and, therefore, is an unlikely provenance for the Middle Run granular skeleton.

Although it is widely accepted that these sediments were deposited in a basin related to the MCR, the mechanism of triggering depositional onset is disputed as either exclusively rift origin (Drahovzal et al., 1992; Stark, 1997a; 1997b), foreland deposition and deformation (Hauser, 1993; Santos et al., 2002), or both (Hauser, 1996; Baranoski et al., 2009). Richard et al. (1997) interpreted the Middle Run, based on observable seismic relationships, to post-date the Grenville and to have been deposited as an alluvial fan seaward across Laurentia. Analyses by Shrake et al. (1990, 1991), Shrake (1991) and Harris (1992) interpreted the Middle Run to have been deposited during an arid time. Middle Run seismic facies is typified by low impedance contrasts, overall poorly reflective, with occasional strong reflections (Shrake et al., 1990; Shrake, 1991;

Figure 3). Bear et al. (1997) discussed an acoustically transparent pre-Mt. Simon sequence in southern Illinois but avoided Middle Run nomenclature. Potter et al. (1997) suggested the presence of the Middle Run below the southern Illinois basin has been severely deformed and imbricated based on the nature of its weak, observable internal reflections. The occurrence of a carbonate member above and within, overall associated with, the Middle Run is introduced by Wolfe et al. (1993), refined by Hauser et al. (2000) and later discussed in detail by Welder (2014). Welder correlated well data from Jay County, Indiana (east of this study area) with seismic reflection to better characterize the occurrence of limestone within the pre-Mt. Simon stratigraphy. Petrographic work by Harris (1992) questioned the carbonate interpretation validity and argued that the unit was volcanic due to low organic content. Later work by Richard et al. (1997) aligned with the earliest description of the facies as a limestone. The relationship between this phosphatic, organic-rich limestone with the Middle Run has yet to be determined (Richard et al., 1997).

Early interpretation by Pratt et al. (1989) suggested the presence of Proterozoic depositional basins, quite possibly pre-dating the Middle Run, across the midcontinent from COCORP reflection data due to a well-stratified, well-reflective sequence deep below the Illinois Basin. A later study (Pratt et al., 1992) termed this unit the Centralia Sequence (Figure 4), which may correlative with rocks of the EGRP observed in core or associated/inclusive depositional units, and is discussed further in subsequent sections. McBride et al. (2003) discussed the occurrence of the Enterprise Subsequence (Figure 5), of the broader

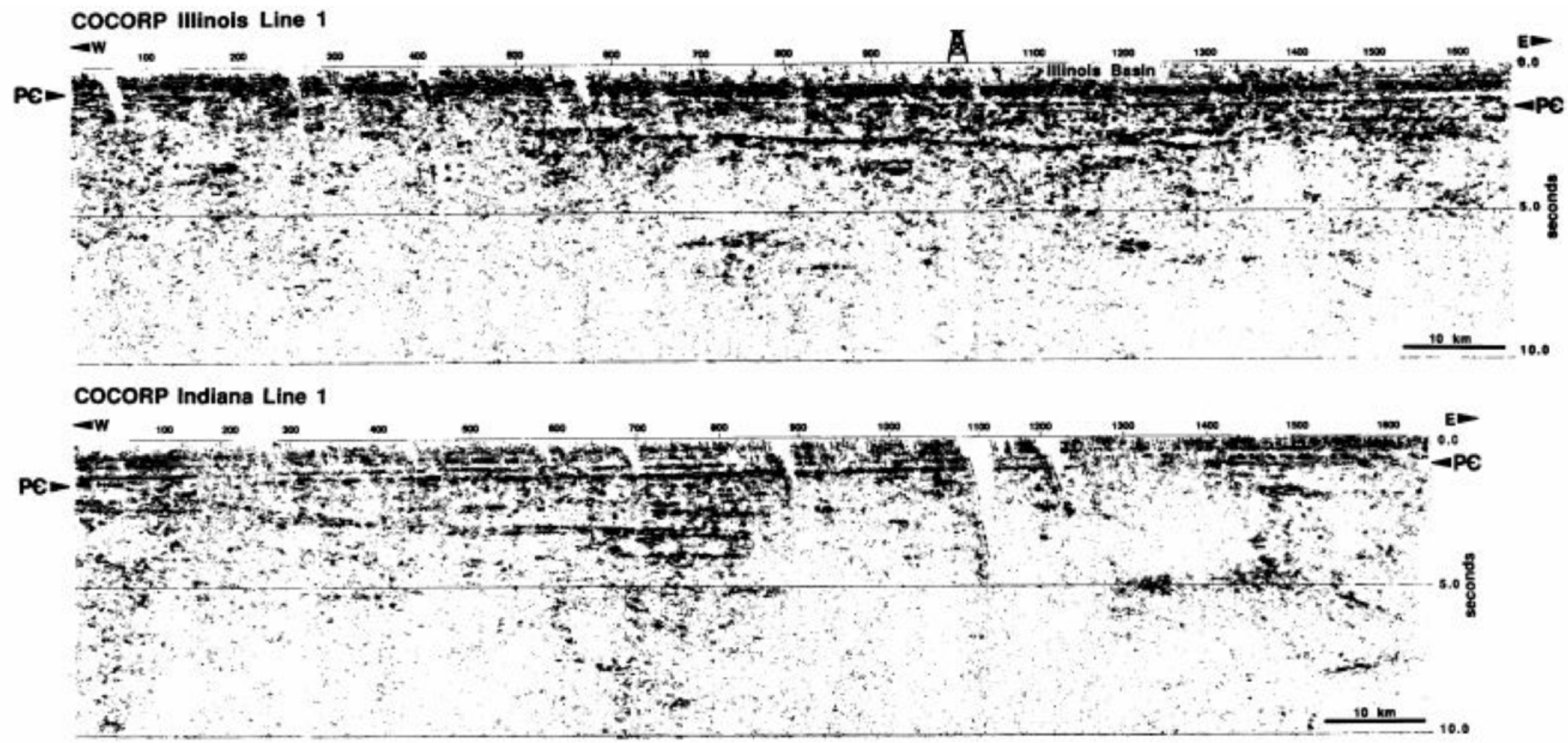

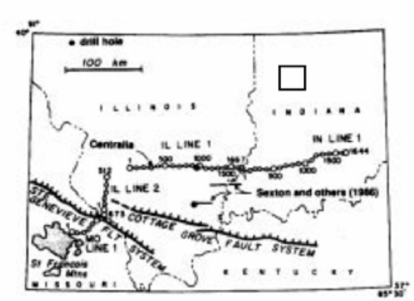

Figure 4 - COCORP 10 s TWT seismic lines across Illinois (top) and Indiana (bottom). The Centralia Sequence is defined as the deep reflective sequence seen on Illinois Line 1. Indiana Line 1 was acquired south of the seismic coverage, indicated on the locus (right), presented here (Pratt et al.,1992).

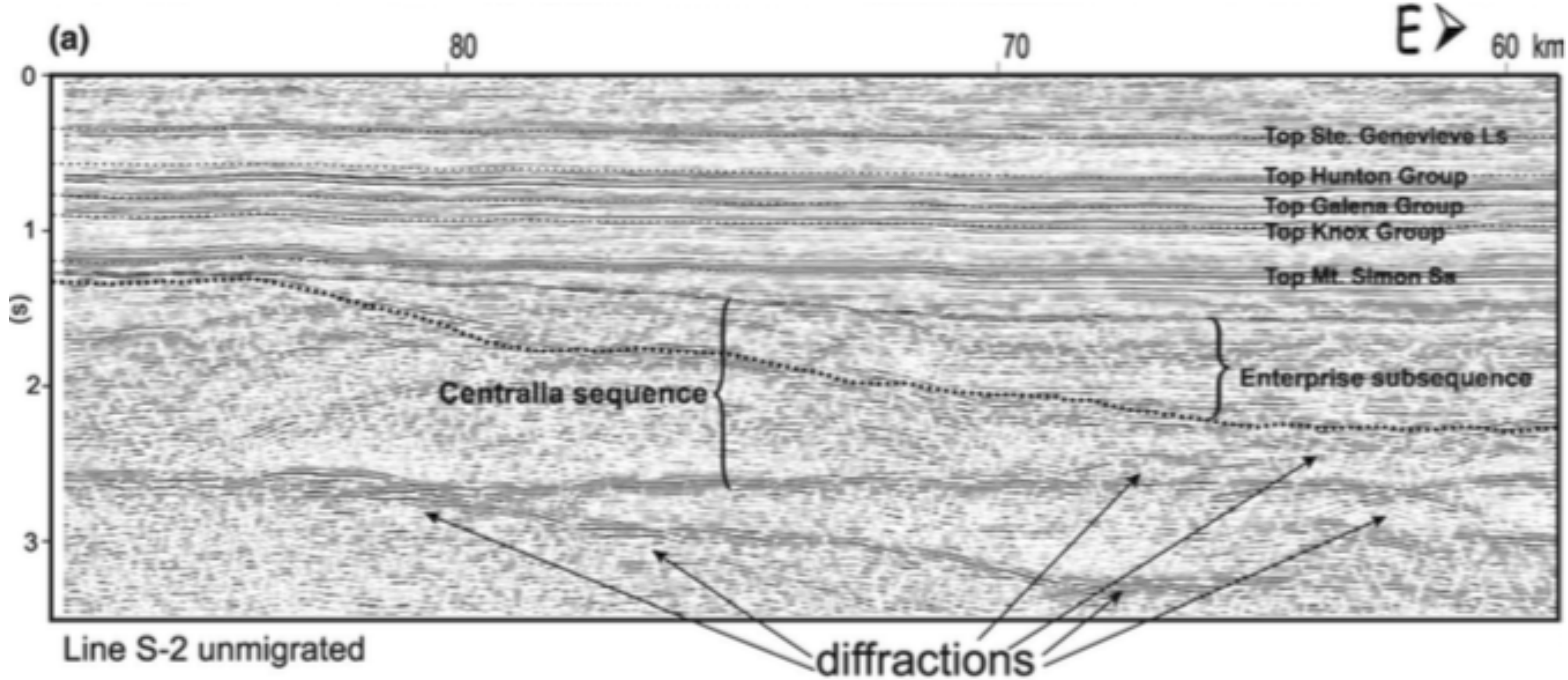

Figure 5 - Enterprise subsequence type section imaged below south-central Illinois. Internal reflections exhibit complex stratal geometries with respect to one another and the broader Centralia Sequence (McBride et al., 2003)

Centralia Sequence below the Illinois Basin as possible basin fill of alternating volcaniclastic and clastic sediments into shallow water, such as nearshore or lacustrine. Reflectors within the Enterprise display seismic signatures indicative of nearshore clastic sedimentation, as outlined in Mitchum et al. (1977). Baranoski et al. (2009) discussed the Enterprise Subsequence as a syn-rift unit deposited during the latter stages of the Grenville orogeny. Absolute dating is, to date, not executed on rocks of this sequence, therefore limiting age determination to pre-Mt. Simon. Comparison of reflections in a volcanic sense with Planke et al. (2000) may suggest massive basalt flows overlain by corresponding and subsequent volcaniclastic deposition.

2.1.3 Paleozoic depositional history

The early Illinois Basin was open to ocean water for much of its existence (Kolata, 1991a). Thus, marine deposition dominates much of the sedimentary record. Lower supersequences outlined by Sloss (1963) are well-preserved and reflected in the basin (Figure 6). Rifting of the Rough Creek Graben (Kolata, 1991b; Catacosinos, 1996), discussed in subsequent sections, resulted in late Precambrian rift-derived arkose basin fill which serves as the onset of Sauk deposition. This unit may be the lithologic twin to the Middle Run Formation of the Appalachian Basin (Baranoski, 2016, personal communication). The deposition of this Precambrian arkosic unit was followed by the deposition of the Mt. Simon in the basin center along with carbonates in shallow water rimming the basin margins, possibly due to thermal subsidence in response to Eocambrian

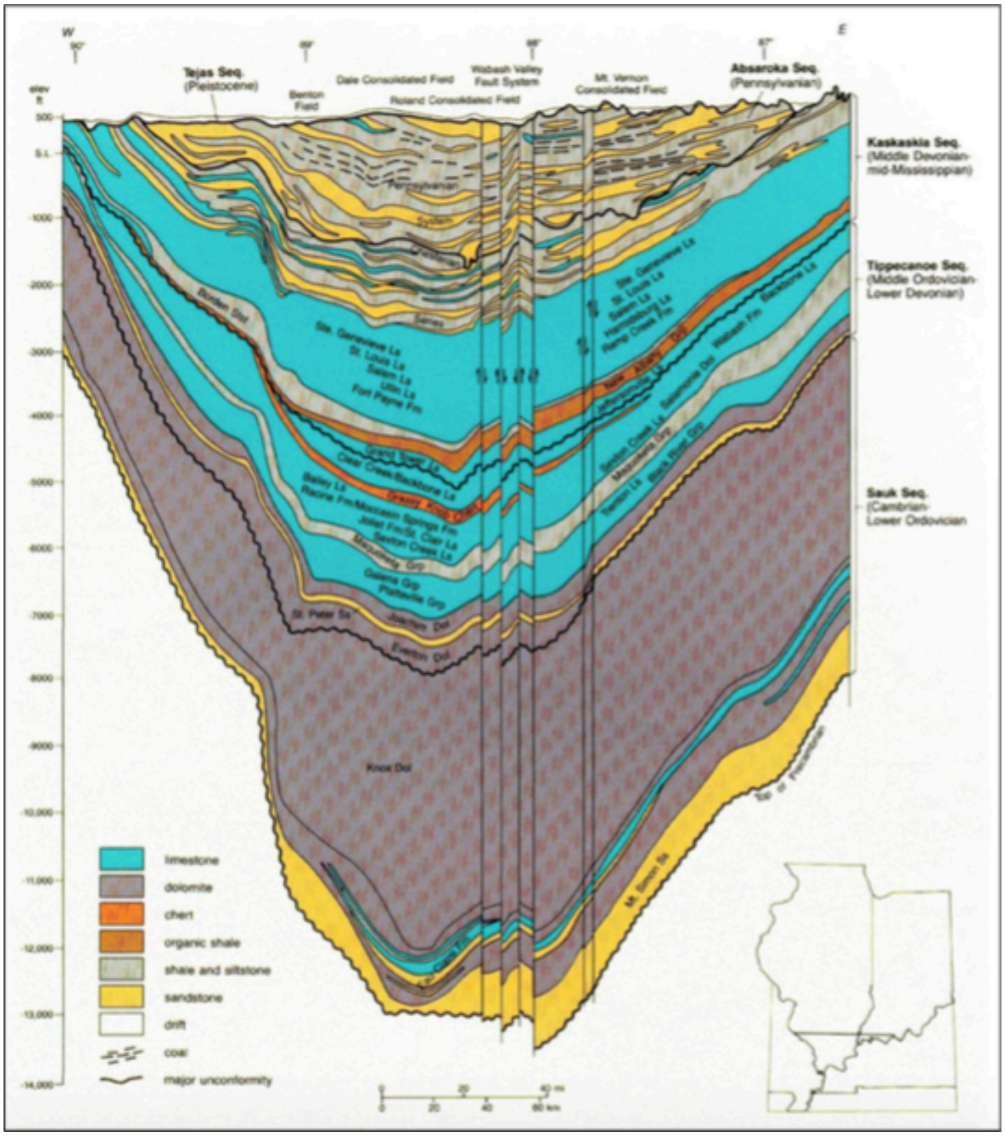

Figure 6 - Geologic cross-section of Illinois Basin strata across depocenter. Note that seismic data presented here image a region to the northeast. Section is greatly vertically exaggerated (Buschbach and Kolata, 1990).The Mt. Simon Sandstone (yellow, base of section), thickens markedly to north, where the Knox Dolomite (purple) and Paleozoic carbonates (blue) and shales (orange) thicken southward towards the depocenter.

rifting (Stark, 1997a). Subsidence acted in response to the deposition of the Mt. Simon followed by the argillaceous Eau Claire Formation. Despite isostatic response to Cambrian deposition, thickness of both the Mt. Simon and Eau Claire is homogenous and suggests relative tectonic quiescence during early Paleozoic time (Furer, 1996). Although extension ceased at the end of Cambrian time subsidence continued throughout the Paleozoic. The basement, at this point, was entirely masked by late Precambrian to late Cambrian sedimentary rocks.

Until the late Ordovician, deposition in the Illinois and Michigan Basins were fairly synchronous. The uplift of the Kankakee Arch began to segregate the two basins, limiting marine influx into the Michigan. The Illinois, however, remained contiguous with the marine environment allowing the deposition of the Trenton Limestone. The end of the Ordovician was marked by a eustatic lowstand in response to glaciation. Therefore, the Upper Sauk and Lower Tippecanoe Sequences are separated by a long stretch of erosion and nondeposition (Kolata and Nelson, 1991). An unconformity representing this hiatus is observable at the top of the Maquoketa Group (Tanner, 1985).

Early Tippecanoe units are carbonate-heavy; subsidence in the basin during this time was fairly subdued. The subduction of the Baltic plate below Laurentia initiated widespread volcanism and uplift. The remnants of the Taconic Orogeny in the basin include the westward fan of clastics derived from uplift. Silurian time saw variable tectonic activity in the basin coupled with rapid subsidence. Sedimentation continued without interruption well into the Devonian until a global eustatic low, at the end of the period, resulted in the unconformity that separates the Tippecanoe from the overlying Kaskaskia Sequence.

Kaskaskian times began in the early Devonian amid a major transgression. During this time the arches that surround the basin acted as broad shoals. Thus, typical marine carbonates and reefs, such as the Wabash Formation, dominated. The collision of proto-Europe with Laurentia triggered Taconic-like uplift and volcanism, the Acadian orogeny, that eventually led to the westward transport and deposition of clastic sediments and the proto-deltaic deposition of the New Albany Shale. The occurrence of the New Albany as a black shale, with trace pyrite, is suggestive of deep, anoxic basin conditions in the southern proto-Illinois while the unit unconformably overlies earlier shallow marine units to the north (Kolata and Nelson, 1991).

Middle Mississippian time was characterized by a high subsidence rate coupled with low sediment loading. This allowed rim carbonates to develop around the margins of the basin and infill was primarily provided through fan deposition of silts and sands (Kolata and Nelson, 1991) and resulted in the deposition of the clastic Borden group (Tanner, 1985). The distribution of these prograding fans was fairly irregular. During St. Louis and Salem deposition, a time of fairly high energy around the basin rim, surrounding arches began exhumation. This excommunication of the basin to marine water allowed for minor salt deposition to occur. The uplift of the Canadian shield provided a heavy flux of clastic sediments to the basin, quite possibly the Cypress Sandstone.

Post-Mississippian strata are absent in the west-central Indianan portion of the basin.

2.2 Tectonic history of the Illinois Basin

2.2.1 Mesoproterozoic tectonics

Initial tectonics in the U.S. midcontinent began in middle Proterozoic time with cycles of anorogenic magmatism (Hoffman, 1989; Atekwanna, 1996; Furer, 1996), resulting in the regional emplacement of the EGRP into and onto the Laurentian upper crust. A major continental rifting event, the Keweenawan (1.30-1 Ga, resulted in a large, arcuate intracratonic igneous province (Chandler, 1983; Van Schmus and Hinze, 1985). Subsequent collision of Laurentia and Amazonia, the South American craton, resulted in the Grenville Orogeny (Chew et al., 2011). Tectonic linkage between the two cratons is evident both geochemically and geologically (Chew et al., 2011). Culotta et al. (1990) and Rivers (1997, 2008) entail polyphase construction of the orogeny, featuring repeated terrane accretion observed in the form of regionally extensive metamorphic rocks. A mosaic of terranes along the eastern margin of Laurentia has led to the distinction between the Shawinigan (1.19-1.14 Ga) (Rivers, 2008; McLelland et al., 2010), Ottawan (1.09-1.02 Ga) (McLelland et al., 2010), and the Grenville front compressional event (~1-0.80 Ga) (Krogh, 1994). Peterman (2016) linked the Grenville tectonic progression to the deposition of the Middle Run (Figure 7). Grenvillian metamorphic rocks are observed along a curvi-linear trend, from outcrop in eastern Canada to subcrop, south to the Mississippi embayment

(Culotta et al., 1990; Thomas, 2005). The thick Cenozoic sedimentary cover obscures the terminus. Geopotential data display a high magnetic curvi-lineament interpreted by many as the GFTZ, a major boundary between distinct basement provinces (Lucius and von Freese, 1988; Pratt et al., 1989; Van Schmus, 1996).

An independent reconnaissance by Stark (1997a) detailed the East Continent Rift Complex as a result of recurrent tectonism across Laurentia during the Proterozoic. This sequence is highlighted by Keweenawan extension possibly forming the half-grabens which received Middle Run sediments and features such as the ECRB (Drahovzal et al., 1992) and English Graben (Stark, 1997b). These extensional structures were then overprinted by Grenvillian front contraction (1,000-880 Ma) which introduced the northwest-southeast structural expression observed across the midcontinent as discussed by Furer (1996). Eocambrian uplift, erosion, and rifting (650-560 Ma) completed the construction of the province. A major caveat, however, is the assignment of Grenville stresses to a finite time window. As outlined by Rivers (2008), the Grenville Orogeny occurred in multiple stages across Proterozoic time (Figure 7). These repeated tectonic episodes would result in much more compression than that suggested by Stark (1997b). These discrepancies, as well as the numerous models for basin evolution and sedimentary progression, exemplify to the complexity and ambiguity of the deeply-buried midcontinent basement.

2.2.2 Neoproterozoic tectonics

The Illinois Basin began development in the late Proterozoic (Furer, 1996), concurrent with the breakup of the supercontinent Rodinia and, thus, Laurentia (Stark, 1997a). Late Precambrian transform faulting within the Rough Creek Graben (RCG) marked the onset of proto-Illinois basin development (Kolata, 1991b; Catacosinos et al. 1996) and the basin subsided through Paleozoic time due to thermal forces. The major formational onset of the Illinois Basin is believed to have occurred in the early Cambrian, when the Reelfoot Rift (RR) was initiated as an aulacogen (Buschbach and Kolata, 1990) contemporaneous with other failed rifts along the southern margin of proto-North America (Oklahoma and Delaware Aulacogens). Northward syn-tectonic thickening of Cambrian sediments is evident in seismic reflection data within and

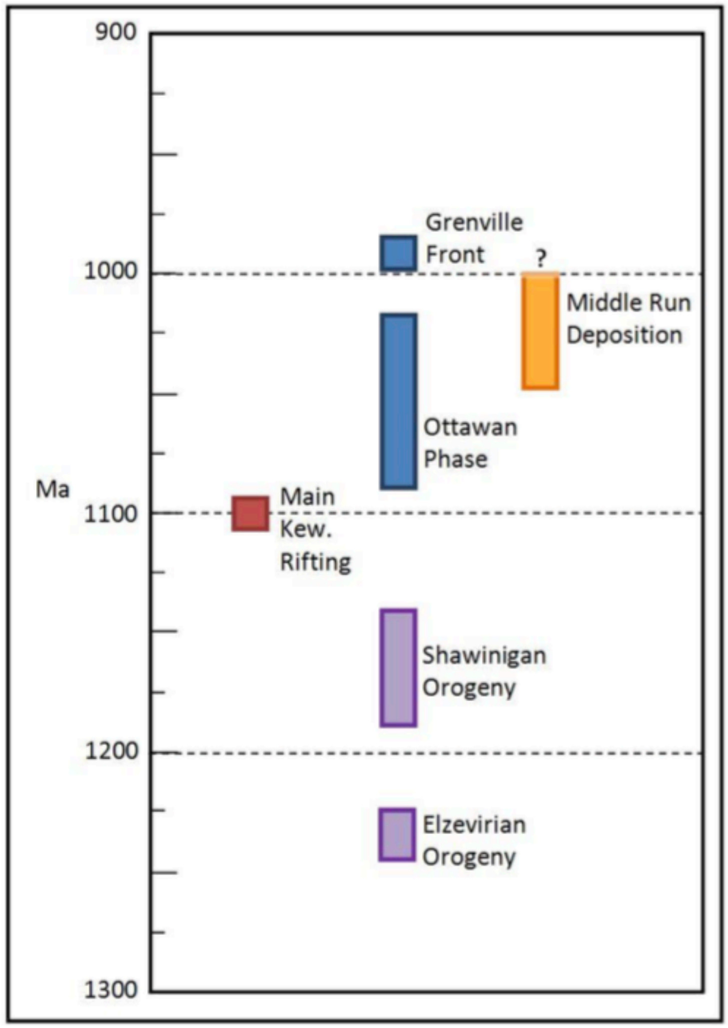

Figure 7 - Chronological synthesis of Grenvillian tectonics. Ages were compiled from numerous sources (Peterman, 2016)

adjacent to the RCG (Drahovzal, 1997; Potter et al., 1997). The geometry of the basin during rifting is well-indicated by the distribution of the pre-Mt. Simon surface (Kolata, 1991b). Intra-plate rifting was following by crustal downwarping in response to the Grenville orogeny, to the east, and the creation of foreland basin that received erosional remnants of Grenvillian thrust sheets (Santos et al., 2002) and granitic highlands (Drahovzal et al., 1992; Hauser, 1993; Furer, 1996; Richard et al., 1997; Baranoski et al., 2009). Vertical faults within the Precambrian, formed during basin genesis, serve as the primary culprit in deformation and reoccurring seismicity (Furer, 1996; Bear et al., 1997; Stark, 1997b; McBride et al., 2014). Subsidence within the basin took place throughout most of Paleozoic time due to continuous deposition and loading, though certain periods (i.e. late Kaskaskia, early Absaroka; early Devonian through Mississippian) experienced faster subsidence than others. During the Paleozoic, the Illinois Basin was continuous with the present-day Black Warrior and Arkoma Basins of Mississippi/Alabama and Arkansas, respectively.

2.2.3 Phanerozoic tectonics

During the early Phanerozoic, the Illinois Basin existed, primarily, as a south-plunging trough open to marine waters. Accessory faults are evident within sedimentary rocks of the Sauk sequence (Stark, 1997a); the thickening of the Knox Group has been attributed to growth faulting (Kolata and Nelson, 1991). Minor deformation is evident in Tippecanoe-aged units. The Taconic Orogeny to the east, however, introduced extracratonic sediments as discussed above as well as some diastrophism. These stresses triggered the Mt. Carmel Fault Zone (MCFZ), a negative flower structure that offsets basement rocks up through the Ordovician Maquoketa Group (Tanner, 1985; Furer, 1996). Flower structures, as described by Harding (1990), are basement-controlled structures initiated during strike-slip tectonism and are comprised for a system of accessory faults that are influenced by a master fault. Surface expression of the MCFZ transects at least a portion of the study area discussed here. Features along the fault include a basinward, westward-dipping master fault and associated synthetic and antithetic faults which, along with drag features, accommodate for displacement along curved fault surfaces (Tanner, 1985).

The basin underwent mild tectonic activity during the Silurian. Kaskaskian movement along the Ste. Genevieve Fault supplied sediments southward and may have encouraged diatreme and plug intrusions. The Acadian Orogeny provided similar structure to the basin as the Taconic did. The uplift of the Kankakee Arch late in Devonian time provided a more effective barrier between the Illinois and Michigan sites (Kolata and Nelson, 1991). Bounding structures around the Illinois basin include the Cincinnati Arch to the east, the Kankakee, Wisconsin, and Mississippi River Arches to the north, the Northeast Missouri Arch and Ozark Dome to the west, and the Nashville Dome along with the Pascola Arch to the south (Buschbach and Kolata, 1990). Folding is evident within Mississippian and Pennsylvanian strata (Kolata, 1991a) which was attributed to the reactivation of basement faults (Drahovzal et al., 1992). It is also postulated that Mississippian deformation is due, in large part, to the collision of

Laurussia and Gondwana (Kolata and Nelson, 1991; Leighton, 1996). Primary compressive stress direction changed continuously through Mississippian time due to the re-organization of continental blocks and outboard arcs (Kolata and Nelson, 1991) along the Laurentian margin. Offset within the MCFZ is evident through Mississippian strata (Tanner, 1985), suggesting renewed movement along the fault during or, likely, after Mississippian time. Contemporaneous and subsequent reactivation resulted in the current state of major intrabasin structures, such as the Rough Creek and Lusk Creek Fault Zones (Heigold and Kolata, 1993). Uplift of the Pascola Arch to the south closed off the basin and provided the geometry known today.

The current structure of the basin is due to a complex tectonic history that requires rigorous geologic and geophysical investigations to interpret. McBride et al. (2014) suggest that deep faults, represented by small offsets, are confined to the basement. Although these faults comprise minimal displacement, their associated stresses may be responsible for reactivated Paleozoic deformation (Furer, 1996, McBride et al., 2014). The overall trend of northeast-southwest structural expression is possibly facilitated by strike-slip faulting within the basin, as is seen in the La Salle anticlinal belt and Cottage Grove Fault System (CGFS). Although few faults that reflect this suspected grain are published, geophysical data support the interpretation; the overall tectonic fabric within the Illinois basin is characterized by orthogonal northeast-southwest (Furer, 1996; Potter et al., 1997) and northwest-southeast striking structures (Furer, 1996). The trend may be responsible for the distribution of a range of geologic factors within the basin, such as responsive structures, igneous intrusions, and warm, mineralized water typical of deeper reservoirs. An episode of Permian mineralization generates a distinct seismic facies in Fluorspar Area Fault Complex (FAFC) seismic data to the south, as well as evidence of faulting occurring as recent as the Quaternary (Potter et al., 1997).

Only a portion of the Illinois Basin is analyzed here. The published and observable structure below west-central Indiana is subtle and much less deformed than that which characterizes the southern reach of the basin in southern Illinois and the Kentucky panhandle. The MCFZ, observed in detail by Tanner (1985) and Furer (1996), offsets strata through the study area. Stark (1997b) suggested that the MCFZ serves as the eastern boundary of the Illinois basin. Though the presence of the structure is well known, its extent is not. Regional features, such as the CGFS, FAFC, RCG, RR, Wabash Valley Fault System (WVFS), and Hicks Dome were analyzed in detail (Potter et al., 1995; Bear et al., 1997; Drahovzal, 1997; Potter et al., 1997) and present a much more complicated structural problem to the south. Still, the data interpreted herein provide similar implications regarding basin genesis.

2.3 Geophysical applications in crustal scale research

2.3.1 Seismic reflection

Seismic reflection data have been extensively utilized to study crustal geometry and characteristics (Sexton et al., 1986; Allmendinger et al., 1987; Pratt et al., 1989; Cannon et al., 1991; Drahovzal et al., 1992; Pratt et al., 1992;

Hauser, 1993; Heigold and Kolata, 1993; Wolfe et al., 1993; René and Stanonis, 1995; Leighton, 1996; Bear et al., 1997; Drahovzal, 1997; Potter et al., 1997; Richard et al., 1997; McBride and Kolata, 1999; McBride et al., 2003; Okure, 2005; Baranoski et al., 2009; McBride et al., 2014; McBride et al., 2016; Peterman, 2016; Figure 3, 4, 5). This method is heavily employed in the Illinois Basin, where numerous data sets revealed a reflective, stratified deep sequence (Sexton et al., 1986; Pratt et al., 1989; Pratt et al., 1992; Hauser, 1993; Heigold and Kolata, 1993; Lidiak et al., 1993; Potter et al., 1995; Van Schmus, 1996; Bear et al., 1997; Drahovzal, 1997; Potter et al., 1997; McBride and Kolata, 1999; McBride et al., 2003; Okure, 2005; Baranoski et al., 2009; McBride et al., 2014; McBride et al., 2016; Figure 4, 5). Crustal character varies considerably to the north below the Michigan Basin as revealed by GLIMPCE profiling (Cannon et al., 1991). The Illinois Basin served as the basis of reflection analysis by McBride and Kolata (1999). The upper crust of the U.S. midcontinent is typified by northwest-thickening basement, coupled with the Mt. Simon, and southwest-thickening Paleozoic strata. Layered reflections suggest an interlayering of unknown compositions (mafic-clastic, mafic-felsic, felsic-clastic?) in the uppermost basement. Applying seismic reflection data to interpret structural settings and characteristics was thoroughly outlined in zonal brackets by Allmendinger (1987).

Pratt et al. (1989) discussed the midcontinent crust based on seismic reflection data across southern Illinois and Indiana and central Ohio. The nature of deep reflectors in the Illinois basin are subhorizontal with a slight eastward dip.

An attempt to correlate reflectors with the St. Francois exposed units was unsuccessful. Although well control in this area is suggestive exclusively of felsic rocks, the amount of parent mafic crust needed to produce such volume is extremely immense. Therefore, it is interpreted that the reflectivity of the layered Precambrian rocks is produced by a predominantly felsic unit interlayered with mafic flows and, possibly, Proterozoic sedimentary rocks Pratt et al., 1989; 1992; Hauser, 1992; McBride et al., 2003). The nature of the reflectors underlying Illinois and Indiana is truncated by the westward-dipping Grenville province (Pratt et al. 1989, Pratt et al. 1992). Precambrian sedimentary sequences related to the Grenville, both syn-kinematic rift basins and a foreland basin, were discussed by Baranoski et al. (2009).

Pratt et al. (1992) also hypothesize that, despite the amount of evidence from shallow-penetrating boreholes, igneous rocks may not comprise the bulk of the midcontinent basement. Although layered volcanics and deep-seated granites are likely present, the amount of crust needed to partially melt the interpreted 6-8 km of crust may reach 80 km, an unrealistic amount with few analogs. Therefore, volcanics and other igneous layers may be the culprit for reflectivity observed in lower intervals, but an appreciable amount of sedimentary strata (volcaniclastic, siliciclastic, or both) may also be present. The presence of igneous rocks in the crustal skeleton suggests that some contact metamorphism probably took place, and biotite and greenschist facies have been reported. Therefore, Precambrian hydrocarbon occurrence is unlikely due to local heating, but if the crust is comprised of lower amounts of igneous lithologies the presence cannot and should not be entirely neglected. Precambrian source rocks are present to the north in Michigan and, in nearby western Ohio, pre-Mt. Simon seismic sequences suggest favorable traps for potential hydrocarbon accumulation (Dean and Baranoski, 2002b).

Seismic reflection was the primary tool used by McBride et al. (2003) to better understand the distribution of Precambrian seismic sequences of the basin by reprocessing industry profiles to extend beyond 4.0 s TWT. The occurrence of highly reflective upper crustal units above pods of discontinuous reflections and numerous diffractions suggests the emplacement of volcanic necks into and extrusion of basaltic flows onto pre-existing granitic country rock. Age relationships suggest these layered units to be much younger than the host into which they were plumbed, most likely rocks of the EGRP. The seismic volume was also used to interpret the relationship of pre-Mt. Simon units to the Mt. Simon, which revealed a conformable contact in many places and an identical northward thickening. Spatial distribution of this unit, the Enterprise subsequence, along with stratal geometry suggest a sedimentary origin. This may also suggest similar provenance of both units.

The Precambrian crust was again analyzed by McBride et al. (2016) and reinforced as a unit comprised of volcanic sills sourced from adjacent magma bodies, both of which may be seen on seismic imagery. This study provides insight into the geometry of the crystalline basement along with the overlying Mt. Simon. Both 2-D and 3-D seismic reflection data are used in this interpretation and prove effective in analyzing the deep crustal structure below the basin.

Although our methodology is limited in comparison to this research, we seek to add similar insight and expand on ideas discussed here and in previously published works. Numerous seismic sections reveal stratified, continuous Paleozoic reflectivity across the Illinois Basin (Sexton et al., 1986; Shrake et al., 1990; Shrake, 1991; Shrake et al., 1991; Drahovzal et al., 1992; Wolfe et al., 1993; Bear et al., 1997; Drahovzal, 1997; Stark, 1997a,b; Richard et al., 1997; McBride and Kolata, 1999; McBride et al., 2003; Okure, 2005; Baranoski et al., 2009; McBride et al., 2014; Welder, 2014; Walker, 2015; McBride et al., 2016; Peterman, 2016).

2.3.2 Potential field

Potential field data also provide insight into crustal structure. Gravity and magnetic data, preferably coupled, provide insight into genesis, metamorphic grade, deformational history, and age relationships of concealed basement rocks (Bickford et al., 1986; Drahovzal et al., 1992; Atekwanna, 1996). In a broad sense, gravity data reveal the spatial shift in density of subsurface rocks and the lateral change in bulk magnetism is measured by magnetic data (Sharma, 1986); magnetism in the subsurface is often produced by varying abundance of magnetite (Lucius and von Frese, 1988). Atekwanna (1996) discussed major Precambrian basement features of the eastern U.S. midcontinent through interpretation of potential field anomalies. She attempts to resolve questions regarding the distribution of these units, of which includes the Eastern Granite-

Rhyolite Province, as well as describing distinct properties seen in gravity and magnetic signals generated by the units in question.

Lucius and von Frese (1988) applied potential field methods, aided by seismic reflection and lithologic data, to analyze and model the deep crustal structure (≥40 km) below Ohio. Coupling gravity and magnetic data permitted the interpretation of two distinct provinces; the discussed anorogenic granite/rhyolite/trachyte is likely correlative to the EGRP. Smaller features, such as juvenile granites and internal complexes typical of heterogenous crust, were also revealed. Nevertheless, it is iterated that such geophysical tools lack the resolution and detail of seismic reflection. These tools are most effective in defining boundaries and regional features.

3. METHODS

3.1 Data acquisition

Seismic reflection data were acquired by Bay Geophysical, for CountryMark, in 2012. Surveys took place, primarily, along roads throughout west-central Indiana (Figure 1). Portions of the subsurface below Monroe, Owen, Putnam, and Morgan Counties are included in the data set. CM-59 (northern Monroe to southeastern Owen; 34.93 km), CM-61 (southeastern Putnam to central Morgan, 30.08 km), and CM-110 (northeastern Owen, 6.54 km) trend east-west. Both of these profiles are bisected by CM-60 (southeastern Owen to northern Monroe; 39.80 km), which runs south-north. The southern terminus of CM-60 roughly corresponds to the western limit of CM-59, but the north end of CM-60 extends beyond its intersection with CM-61. CM-110 roughly bisects CM-61 through northeast Owen County. All four seismic surveys listened for 2.0 s TWT.

A *Vibroseis* source was employed for each of the surveys, sweeping 8-125 Hz at each shot point. Shot points were spaced 110 ft. apart and receivers were located at every 55 ft. Thus, interpreted CDP locations are spaced 27.5 ft. from the adjacent point. The geometry of the local roads resulted in irregular profile geometry, which is accommodated for during by static corrections during data processing. Examples of these deviations include the sharp turn in CM-59 and the broad southwestern bend in CM-60. Processing of the data was also done by GeoConcepts, Inc. and the resultant common depth point (CDP)-stacked, migrated images were included in the data set donated by CountryMark.

3.2 Data re-processing

3.2.1 Re-processing steps (CM-59)

In an attempt to amplify basement reflection events, line CM-59 was re-processed from raw SEG-Y data in Halliburton's *ProMAX 2-D* (Figure 8A). The donated seismic volume was processed with an exploration focus on Paleozoic units (Figure 8B); I focused on enhancing reflections of the interpreted basement, between ~1.0 and 2.0 s TWT. Data were processed initially in the form of shot gathers, where all data were generated from a single shot point at the surface. Once line geometry was input, dead or inconsistent traces within each gather were picked for killing. Creating a kill table and applying kills omits these traces from the final stack. Most shot gathers contained a completely "silent" trace, where no seismic data were received. This may be due to an open take-out (receiver-cable connection). Some traces were dominated by a 60 Hz signal, the Mains electricity frequency, which suggests leakage to ground in some geophones or cables. Most of the raw data contain a relatively narrow refraction window. Refractions are typified by linear moveout events, where refractions are received in a linear style with increasing offset. Top muting, removing only selected early-time portions of a gather, effectively removes refraction events and prevents them from entering the final stack.

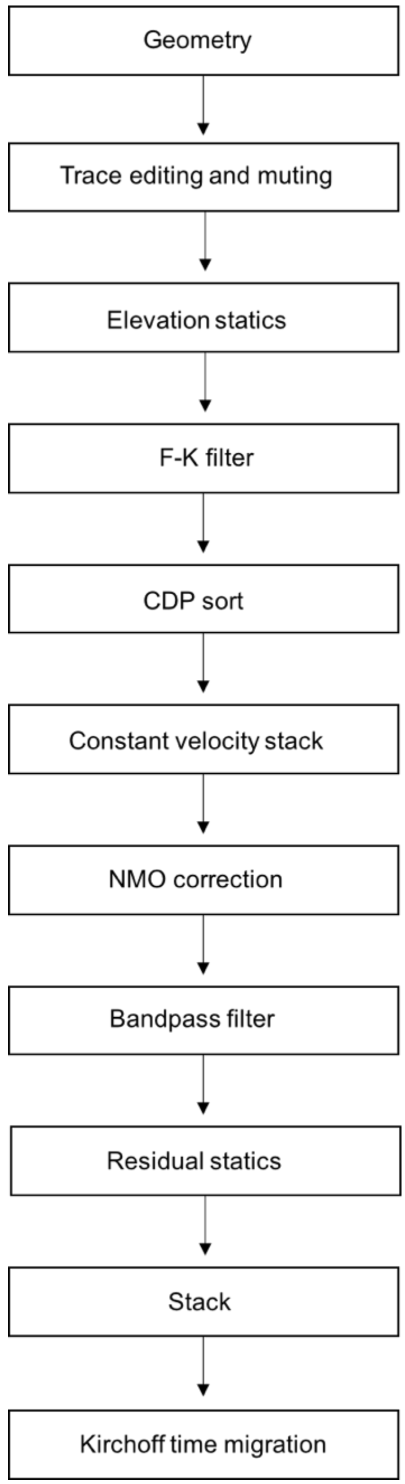

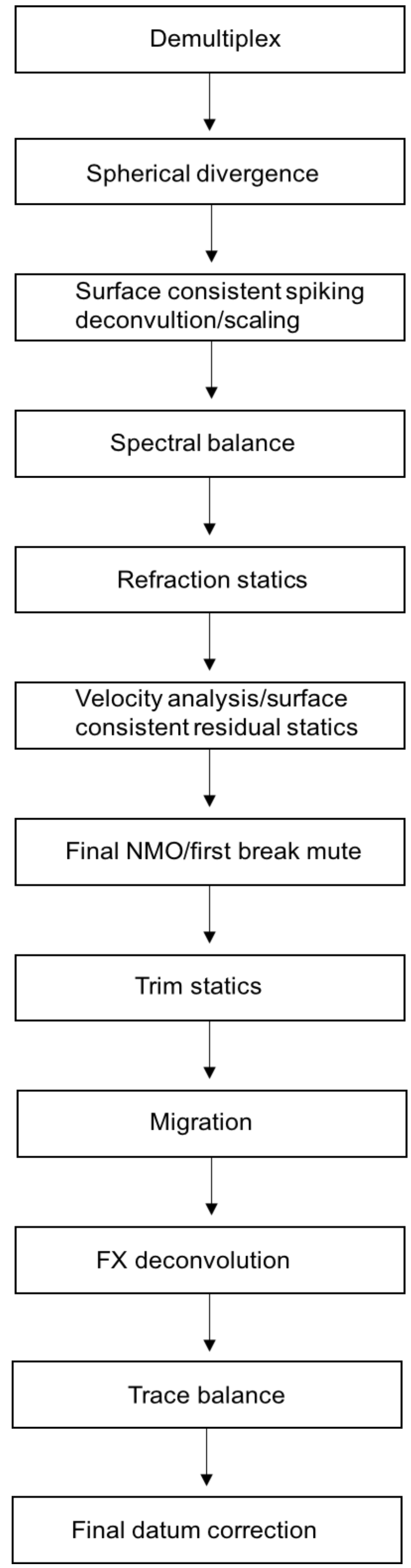

Figure 8 - A) seismic processing flow from re-processing done at Wright State University (left); B) processing supplied from SEG-Y headers by GeoConcepts, Inc (right). WSU processing focused on enhancing and amplifying deep reflections while GeoConcepts processors focused on Paleozoic hydrocarbon targets.

Although refractions were minimal in these data, surface waves, or ground roll, were a predominant source of noise that required removal during pre-stack processing. Ground roll behaves as a low velocity waveform in seismic acquisition, therefore masking refraction and, most importantly, reflection events. Attenuating this interference is not as simple as creating top mutes. A more elegant and rigorous filter must be applied; frequency-wave number (F-K) filtering allows the picking of a certain range of frequencies and wave number ($1/\lambda$) within a polygon; events which may either be accepted or rejected at the preference of the processor. Reflections and ground waves are easily distinguished in F-K space, as reflections tend to be closer to the zero wave number area and low frequency events, such as ground roll, plot closest to the abscissa. The ground roll in this data volume, however, was of higher frequency and the selection of boundaries was often ambiguous. The F-K analyzer in *ProMAX* displays time-offset (T-X) in an adjacent window, thus allowing quality control in defining polygonal boundaries.

Data were sorted into CDP gathers following F-K analysis. These gathers display all data generated from a single point in the subsurface. Since data were collected via a *Vibroseis* roll-on method, starting and ending CDP's yielded little data. These low-fold areas were taken into account during subsequent processes. To minimize the artifacts associated with low-fold data, the center portion of the line was analyzed. 600 central CDP's were employed to run through constant velocity stacking, a method designed to obtain appropriate root-mean-squared (RMS) velocities for intervals in the subsurface. This process is pivotal in improving seismic imagery; my focus was on basement velocity and applying the most proper velocity to amplify the truest reflectivity.

Velocities vary in the subsurface based on degrees of lithologic differentiation. Honoring basic geologic principles, velocity generally increases with depth based on compaction sourced by overburden aggrading and the eventual contact with crystalline, high-velocity crustal basement rocks. The quantitative velocity, however, is important in seismic processing in correcting for normal moveout (NMO). Contrary to linear moveout, NMO is characterized by hyperbolic style of events due to a non-linearly increasing pathway distance between source and receiver during acquisition. NMO is calculated by:

$$t_{NMO} = \frac{\sqrt{x^2 + 4z^2}}{V_{RMS}} - \frac{2z}{V_{RMS}}$$

NMO correction restores seismic events to their proper position in the subsurface. Since Illinois basin strata are relatively horizontal and undeformed, the principle of NMO is viewed here as viable. Applying the NMO corrections with appropriate velocities produced few laterally continuous reflections. A bandpass filter, allowing only a certain range of frequencies through, was applied a 6-12-24-48 (Hz). The bandpass exposed multiple continuous horizons suitable for residual statics selection and correction.

Residual statics is a processor that shifts reflectors at improper times to a specific datum. The continuous reflections sought in NMO correction and bandpass filtering are key for this and serve as the datum for autostatic shifting. This particular procedure was rigorous here; converging the data took close to a full day to run and, initially, would not converge. Convergence criteria, a time unit used as the minimum sum of convergence under a Cauchy sequence, were established for various horizons empirically. Criterion ranged from 0.12-0.46 ms with no true relationship with depth. Initially, one negative reflection was used as a horizon due to continuity across the section. This, however, produced an erroneous gather with events occurring in improper locations in time. To ensure that autostatics were accounted for at greater depths, laterally continuous sub-1.4 s reflections were picked as horizons where appropriate. The array of autostatics horizons were spliced together and applied. Applying Kirchoff migration to the data returned spurious events, such as dipping units, to their original positions in the subsurface. Migrating seismic reflection data also collapses diffractions and creates a final interpretable cross section of the acoustic variations in the subsurface. The final results of re-processing were compared to the donated set of stacked images and aided in interpretation.

3.2.2 Calculation of CDP coordinates (CM-59, 60, 61)

Importing enhanced, migrated data acquired from CountryMark into *Petrel* produced reflection planes displayed geographically according to shot point. Proper interpretation requires CDP coordinates to be displayed against TWT. *ProMAX 2-D* provides CDP computation through the import of source and receiver coordinates. Source and receiver positions loaded into *ProMAX 2-D* need to be monitored for error, as some raw data require correction. Errors range from unwanted characters (asterisks) appearing in the data or station numbers cycling instead of increasing sequentially. Once these variables are corrected, CDP locations may be binned. Binning is the process of assigning a specific CDP to a grid cell in the subsurface. Binned data may then be uploaded into *Petrel* for interpretation. This portion of data preparation was done after initial interpretation in *Petrel* revealed the nature of each survey in space.

3.2.3 Correction of spatial coordinates

CDP coordinates were stored in the trace headers of all seismic data as integers by multiple real Indiana State Plane coordinates by 10. This was problematic in initial data load in *Petrel*. The Trace Header Math processor in *ProMAX* was employed to divide these values by 10 and produce real coordinate values within the SEG-Y file. Uploading the corrected CM-110 SEG-Y revealed an apparent reversed polarity of the data. Positive reflections within bisecting CM-60 corresponded with negative events in CM-110 and vice versa. The New Albany reflector, the uppermost negative underlain by a strong positive, indicated the change. A phase rotation of 180° was applied, following an unsuccessful trace reversal, restoring wavelets to proper polarity.

3.3 Geophysical well log correlation

Bulk density, travel time, and gamma ray logs from the Pensinger #1 well in Clay County were utilized here for correlation of logged geologic data with seismic reflection. The well penetrated 6,785 ft. of Illinois basin stratigraphy and reportedly bottoms in the Mt. Simon. The driller’s report was employed for picking formation tops. Data for all wells (oil, gas, dry hole, etc.) are available through Indiana Geological Survey (IGS)'s Petroleum Database Management System (PDMS) and the state's Department of Natural Resource (DNR)'s oil and gas database. Correlation of data was completed in *Kingdom.*

Importing bulk density and travel time logs into *Kingdom* allows for the calculation of acoustical impedance (I) and, in turn, reflection coefficients (R). *Kingdom* automatically generates corresponding velocity values from the travel time logs due to their inverse proportionality, where:

$$\left(\frac{\mu s}{ft} * \ 10^{-6} = \frac{s}{ft}\right)$$

$$V = \left(\frac{1}{\frac{s}{ft}} = \frac{ft}{s}\right) * 0.3048 = \frac{m}{s}$$

The product of bulk density and velocity, together, defines acoustical impedance, a property discussed by many (Reynolds, 2011) as the simple parameter of reflection seismology.

$$I = \rho V$$

Differences and shifts in impedance produce seismic reflections. Assuming a lower (2) and upper (1) medium, we may calculate reflection coefficients, by:

$$R = \ (\rho_2 V_2 - \rho_1 V_1)/(\rho_2 V_2 + \rho_1 V_1)$$

Extracting a statistical wavelet from a certain time window within a range of CDP's produces frequencies typical of a specific range of reflection events Importing CM-60 to *Kingdom* allowed for the extraction of frequencies from 0.10 – 0.75 s TWT from a small range of CDP's. The extracted wavelet was applied to a synthetic seismogram, a trace generated by convolution of the extracted wavelet with the reflectivity time series. Since the Pensinger #1 well was drilled to the west of CM-60, events are expected to appear in well log and synthetic data below their corresponding reflection due to a general basinward (south, southwest) dip of Paleozoic strata. A reference datum (700 ft.) and replacement velocity (12,500 ft/s) were provided with the seismic volume and applied to this data set. The replacement velocity is empricial, based on a reasonable value for shallow bedrock in the region (Hauser, 2017, personal communication). The Pensinger #1 was logged from 235-6,785 ft. Therefore, applying the velocity to the unsampled upper 235 ft. provided an appropriate correction and positioning of the log.

Velocity analysis done by *Kingdom* provides corresponding TWT values (Figure 9). The same sequence of CDP's applied to wavelet extraction was displayed in a track alongside the well logs for direct correlation onto the seismic reflection data, CM-60 (Figure 9). The digitized and imported gamma ray log served as a simple correlation tool; discrepancies between formations in gamma ray logs are marked and easily distinguishable, particularly between shales and non-shales (Prothero, 2004). The Trenton reflection, typically a strong positive between two negative reflections (Watts, 2016, personal communication), served as the marker horizon for quality control on the well tie. Tops for the New Albany, Trenton, and Knox were easily identified through the well tie. Tops of the Eau Claire and Mt. Simon, however, were picked independent of the driller's log.

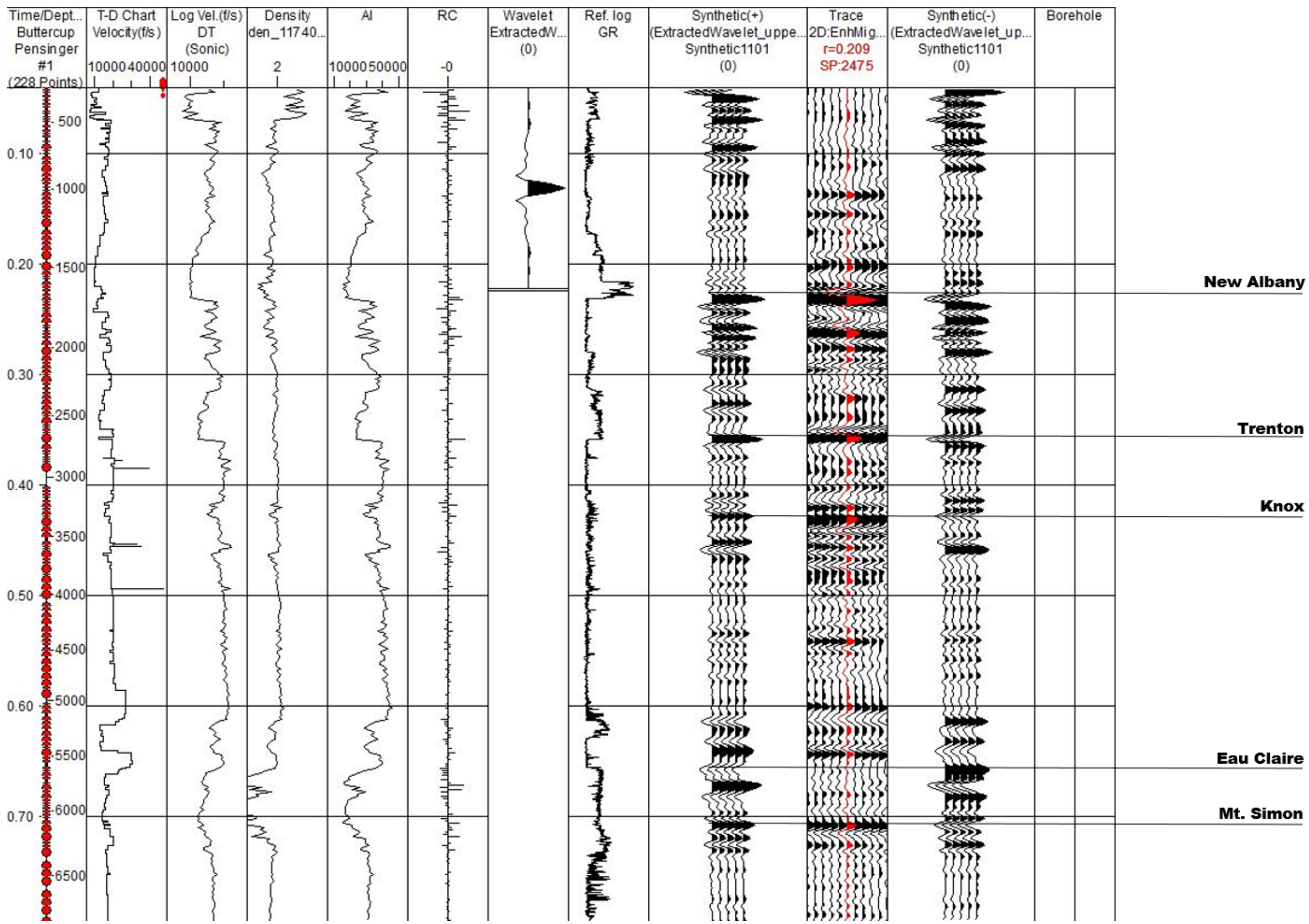

Figure 9 - Synthetic seismogram and well tie from Kingdom. Prominent Paleozoic reflectors are labeled. Wavelet for convolution with time series was extracted from CM-60 allowing projection into the seismic from the Pensinger #1.

Velocity changes typical of each formation did not correspond to their placement in depth and, thus, facilitated a more quantitative top pick. The top of the pre-Mt. Simon is not controlled by well data and its top was picked solely on reflective properties. The Pensinger #1 bottoms in the Mt. Simon and no well within and reasonable radius is available to correlate. Our pick is entirely qualitative, a problem faced and dealt with similarly by Bear et al. (1997). Since no known or available well control exists in west-central Indiana to constrain the top of the pre-Mt. Simon, the boundary was selected solely on seismic character. A basal conglomerate, likely an erosional remnant predating the primary Mt. Simon depositional episode (Wolfe et al., 1993), is reported at the type locality (Shrake et al., 1990) and may produce a positive reflection at the top of the pre-Mt. Simon stratigraphic package. These data, however, reveal higher continuity in an associated negative reflection at the Mt. Simon base. This negative event was selected due to its distribution across the data.

3.4 Data visualization

Schlumberger's *Petrel* was the primary interpretation software package utilized here. Migrated, binned SEG-Y data were entered and displayed in three-dimensional space, as a fence diagram. 3-D visualization allows for regional correlations to be made and to understand the broad structure and stratigraphic trends within the basin (Figure 10). Reflections were tracked and horizons picked with the 2-D guided autotracking tool. This utility allows certain events to be interpolated by amplitudes. Picks were refined with the manual autotracking tool, which allowed for correlation across a zone of variable amplitude. Adjacent positive wavelets, in some cases, skewed the autotrack and caused a mis-tie between CDP’s. The manual tracking tool was employed to precisely pick correlation points. Once initial horizon tracking was completed, fault traces were manually interpreted due to visible offsets and diffraction clusters. Diffractive zones typically displayed some evidence of offset; variability along a geological

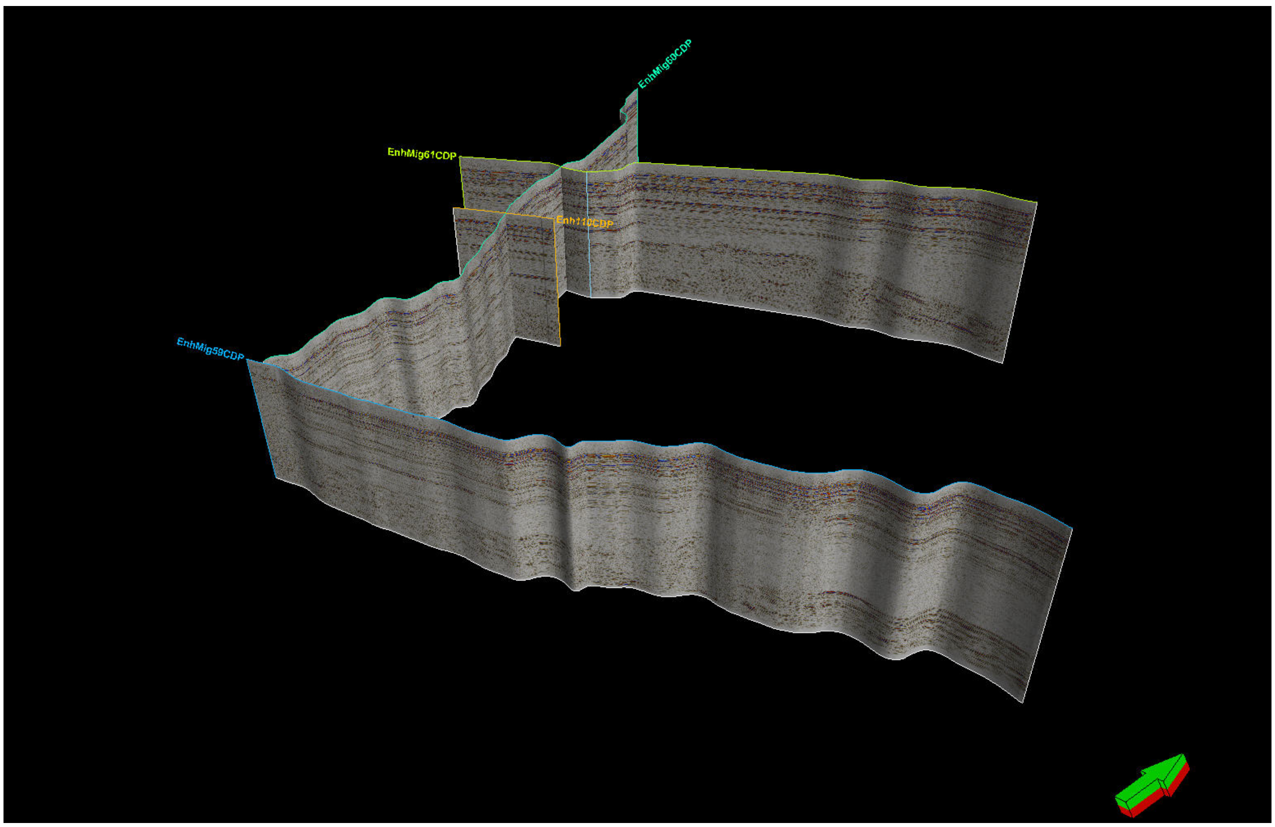

Figure 10 - 3-D view of 2-D seismic reflection data in Petrel. Note the inclination of the data with respect to north. Sections are binned into CDP's and, thus, are not identical with roadways. Refer to Figure 1 for scale.

surface, such as that produced by faulting, causes reflections to appear jumbled and discontinuous due to Fresnel zone effects.

Horizon tracking generally began on CM-59 where prominent reflections, especially those observed below ~1 s, are easily identifiable. Initial tracking along interfaces between three initially interpreted sequences of unique seismic character was followed by individual, internal reflection picking throughout the data set. The intersection between lines served as the correlation point and allowed horizons to be picked consistently in all four 2-D profiles (Figure 10). Although displaying wiggle traces is a utility offered in *Petrel* (Figure 11), data were initially analyzed in a bitmap scale of red (positive reflection) against blue (negative). Manual interpretation, for interpolating weak and discontinuous

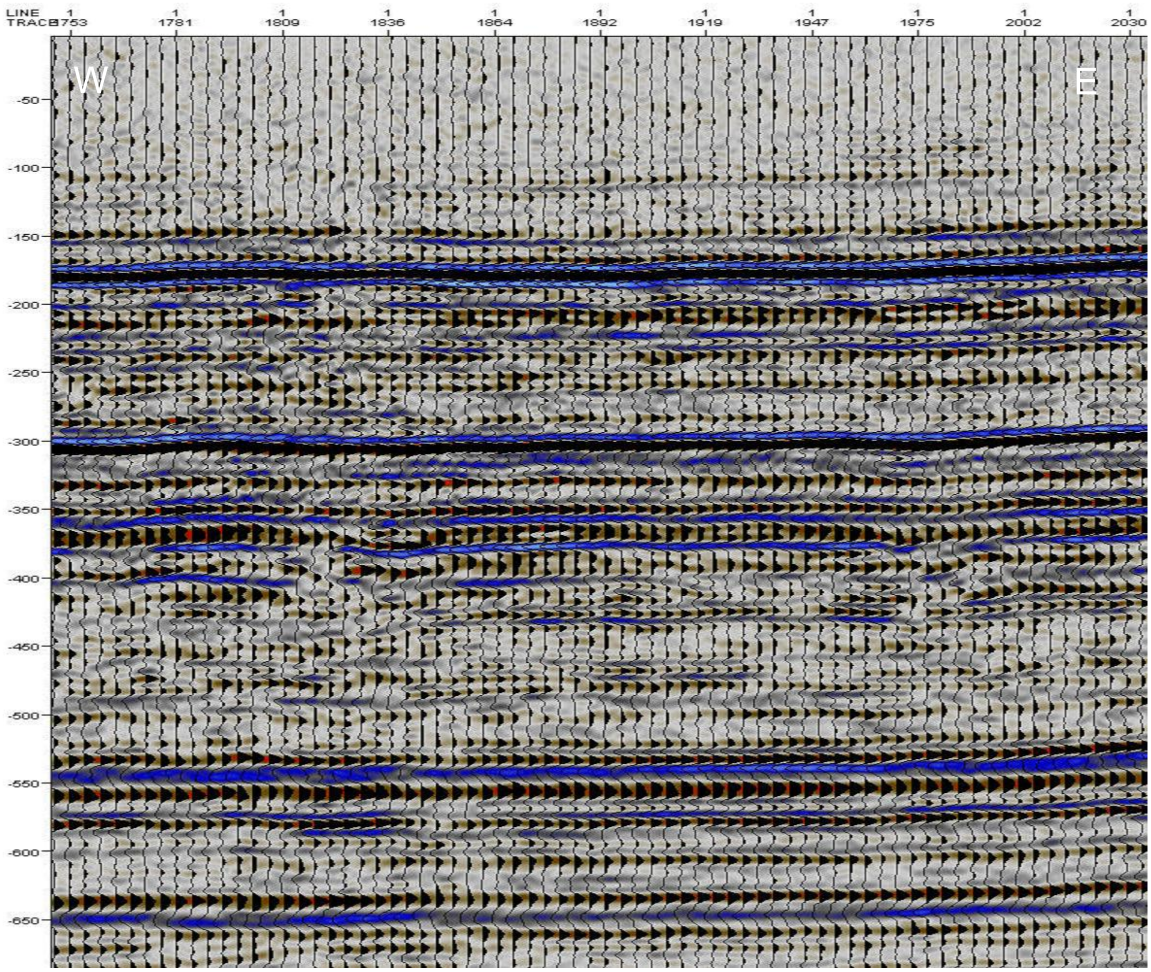

Figure 11 - Portion of CM-59 exhibiting both bitmap color scheme and wiggle traces. Positive reflections correspond with reds where negatives correspond with blue. Wiggle traces are useful in low amplitude regions of the seismic. Vertical axis is in TWT.

segments of reflections, utilized wiggle trace to pick true peaks and troughs. *GSEGYview*, freeware available for public download, provides a simple interface to display SEG-Y data. Variable area display on *GSEGYview* is not available in *Petrel.* Visualizing seismic data in *GSEGYview* helped amplify subtleties that were not apparent in *Petrel*. No horizon tracking utility is available in *GSEGYview.*

3.5 Potential field data

Availability and accessibility are two primary advantages of potential field data, both gravity and magnetic. Data are made available to the public by the United States Geological Survey (USGS) on their on-line database (United States Geological Survey, 2014; Figure 12A, B). Gravity data may be viewed as either isostatic or Bouguer; magnetic data are aeromagnetic. Station spacing is not specified by USGS and may be so coarse that small anomalies are aliased. Still, correlation between potential field data is permissible. The Pan American Center for Earth and Environmental Studies (PACES) at University of Texas at El Paso (UTEP) provides high-resolution regional geopotential data for public download (University of Texas at El Paso, 2013). Aeromagnetic data were collected through an air survey, flown at ~305 m altitude by a USGS geophysical team. Wavelengths of 500 km, or greater, were removed from the data before release. Gravity (Figure 13A, B) and aeromagnetic (Figure 14A, B) data were extracted from the site to construct regional anomaly maps. Data were extracted as a .csv file and opened in *Excel*. For gravity, Bouguer anomaly values and spatial coordinates (NAD83) were imported into ESRI's *ArcCatalog* to construct a geodatabase. The geodatabase was added as a layer, on top of a county base map, in *ArcMap*. Spatial geopotential data was then entered and contoured in *Surfer*, exported as a shapefile (.shp), and added as a layer in *ArcMap*. Kriging, a geostatistical interpolation method, is facilitated by *ArcMap*. This provides a shaded relief map to correlate with imported contour .shp data from *Surfer* and more satisfactory interpretation. Additionally, CountryMark donated high resolution aeromagnetic (HRAM) data (Figure 15A, B).

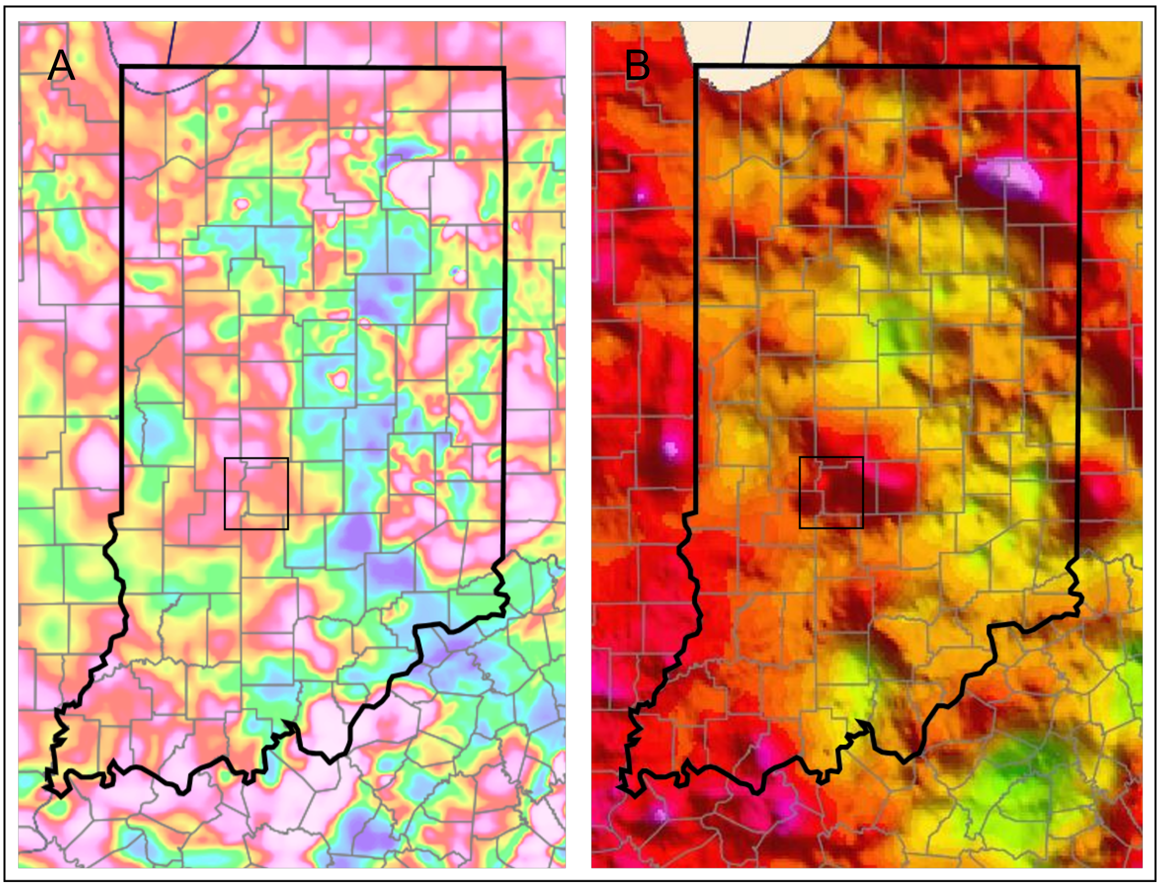

Figure 12 - A) regional aeromagnetic data provided by USGS (left); B) regional Bouguer gravity data provided by USGS (right). Seismic coverage is indicated by square centered over west-central Indiana.

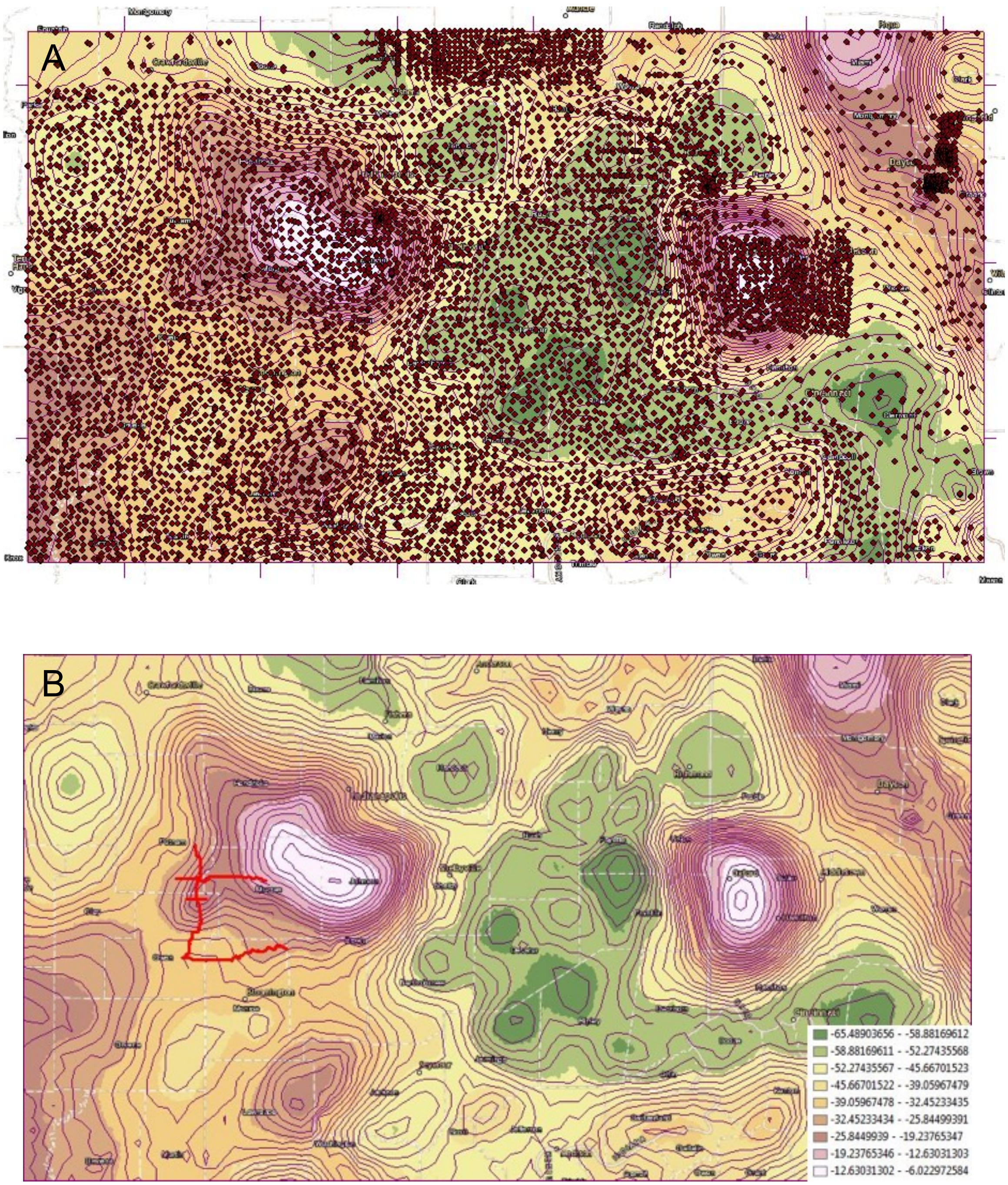

Figure 13 - A) Bouguer gravity stations compiled by UTEP PACES project (top); B) regional Bouguer anomaly map of southern Indiana and western Ohio (bottom). Seismic coverage is indicated by red survey lines. Note the broad low (green) below east-central Indiana and circular to ovoid positive anomalies (red to white) centered below Hamilton County, Ohio and Morgan County, Indiana.

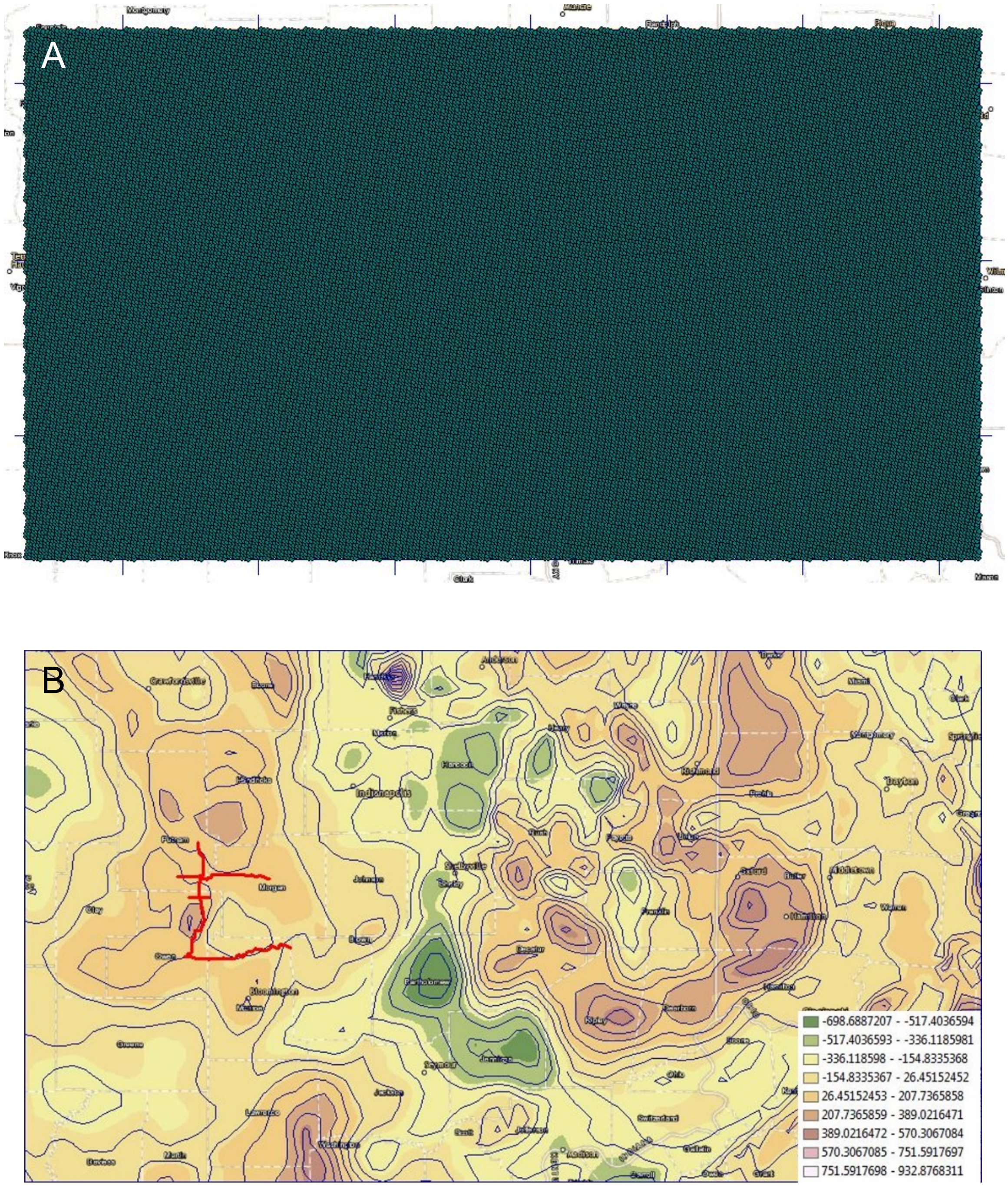

Figure 14 - A) Aeromagnetic stations compiled by UTEP PACES project (top); B) regional aeromagnetic anomaly map of southern Indiana and western Ohio (bottom). Aeromagnetic survey was flown by USGS at ~305 m altitude. Seismic coverage is indicated by red survey lines. Note the regional ring-shaped anomaly below eastern Indiana and western Ohio. A small positive anomaly is observable below northeast Owen County near the trace of CM-60.

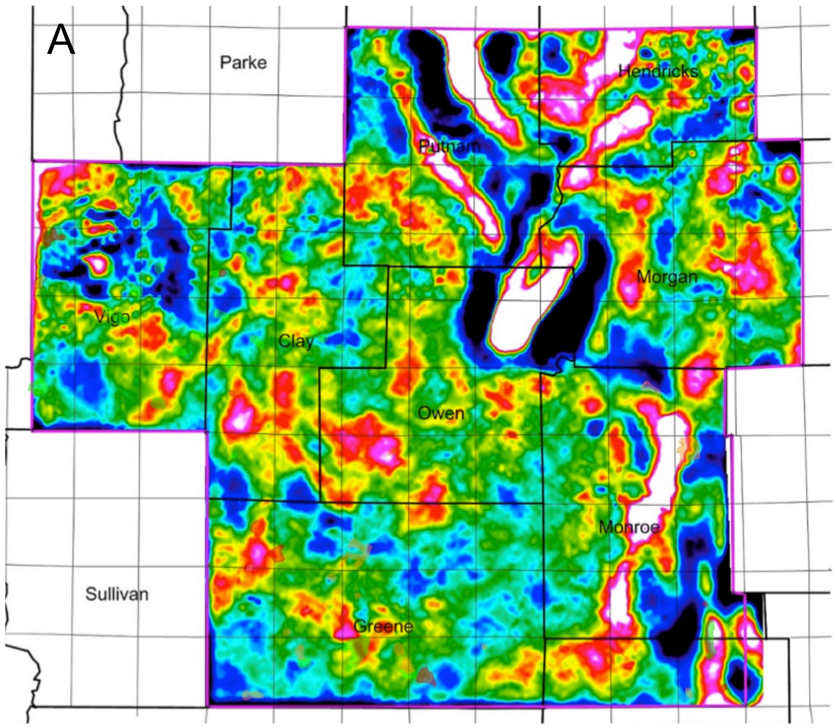

Figure 15 – A) Regional high-resolution aeromagnetic (HRAM) data supplied by CountryMark (top). Radial, linear anomalies to the north and subparallel high to the southeast display systematic distribution; B) local magnetic high centered below northeast Owen County, Indiana (right). Annotated seismic lines (CM-59, 60, and 61) by Walker (2015) indicate basement "highs."

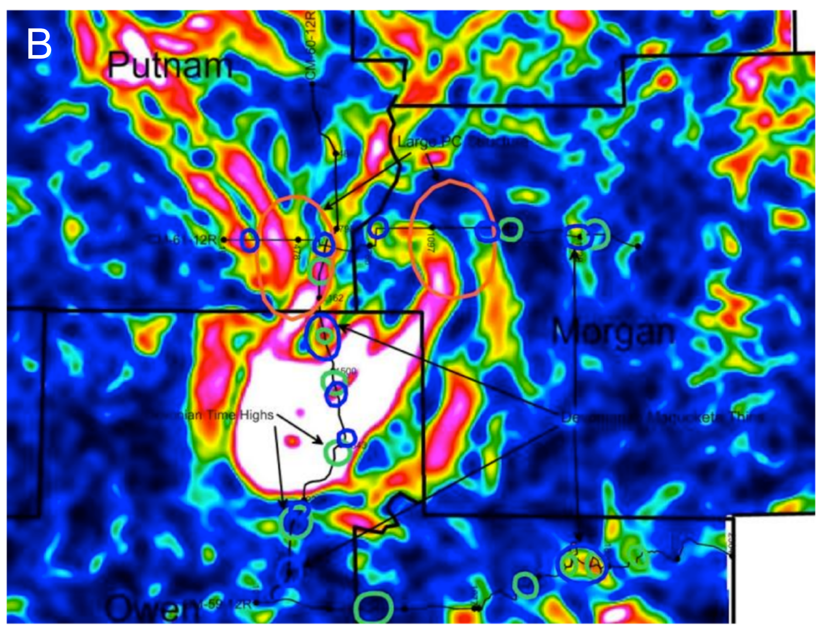

4. RESULTS

4.1 Seismic reflection

CM-110 data presented here were not migrated contrasting the post-stack migration performed on CM-59, 60, and 61 (Figure 8B). A major pitfall of 2-D seismic interpretation is the affect that out-of-plane migration artifacts have on the profile; that is, the incorporation of reflection events from positions adjacent to the actual survey into acquired and displayed data. The offset of these CDP's creates a cross-cutting phenomena through surrounding reflections in the profile and are, for the most part, readily identifiable. However, interpretations here assume that all reflection events aside from explicit artifacts are indeed in the plane. It is worth noting that some reflective packages and intervals may be a product of the migration of lateral events into our seismic section, making the interpretations described here subject to skepticism. Characteristics of each line will be reported along with our re-processed version of CM-59.

Marker horizons, such as the regionally negative New Albany and positive Mt. Simon tops, were picked on each section (Figure 16). Well data constrained the tops of the Eden (emerald on *Petrel* screen captures), Trenton (light red), Knox (gold), Eau Claire (pink), and Mt. Simon (violet) (Figure 16). The base of the Mt. Simon (lime) was identified based solely on seismic character, as was the top of a distinct basal sequence (red) discussed herein. Other prominent reflections within each of the formations identified above were tracked for structural and stratigraphic trends and are discussed as pre- or post- with respect to adjacent to well tied horizons. Offsets, discussed herein as faults, are described in a geologic context (normal, reverse, etc.).

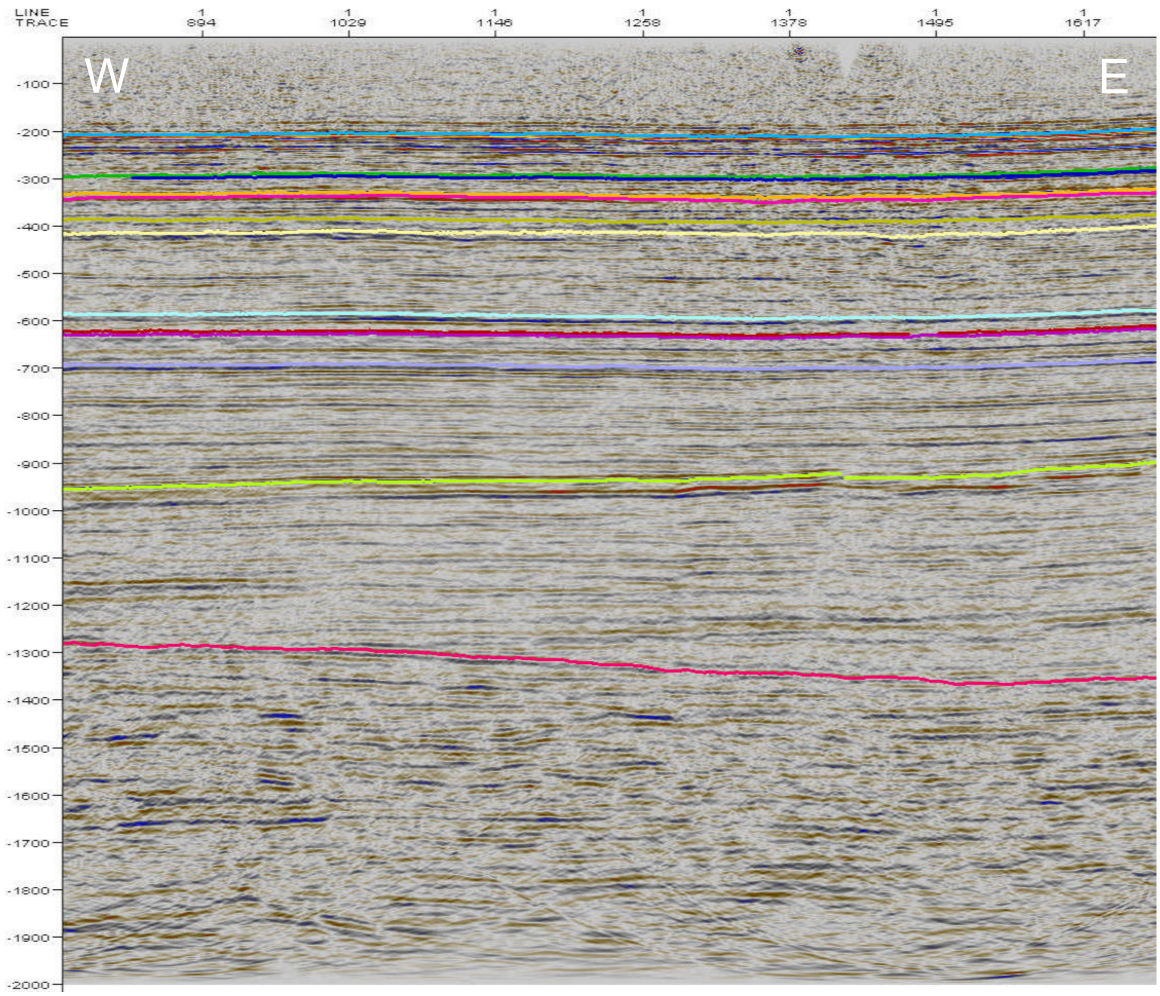

Figure 16 – Typical seismic stratigraphy interpreted through seismic coverage. Prominent internal reflections are picked along with basal pre-Mt. Simon reflective sequence (red), pre-Mt. Simon poorly reflective (lime), Mt. Simon (violet), Eau Claire (maroon), Knox (gold), Trenton (light red), Eden (emerald), and New Albany (cyan). Vertical axis is in TWT. Section is displayed ~1:1 @ 6 km/s.

4.1.1 CM-59 (industry processed)

CM-59 (Figure 17; Appendix 1) begins at the southeastern corner of Owen County and runs east to the northeastern corner along the eastern limit of Monroe County. Line geometry is fairly uneven and jagged to accommodate roadways along which the *Vibroseis* source could effectively navigate and induce signal. Several junctions of the line feature sharp bends that must be accounted for both in processing and interpretation of the data. The profile totals over 35 km and intersects the southern end of CM-60 in Spencer, Indiana.

The ends of the line, areas of low-fold coverage, are not interpreted here due to visible artifacts of processing that induce an over-correction to events. A well-stratified, reflective sequence is present in the first ~1 s TWT of the record. Broad, open folds typify this sequence and occur in a variety of apparent wavelengths. Reflections are continuous aside from a zone of major discontinuity, typical of complex faulting and analyzed here as such, that offset horizons and persist towards, and perhaps beyond, the base of the record from CDP ~3560-3830 (Figure 18). Shallow high-amplitude reflections display a shift from horizontal to the east to a west, down to basin, dip west of this diffractive zone. This feature is comprised of one master fault, which penetrates beyond the Eden, and appears to extend down to ~1.60 s TWT. The master fault appears listric. Three antithetic patterns also offset reflections and merge in an apparent asymptotic style with the master (Figure 19A). A small synthetic offset displaces a negative-positive couplet at ~0.33 s TWT (Figure 19B) The Eden reflector is offset by 20 ms by the master fault and the Mt. Simon exhibits throw of 13.56 ms.

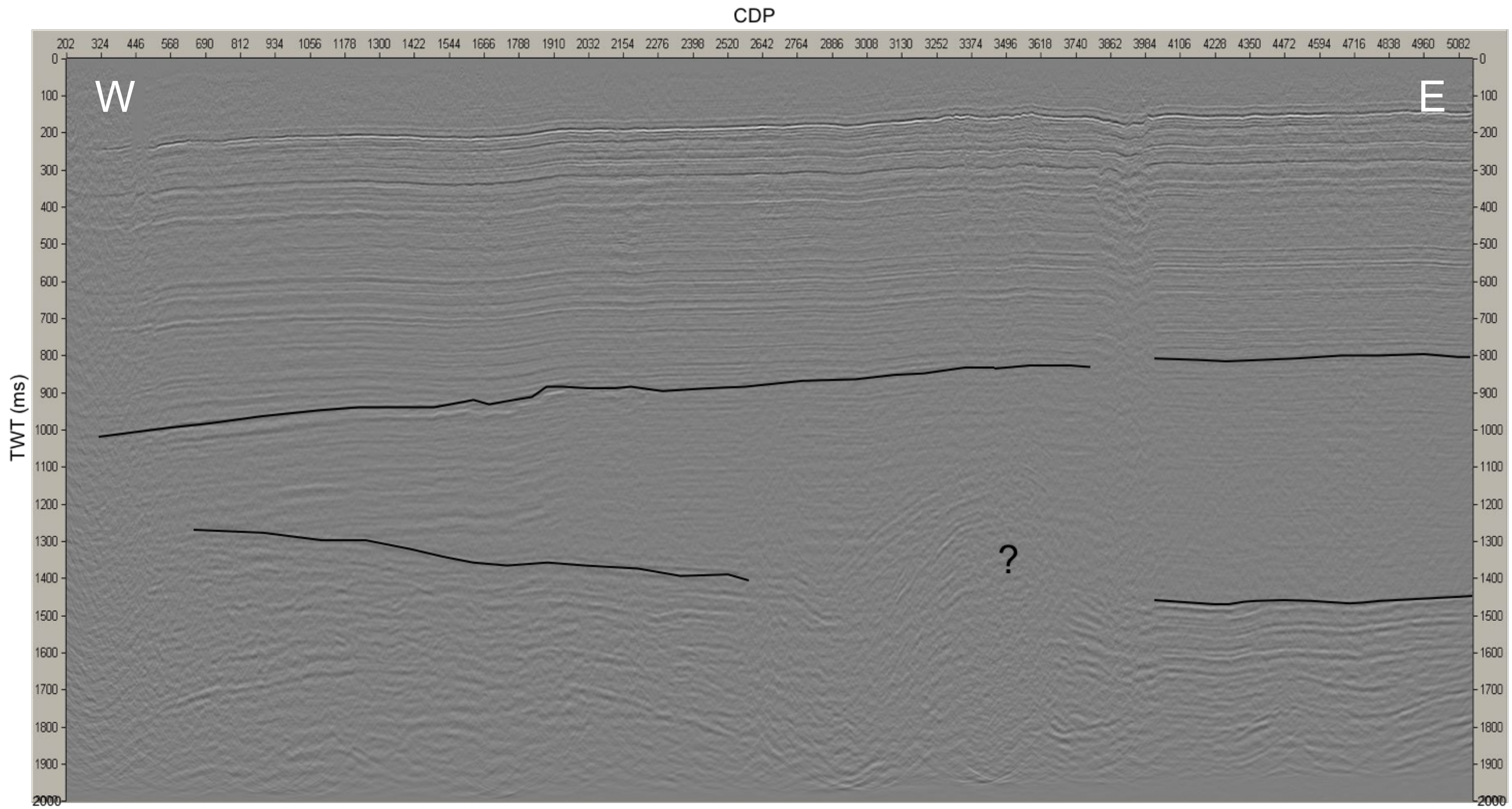

Figure 17 - CM-59 displayed in variable density in GSEGYview. Distinct pre-Mt. Simon seismic sequence tops are indicated. Note seismic contrasts between the poorly reflective upper sequence and the stratified, reflective basal unit. Section is displayed ~3:1 @ 6 km/s.

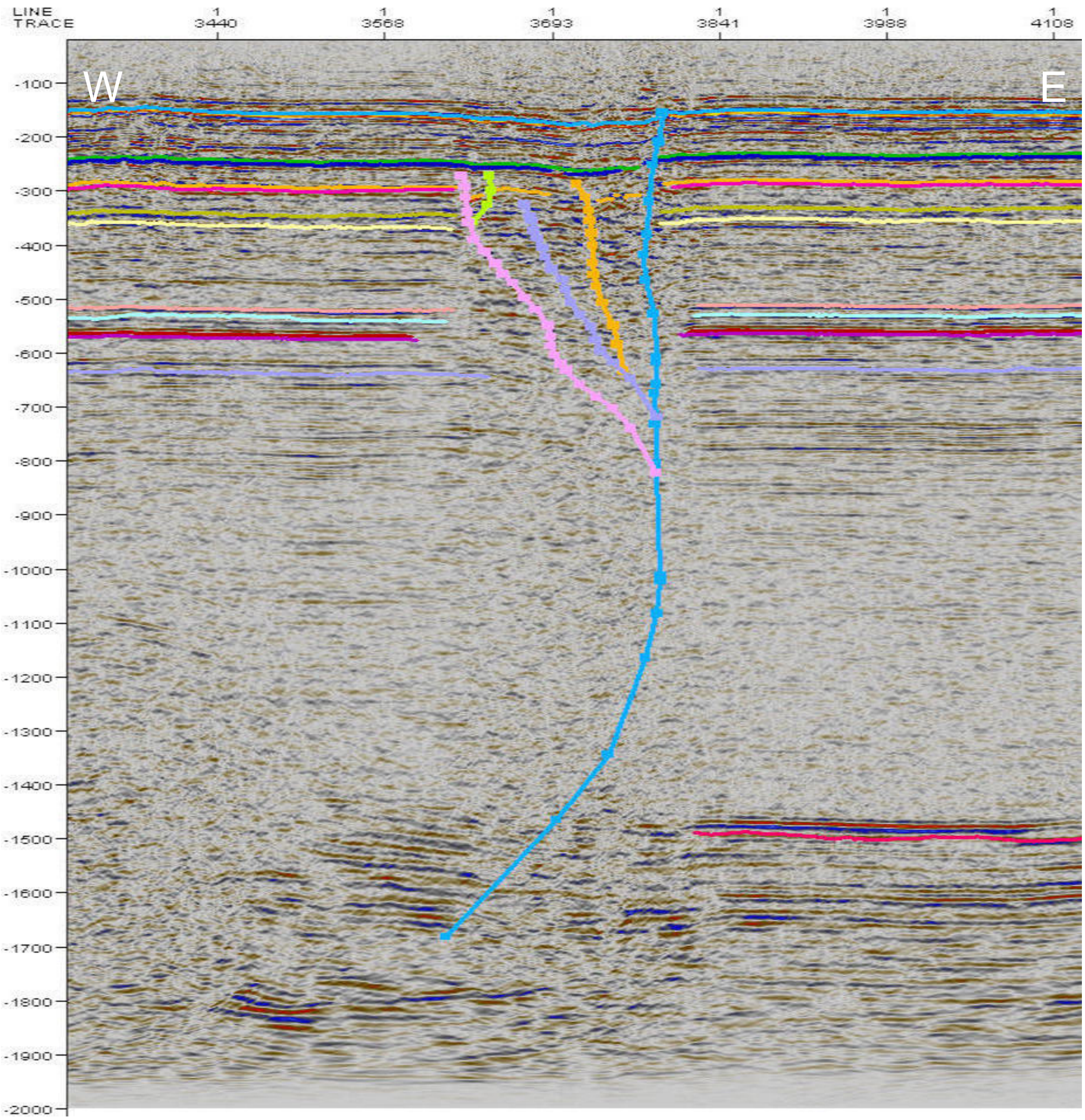

Figure 18 - Mt. Carmel fault zone (MCFZ) on CM-59. Discontinuity persists within a wide zone but observable normal offset in the basement (see Figure 19b) suggests a relatively vertical master fault. Section is displayed ~1:1 @ 6 km/s.

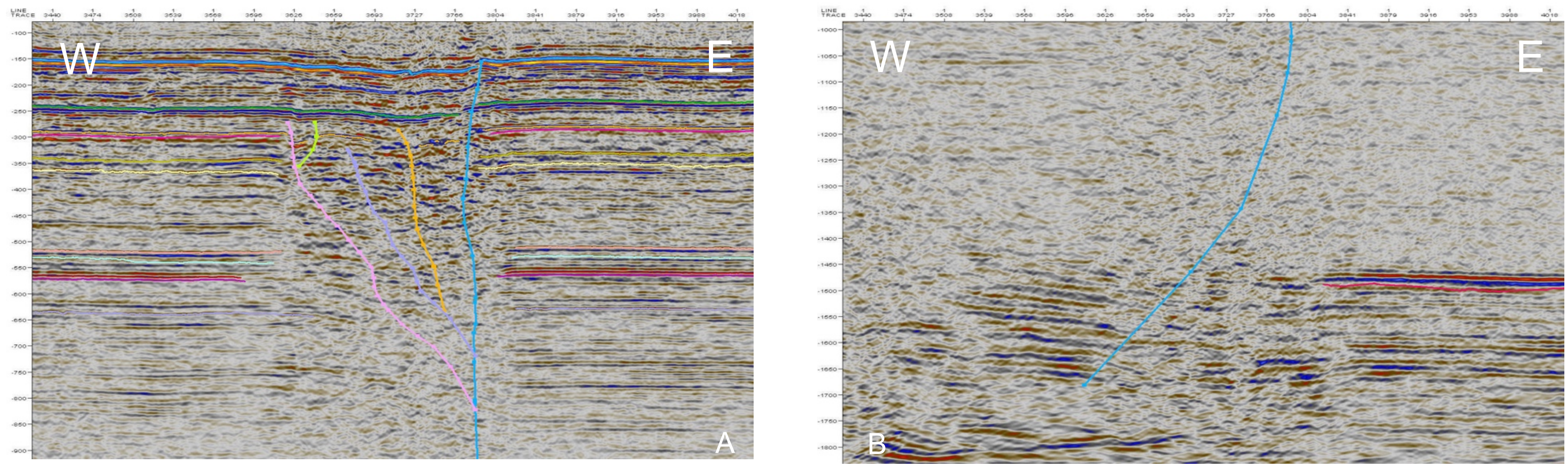

Figure 19 - A) upper "flower" of MCFZ offsetting Paleozoic reflections. Note the master fault (blue) offsetting beyond the New Albany (cyan). Three primary antithetic limbs contribute to deformation (left); B) interpreted MCFZ master fault root. Normal offset of reflection package (positive (sequence top)-negative-positive) indicates faulting. Change in dip to the west of the proposed fault base may link to the apparent structural high on CM-59 or indicate rotation in the hanging wall (right).

Antithetically faulted events exhibit much less displacement. Additional normal faulting, though down to the east, is interpreted to offset horizons into the Knox below CDP 270. Normal offset is apparent towards the base of the section, along with apparent hang wall block rotation (Figure 19b).

The Eden loses amplitude, considerably, west of CDP ~825. The Eden is again observable between CDP ~325-425. The Knox exhibits similar reflection style from east to west. In places east of the diffractions the wavelets briefly transition to double-lobed becoming more consistent to the west of the profile. The horizon appears depressed below CDP ~4465-4480. No adjacent reflections exhibit similar morphology directly above or below. The base of the Mt. Simon, and loosely interpreted top of the Precambrian, is easily distinguished as a positive reflection, likely due to the basal conglomerate of the package (Shrake, 1991; Shrake et al., 1991). This positive horizon, however, is not continuous throughout the seismic network. An overlying negative reflection was picked based on its continuity throughout the sections (Figure 20). A double-lobed positive reflection, juxtaposing two negative events, dips slightly west at the base of the Mt. Simon roughly continuous with the pre-Mt. Simon top pick (Figure 21). This feature is evident from CDP ~1980 to the profile limit. My interpretation of the pre-Mt. Simon record within the Illinois Basin stratigraphic succession is exclusive to this zone.

A poorly reflective unit which occurs from ~0.95-1.50 s TWT on the eastern limit of the line at its thickest underlies the basal Mt. Simon reflection. The unit contains multiple sporadic and discontinuous reflections of generally

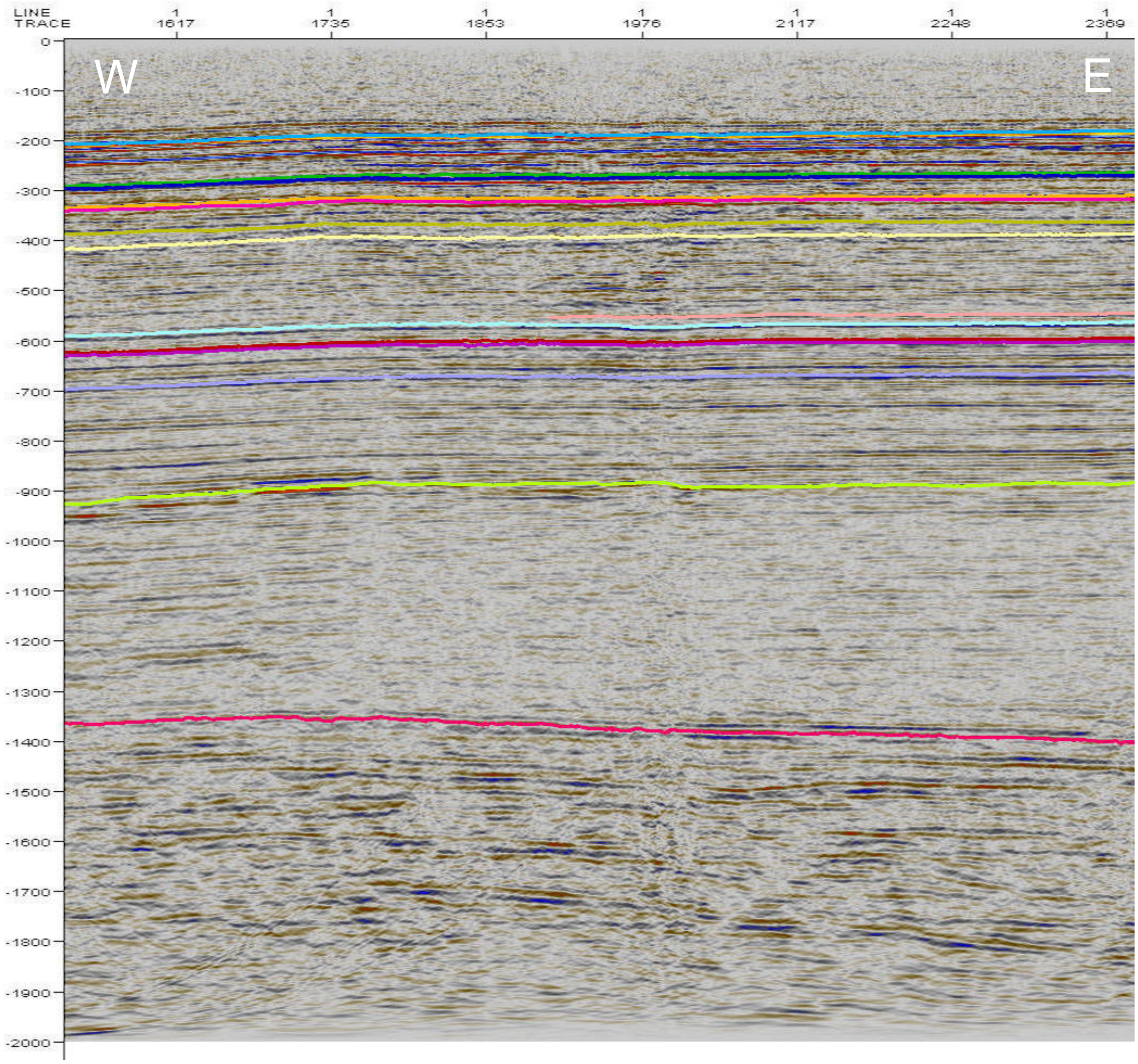

Figure 20 - Base of Mt. Simon (lime), ~910 ms, based on change in seismic character from reflective within the Mt. Simon (violet) to poorly reflective below. This upper pre-Mt. Simon sequence is comprised of discontinuous, weak reflections, some of which could be multiples. An underlying, well-reflective sequence is observed at the base of the record and throughout seismic data. Internal reflections of the poorly reflective package parallel those within the basal unit (Figure 17) Section is displayed ~1:1 @ 6 km/s.

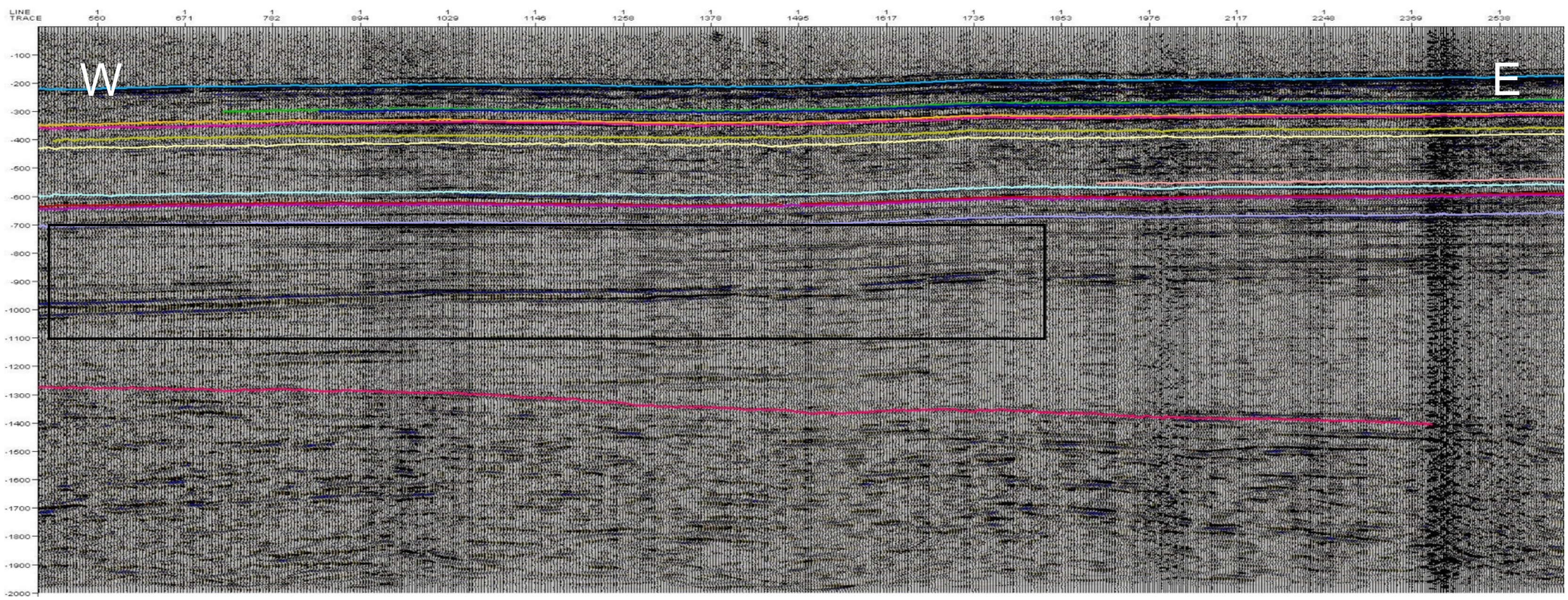

Figure 21 - Split positive reflection juxtaposing two negatives, including top of pre-Mt. Simon, on CM-59. The horizon dips slightly west in concordance with the overlying Paleozoic sequence but is discontinuous. A similar feature is observable on CM-61. Section is displayed ~1:1 @ 6 km/s.

weak amplitude. In a broad sense, this package is weakly reflective compared to the overlying Paleozoic sequence and underlying basement reflections. From the western limit of the profile, the zone thins markedly where it nearly terminates between the basal Mt. Simon and underlying reflections; the western limit is obscured due to the low-fold data of the western limit of the profile. Internal Mt. Simon reflections onlap the sequence (Figure 22) It appears to rest conformably upon the lowermost sequence. Conformable reflections are of low amplitude and appear to be overprinted by multiples, likely peg-leg, generated by the top of this pre-Mt. Simon sequence poorly reflective.

The basal portion of the record, which extends from the base of this poorly reflective sequence to the end of our record, is characterized by sub-horizontal, well-stratified, high-amplitude, discontinuous reflections. Migration artifacts, which appear as broad concave downward events through seismic data, are prevalent and easily identified within this sequence and are taken into account when interpreting data in a structural sense. Zones of internal reflections display stratal geometry that is discussed here in terms first introduced by Mitchum et al. (1977). Upper boundary toplap and basal onlap are visible in portions of this lowermost sequence and appear to form discontinuous wedges through the section. An apparent high, comprised of weak and sporadic reflections, is observable from CDP ~2740-3480 adjacent to the master fault that offsets reflections down to 1.70 s TWT. West of the discontinuous channel characteristic of the offset zone, reflections within the lower sequence transition to an apparent

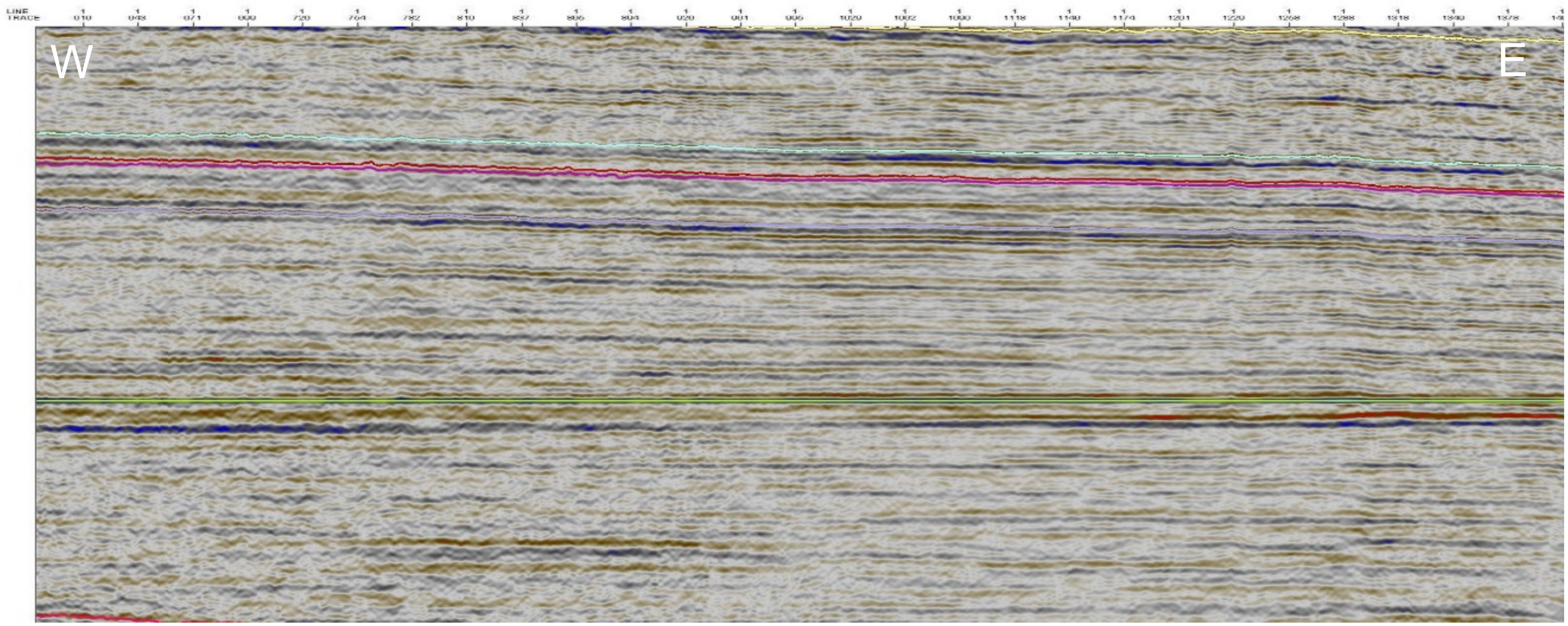

Figure 22 - Flattened top of upper pre-Mt. Simon (lime) sequence showing onlap of internal Mt. Simon reflections onto the boundary. Section is displayed ~1:1 @ 6 km/s.

eastward dip. An internal, convex upward, bowl-shaped negative horizon is centered below CDP 1030 between 1.67-1.70 s TWT (Figure 23). This lower reflective sequence shallows to the west where it appears to subcrop near the base of the Mt. Simon.

4.1.2 CM-59 (re-processed)

Re-processing of CM-59 (Figure 24) focused on amplifying deep reflection character, presumably of basement rocks, that may have been neglected in original processing due to Paleozoic focus. Deeper reflections are indeed more prominent after re-processing and appear far more continuous than those seen in the lowermost sequence in the original CM-59 section. The top of the poorly reflective sequence is resolvable and the uppermost sequence thickens to the west. Resolution of internal reflections of the upper two sequences, however, is poor and does not allow for robust interpretations. Only the uppermost reflections display similar continuity to those of the shallowest sequence observed in the industry processed data. The diffractions and structural high previously are not present, though discontinuity of the lowermost sequence between CDP ~2530-3440 spatially correlates with the convex upward structure observable in the industry processed section. Weak stratal relationships within the lowermost sequence exist within the basal sequence. The eastern base of the Mt. Simon appears much more coherent across the section. This boundary is not distinguishable east of the MCFZ on the industry processed stack.

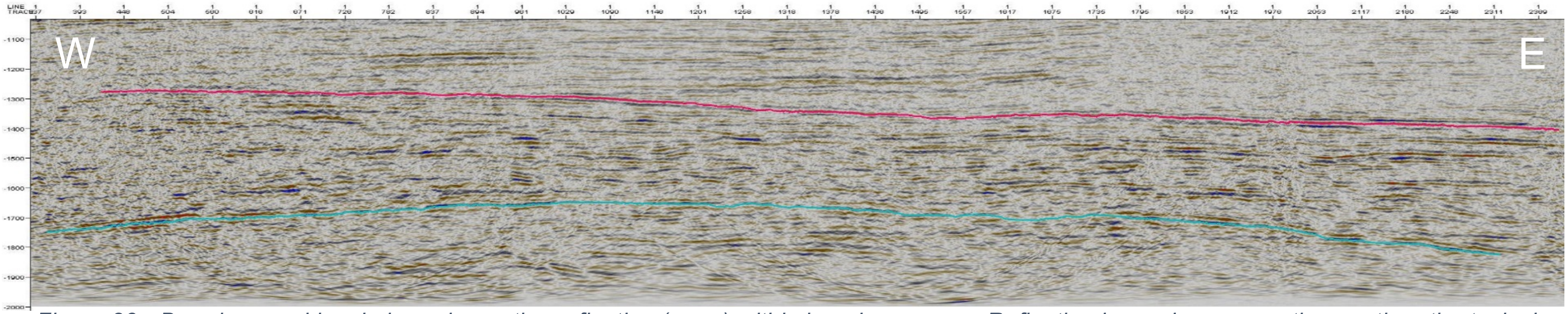

Figure 23 - Broad upward bowl-shaped negative reflection (aqua) within basal sequence. Reflection is much more continuous than the typical discontinuity seen within the unit. Section is displayed ~1:1 @ 6 km/s.

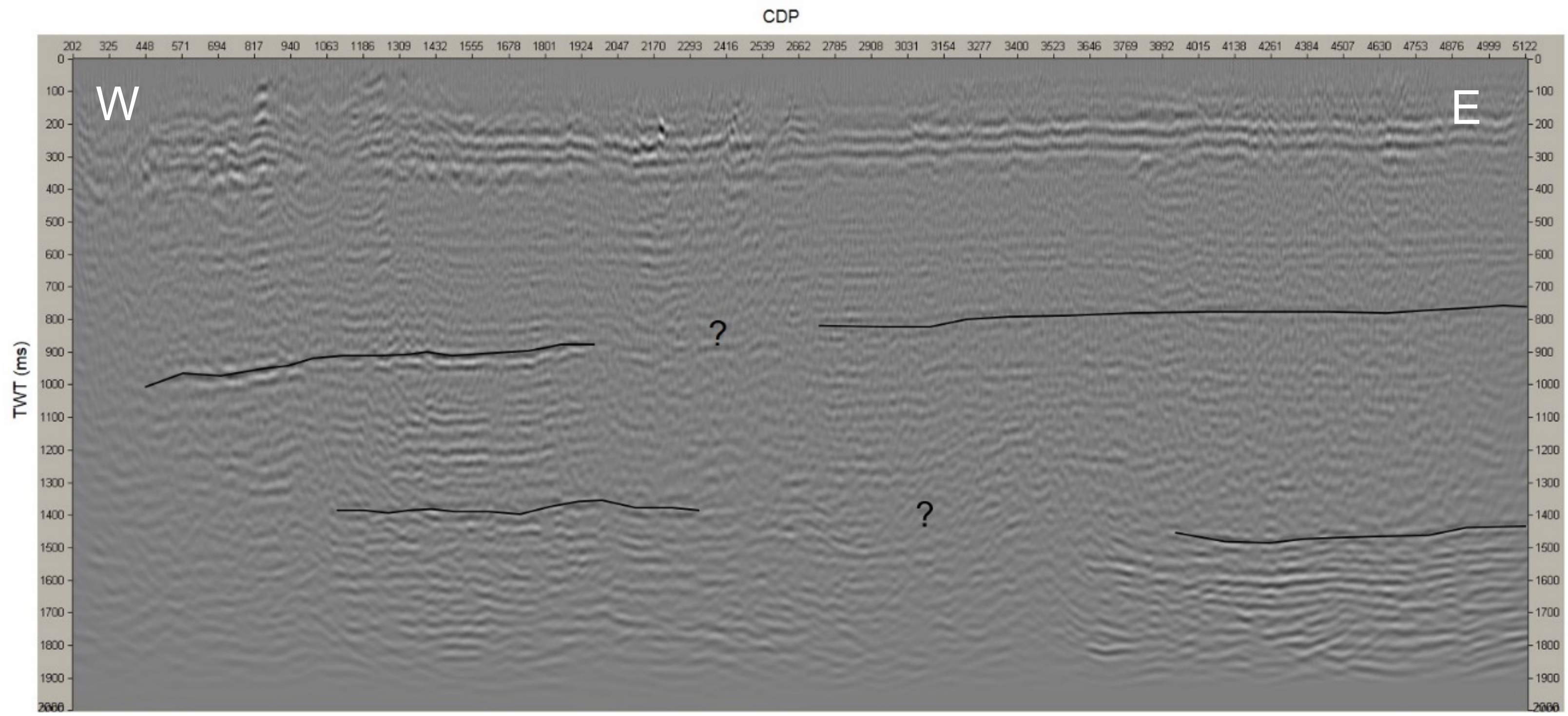

Figure 24 - Re-processed CM-59. Figure 8a summarizes processing steps. Revealing basement reflectivity was emphasized, thus, losing resolution in Paleozoic section. The interpreted base of the Mt. Simon (lime in Petrel sections) is interpreted here in the eastern portion of the stack. This horizon loses amplitude and is not tracked east of the MCFZ in seismic data processed by GeoConcepts, Inc. (Figure 8b). Top of the basal well reflective sequence is indicated. Section is displayed ~3:1 @ 6 km/s.

4.1.3 CM-60

The obvious regional structure and distribution of sequences seen in CM-59 is absent from CM-60 (Figure 25, Appendix 2). Reflections from the top of the record to the base exhibit relatively horizontal attitude though appear to thicken and deepen to the south. Initial horizon picking between the two east-west sections, CM-59 and 61, revealed an apparent dip to the south due to negative offset (lower position in time) in 59 reflections correlative to 61 events. The Eden reflector appears intermittent from CDP ~5075 north to ~3560 where it terminates. Knox reflections, both top and internal, shift between single and double-lobed.

A positive reflection at the base of a series of relatively continuous reflections below the Mt. Simon top overlies a zone of acoustic transparency correlative in time with the thinning portion observed in CM-59. The poorly reflective sequence is observable across CM-60 and exhibits relatively uniform thickness throughout with the exception of a thinned segment across a shallowing of the underlying, lowermost reflective package (Figure 26). The high-amplitude sequence appears well-stratified and horizontal; unlike CM-59, internal reflections display little complexity in total. Few intervals of the sequence emulate the baselap observed on CM-59.

Weak internal reflections of the pre-Mt. Simon are concordant with the top of the deeper reflective facies. Reflections of the basal sequence, which is topped by a discontinuous but high-amplitude event, shallow towards the base of the Mt. Simon between CDP 930-3350. The poorly reflective pre-Mt. Simon

Figure 25 – CM-60 displayed in variable density in GSEGYview. Distinct pre-Mt. Simon seismic sequence tops are indicated. Note seismic contrasts between the poorly reflective upper sequence and the stratified, reflective basal unit. Section is displayed ~3:1 @ 6 km/s.

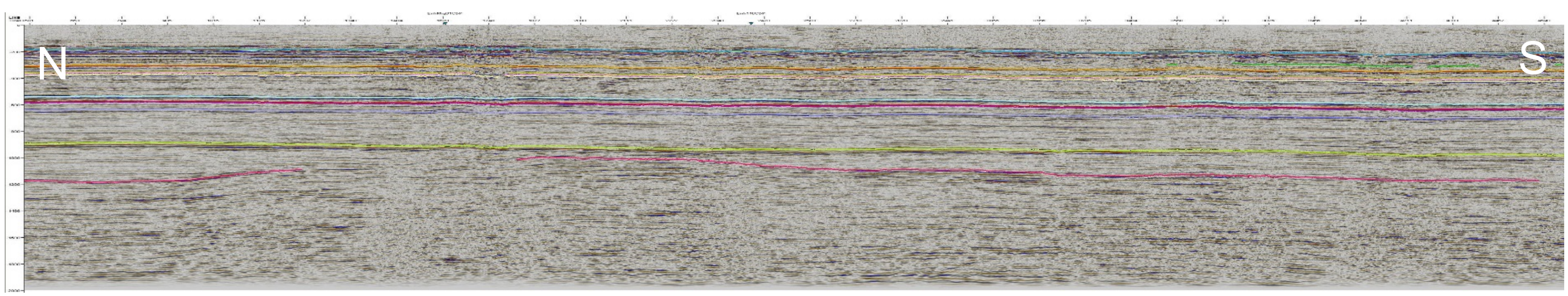

Figure 26 - Apparent structural high of basal sequence on CM-60. The overlying poorly reflective sequence thins markedly up to and across the high both to the east and west. Section is displayed ~1:1 @ 6 km/s.

sequence, correspondingly, thins across the interval; a positive internal reflection observable within this package continues across the peak of this apparent structural high. Reflections in the lower unit appear much more chaotic and diffractive with respect to other internal reflections across the sequence laterally. To the east, below CDP 4050-4950, a negative continuous event shallows and flattens westward.

4.1.4 CM-61

The uppermost sequence of reflections thickens to the west, similar to CM-59, though no major fault-related discontinuities interrupt the continuity of the events across the section (Figure 27, Appendix 3). The sequence exhibits broad, open folding across the section. These features do not offset the continuous Post-Knox reflector. High-amplitude reflections at the top of the Knox are continuous but chaotic, shifting between single- and double-lobed character. This creates undulation of horizon picks across the section. Reflection splitting is also evident in the Mt. Simon reflector. Similar to CM-59, a split positive reflection bounded by two strong negative horizons at the apparent base of the Mt. Simon and dips gently west from CDP ~1630 to the edge of the section.

The sequence of low reflectivity appears much thicker to the east in this profile but thins considerably to the western limit of the section. The basal reflective package shallows westward in compensation to the thinning transparent unit. The topography expressed by the lower sequence appears more complex and undulatory than that observed on CM-59. Two convex upward

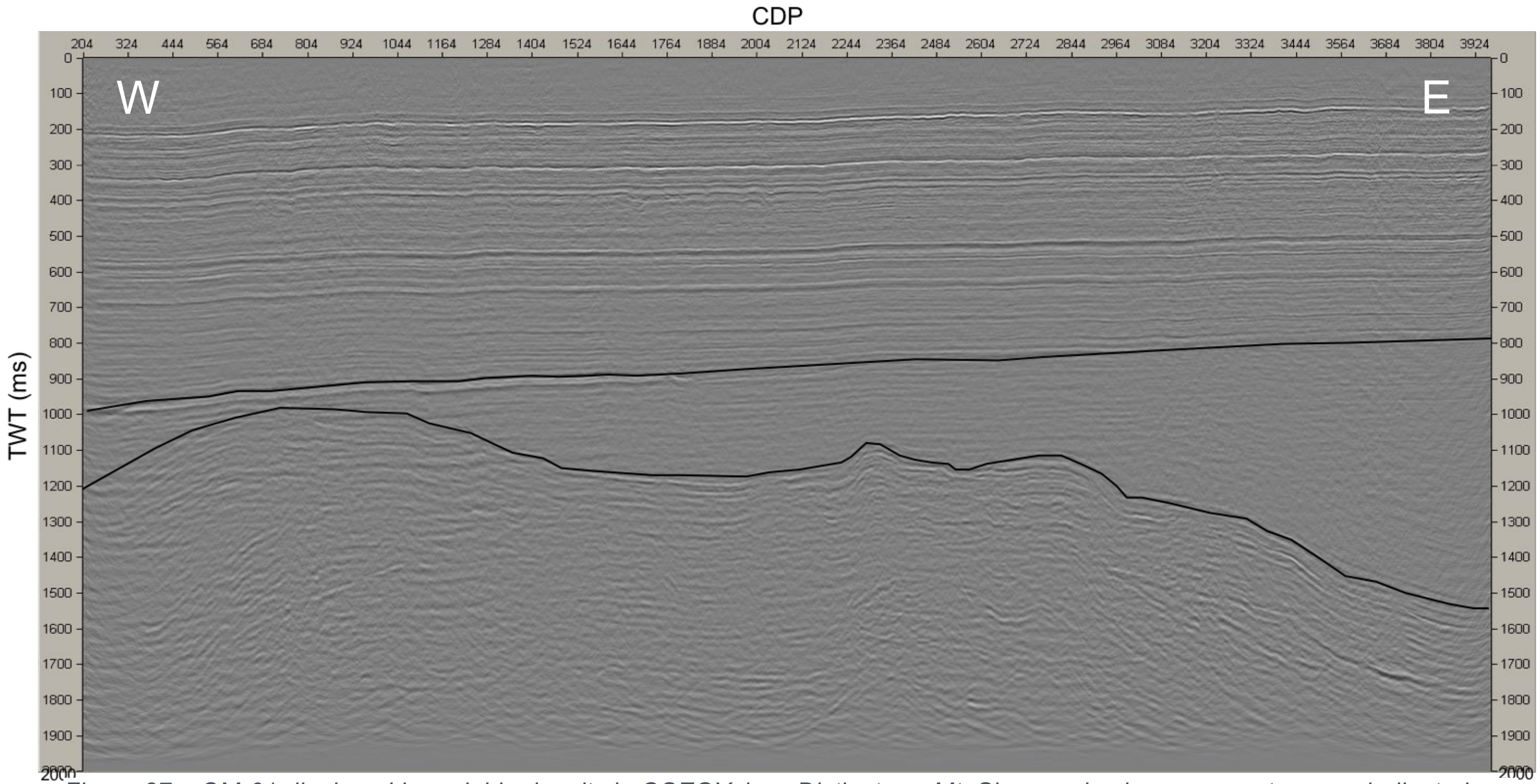

Figure 27 – CM-61 displayed in variable density in GSEGYview. Distinct pre-Mt. Simon seismic sequence tops are indicated. Note seismic contrasts between the poorly reflective upper sequence and the stratified, reflective basal unit. Poorly-developed internal reflections of the poorly reflective sequence parallel those of the basal package. This especially apparent below the eastern edge of the section where apparent multiples overprint the reflections. Section is displayed ~3:1 @ 6 km/s.

structures exist in this sequence, cutting up through the overlying acoustically transparent interval (Figure 28). The weak reflections present within the overlying package appear concordant with the top of the basal sequence in places while onlapping in others. Unlike the convex upward structure observed on CM-59 reflectivity is well-preserved in the zone and events remain continuous. The high-amplitude horizon picked as the top of the unit is continuous across the section and internal reflections are generally of well-defined reflectivity. Internal Trenton reflections exhibit enhanced reflectivity above these features. Similar relationships, those of onlap, toplap, and erosional truncations, as evidenced in the lowermost sequence of CM-59 are present on -61 (Figure 29).

4.1.5 CM-110

CM-110 (Figure 30, Appendix 4) was incorporated to constrain deep reflections in the center of CM-60 where coverage from bisecting lines is absent. Reflections of CM-60 were correlated for horizon picks. Reflections in the upper portion of the section are continuous and exhibit westward thickening, similar to that seen in east-west lines CM-59 and- 61. The poorly reflective sequence underlying the shallow reflective package thins considerably from east to west. The basal reflective unit, as observed in CM-59 and -61, shallows and nearly abuts the base of the Mt. Simon. Weak internal reflections of the overlying sequence appear to terminate against the top of the basal unit. Below CDP 350, the top of the basal seismic sequence appears offset in a normal, down to the east sense.

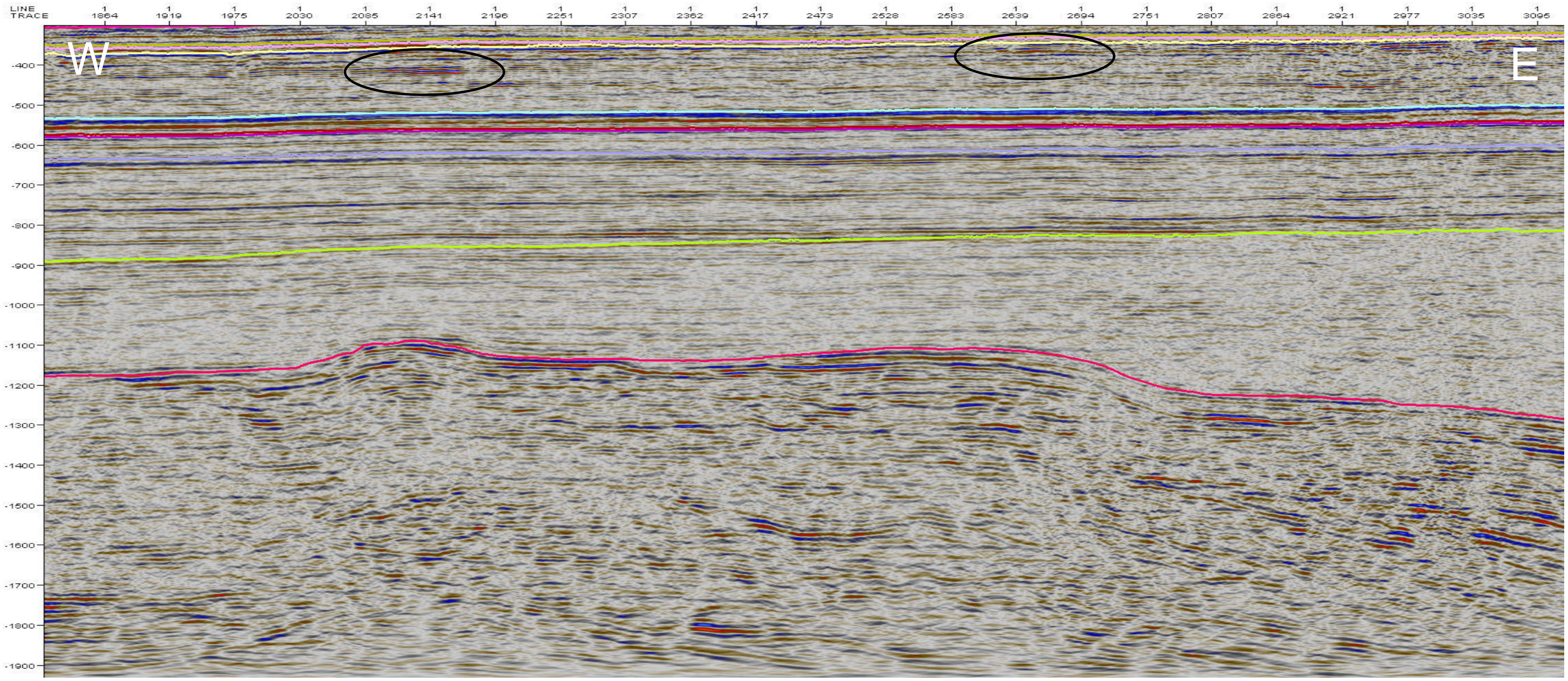

Figure 28 - Structural highs of the basal sequence on CM-61. Zones of enhanced reflectivity are located above these features and may have been controlled geologically by basement highs. Section is displayed ~1:1 @ 6 km/s.

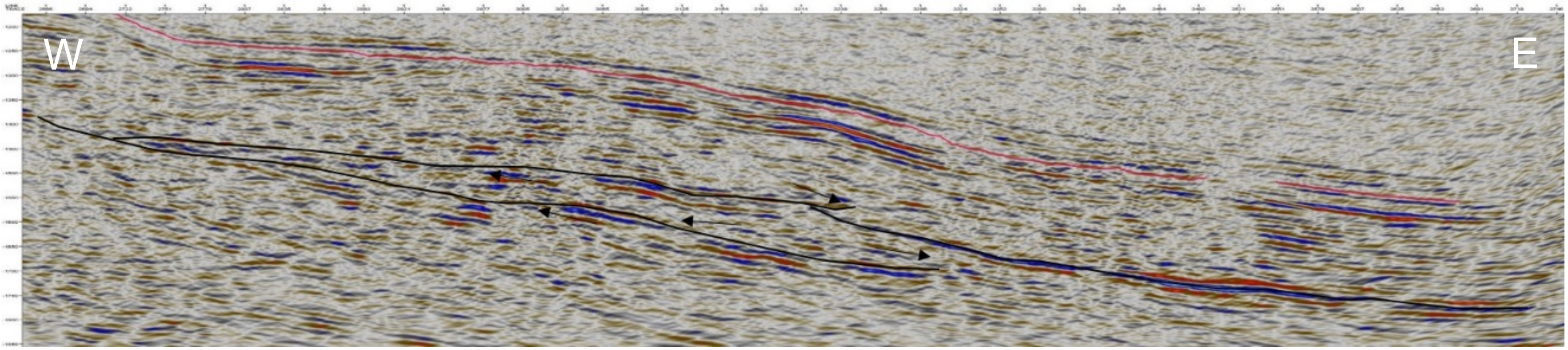

Figure 29 - Subsequence within the basal unit exhibiting stratal geometries indicative of deposition. Other discontinuous, complex sequences are observed in CM-59 and 61. Section is displayed ~1:1 @ 6 km/s.

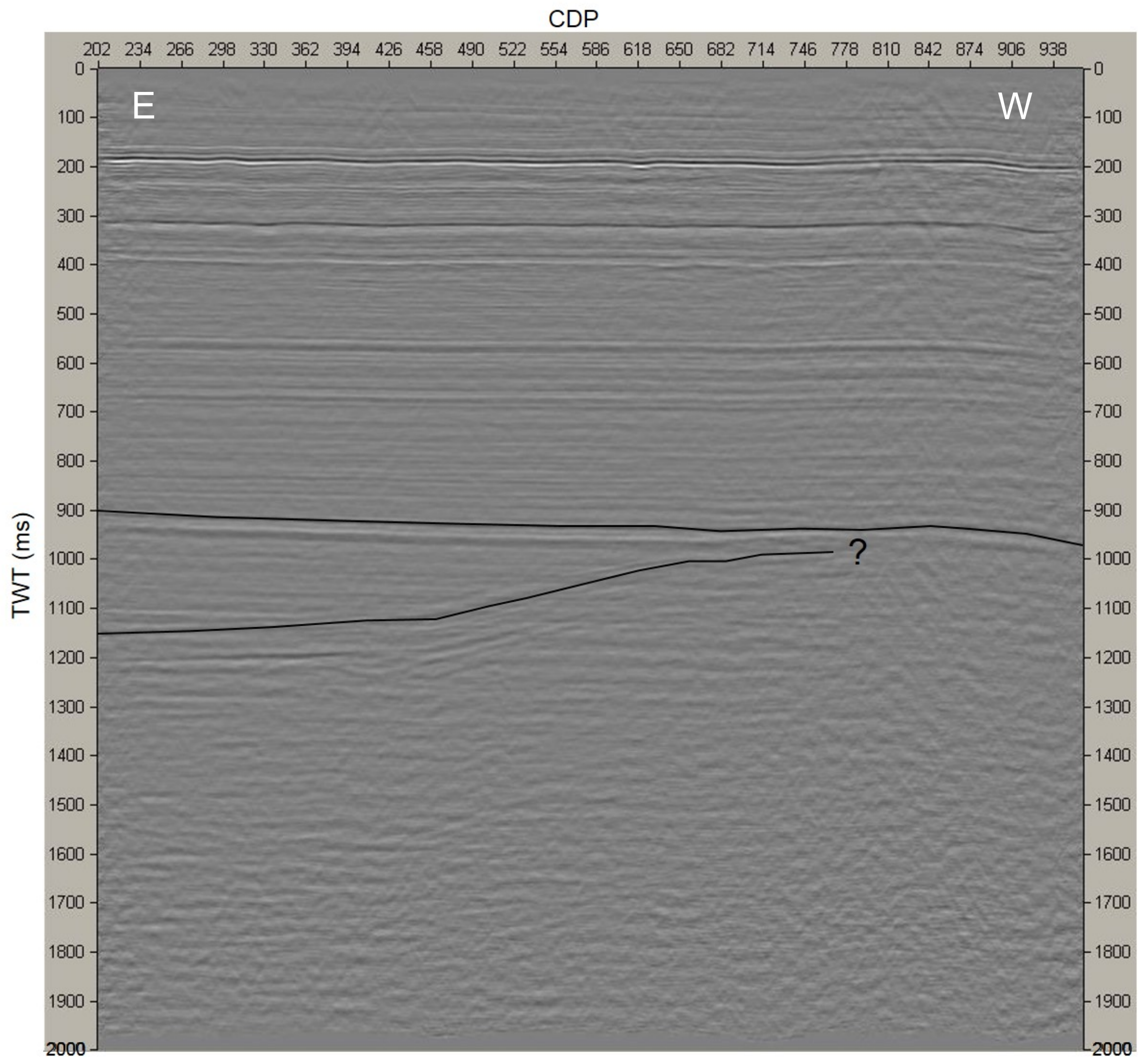

Figure 30 – CM-110 displayed in variable density in GSEGYview. Distinct pre-Mt. Simon seismic sequence tops are indicated. Note seismic contrasts between the poorly reflective upper sequence and the stratified, reflective basal unit. Section is displayed ~1:1 @ 6 km/s.

4.2 Potential field

4.2.1 Bouguer gravity

Bouguer gravity data across southern Indiana display a relatively gentle gradient across the region (Figure 13B). The region is characterized by relatively low Bouguer anomalies with sporadic highs showing no systematic distribution. Gravity increases from east to west across the state, towards the depocenter of the Illinois Basin. A broad gravitational low, low-amplitude, long wavelength anomaly extends from western Ohio and northwestern Kentucky into eastern Indiana. Ovoid to circular anomalies are centered below northwestern Decatur, northwestern Ripley, and northeastern Jennings, and the boundary between Fayette and Franklin Counties. High-amplitude, short wavelength gravitational highs below Hamilton County, Ohio and Morgan County, Indiana flank the broad, regional low of southern Indiana. An additional isolated high is produced below Lawrence County, Indiana. The gravitational high below Morgan County extends to the southeast through Johnson County and to the northwest to Hendricks County and likely beyond. An adjacent high, centered below the intersection of Morgan, Putnam, and Owen Counties, corresponds with the shallowing of the well-reflective sequence observed in CM-60, -61, and -110. A high wavelength anomaly to the southwest of seismic coverage continues beyond the area of coverage.

4.2.2 Aeromagnetics

A regional ring-shaped anomaly is observable below southeastern Indiana into western Ohio. Isolated peaks below eastern Ripley County, Indiana, and western Hamilton County, Ohio yield signatures of 472.2, 487.2, and 521.8 nT and are flanked by magnetic low (-702.5 nT) centered below Columbus, Indiana. These anomalies collectively form a regional ring-shaped anomaly. High magnetism continues east near Middletown, Ohio, adjacent to the ODNR-1-88 seismic transect. A broad, regional low flanks the western edge of the ring. Overall, southern Indiana produces a relatively high regional signature (Figure 14B). Northwestern Washington and southeastern Lawrence County are underlain by a magnetic high trending, roughly, north-south. Near the gravitational high correlative with the intersection of CM-60 with CM-61 and -110 is a local northeast-trending magnetic high in the northeast corner of Owen County. This anomaly is located south of CM-110 and west of CM-60 which traverses along the eastern margin of the feature. Associated radial, elongate magnetic highs to the north of the Owen anomaly are resolved in HRAM data (Figure 15A, B). Flanking minima, not observed on USGS or UTEP data, bound the anomaly to the northwest and southeast (Figure 15B). A morphologically similar anomaly to the radial highs trends roughly north-south through eastern Monroe County and across CM-59. This anomaly is not accompanied by flanking minima.

5. DISCUSSION

These data are interpreted in a regional geologic framework. Subsequent sections will detail various interpretations of crustal evolution incorporating all geophysical data previously discussed. I will first define each pre-Mt. Simon seismic sequence based on definitive intrinsic properties. The Paleozoic section will not be re-defined due to its distinct seismic character and geophysical and geologic correlation from Pensinger #1 well logs (Figure 9) and reports. Geologic interpretations will then be discussed in the context of these sequences.

5.1 Seismic sequence nomenclature

5.1.1 Wilbur sequence

The poorly reflective sequence underlying the Mt. Simon is termed here the Wilbur sequence for the location of its thickest presence, on CM-61 (Figure 27, Appendix 3), below the town of Wilbur, Indiana. Internal reflections parallel the underlying reflective package and are overprinted, in places, by multiples derived from various intervals within the Paleozoic. Peg-leg multiples from the strong basal reflector overlying the Wilbur towards the western edges of CM-59 and -61 produce apparent onlap with the top of the underlying reflections (Figure 21). Aside from acoustic transparency, the Wilbur is typified by marked westward thinning across west-central Indiana accompanied by shallowing of the underlying sequence and thickening of the Paleozoic (Figure 15, 27, 30; Appendix 1, 3, 4). Deformation within the sequence, primarily within the MCFZ (Figure 18), is not well-imaged due to the poor reflective properties of the unit. Reflections do, however, terminate in an apparent angular unconformity against the inferred base of the Mt. Simon. This is especially evident at the eastern edge of CM-61 where Wilbur reflections dip steeply east, conformable with inclined underlying reflections (Figure 27, Appendix 3).

A lack of reflectivity suggests homogenous geologic composition. This sequence resembles the seismic facies which aided Middle Run definition at its type locality (Shrake et al., 1990; Shrake, 1991; Drahovzal et al., 1992; Figure 3) in Warren County, Ohio, due east of seismic coverage presented here. Other midcontinent seismic data (Wolfe et al., 1993; Drahovzal, 1997; Richard et al., 1997; Baranoski et al., 2009; Peterman, 2016) have also been interpreted to image the Middle Run seismic facies. The relatively homogenous lithic arenitic composition of the Middle Run (Shrake et al., 1990; Shrake, 1991; Shrake et al., 1991; Drahovzal et al., 1992; Harris, 1992) may generate low reflectivity. Interbedded shales and siltstones, reported from core at the type locality, may cause the intermittent, discontinuous reflections within the sequence. Basalts and other volcanics, locally associated with the Middle Run (Drahovzal et al., 1992; Drahovzal, 1997) may also produce reflections of higher amplitude. The strong, split positive reflection observed at the base of the Mt. Simon, top of the Wilbur sequence (Figure 21), is interpreted as a volcanic flow or sill due to its seismic character, multiple production, and local distribution. Dawson (1960) reported basalt in what he interpreted as the Mt. Simon from the Lawrence County deep well, though core descriptions suggest the presence of the Middle Run and, thus, its associated volcanic component.

5.1.2 Quincy sequence

Stratified, discontinuous, high-amplitude reflections characterize the base of the seismic record interpreted here. This unit is termed the Quincy sequence due its subcrop below Quincy, Indiana imaged by CM-110 (Figure 30, Appendix 4). The Quincy shallows nearly 0.60 s to the west. Reflections towards the top of the sequence are relatively continuous across the section. Internal reflections exhibit complex stratal geometries (Figure 29). Several discontinuous yet observable unconformity-bounded sequences, discussed here as subsequences, comprise the Quincy. These subsequences are observed, primarily, on CM-59 and -61. Subsequence tops and bases are relatively continuous opposed to the discontinuous occurrence of internal baselapping reflections. In contrast to the overlying Paleozoic sequence, the Quincy appears structurally complex in addition to its stratigraphic intricacies (Figure 23, 26, 28). Parallel reflections within the Wilbur suggest a Quincy-controlled structural grain was removed by erosion predating Mt. Simon deposition. Both broad structural highs, such as that imaged to the apparent west of the MCFZ, and local highs, as observed on CM-61, characterize the morphology of the package. Apparent three-way closure of the sequence is imaged where the Quincy on CM-60 shallows to the north and is crossed by both CM-61 and -110 (Figure 31). The sequence appears to begin to thicken west of the structural high imaged by CM-61, facilitating the interpretation of a previously unmapped structural dome.

Pre-Mt. Simon reflectivity has been widely reported in midcontinent seismic surveys (Sexton et al., 1986; Allmendinger, 1987; Pratt et al. 1989; Cannon et al. 1991; Drahovzal et al. 1992; Pratt et al. 1992; Hauser, 1993; Heigold and Kolata, 1993; Wolfe et al., 1993; Leighton, 1996; Bear et al, 1997; Drahovzal, 1997; Potter et al., 1997; Richard et al., 1997; McBride and Kolata, 1999; McBride et al., 2003; Okure, 2005; Baranoski et al., 2009; McBride et al., 2014; McBride et al., 2016; Peterman, 2016). Pratt et al. (1992) broadly termed the Centralia Sequence as the reflective sequence underlying the Phanerozoic cover of the midcontinent (Figure 4). Ground truth with core in Illinois enabled the initial correlation of the Centralia with the EGRP although it has been interpreted that the Centralia may represent depositional lithologies (Pratt et al., 1992; McBride and Kolata, 1999; Baranoski et al., 2009). I avoid this terminology due to the lack of a geologic analog in west-central Indiana, though the correlation of reflections below Illinois with those presented here may be permissible.

Seismic stratigraphic relationships such as those first discussed by Mitchum et al. (1977) within the Quincy suggest, at least in part, a depositional origin. A similar interpretation was made by McBride et al. (2003) in naming the Enterprise subsequence below central Illinois (Figure 5). The relationship of this stratigraphic package with the EGRP and Middle Run is unknown. Volcanic sills

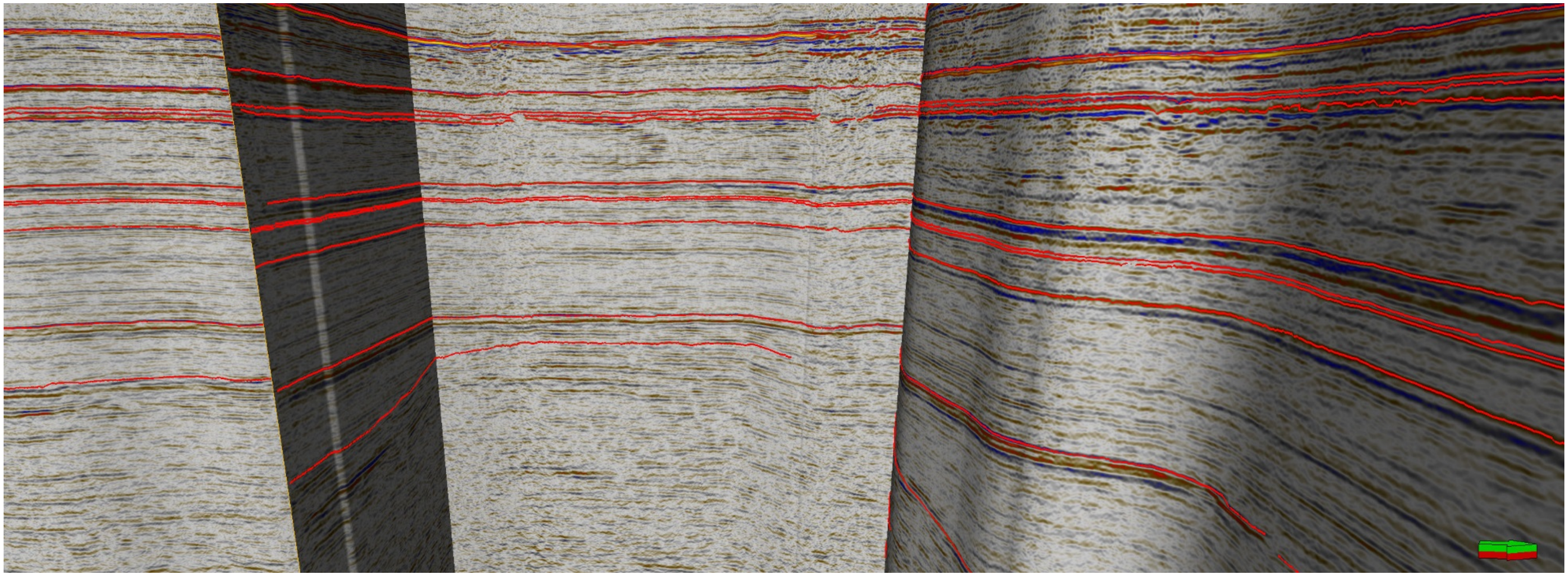

Figure 31 - 3-D view of three-way closure, structural doming, below northeastern Owen County. Note the lowermost reflection shallowing west on CM-110 (south, left) and CM-61 (north, right) towards CM-60. This horizon also shallows on CM-60.

and flows may constitute a portion of the well-reflective seismic facies. The possibilities of depositional basins superimposed on the EGRP was first introduced by Pratt et al. (1989). Therefore, interlayering of clastics, volcaniclastics, and volcanics may comprise the skeleton of the Quincy sequence. Geopotential data, discussed in subsequent sections, assist in characterizing the lithologic properties. Regardless, sequence origin is interpreted here as depositional and controlled primarily by surface processes.

5.2 Geologic interpretation

Interpretation will be discussed with respect to the relative timing of Middle Run deposition along with its underlying reflective seismic sequence. Age determination, geochemically and geophysically, of the Middle Run in Ohio has varied between pre-Grenville compression (Drahoval et al., 1992; Harris, 1992; Hauser, 1993; Peterman, 2016; Moecher et al. 2017) and syn-Grenville (Santos et al., 2002). The Middle Run is discussed here as a stratigraphic datum. These data, in a regional context, suggest two possible scenarios (Table 1).

5.2.1 Pre-Middle Run deposition

One possibility of origin is the deposition of both Quincy and Wilbur sequences pre-dating the Middle Run and its associated reflective package. The localized gravity high below the intersection of CM-60 with CM-61 and -110 (Figure 13B), where the Quincy exhibits apparent three-way closure (Figure 31), may be the product of denser rocks displacing the low density, overlying

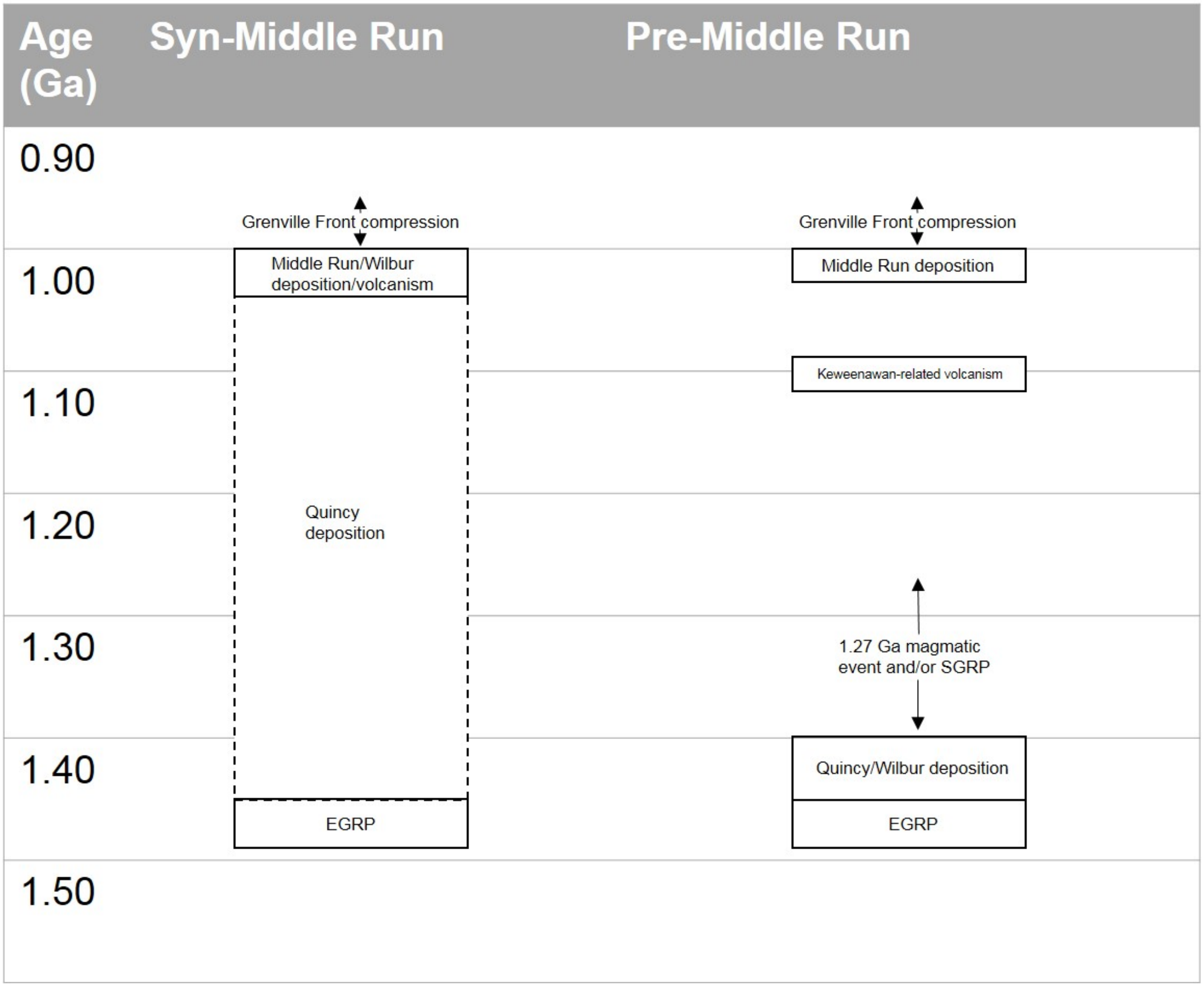

Table 1 - Syn- and pre-Middle Run scenarios of emplacement, deposition, and deformation interpreted from seismic reflection data.

sedimentary rocks of the Wilbur. Rhyolites, possibly associated with EGRP-related volcanism, flowing into sporadic basins across the midcontinent may interlayer weathered volcaniclastics from the caldera complexes scattered across the craton during Proterozoic time (Kisvarsanyi, 1980; Sides et al., 1981; Lidiak et al., 1993; McBride et al., 2003). Caldera collapse, modeled by Kisvarsanyi (1980) and interpreted below Illinois by McBride et al. (2003), would then be followed by intrusions into fractures surrounding the magma chamber. A sedimentary apron, comprised of volcaniclastics and clastics, may then accumulate around the volcanic center and into basins surrounding volcanic highs. The large, circular magnetic anomalies below eastern Indiana and western Ohio likely are the produced these buried caldera complexes (Figure 14B). This depositional episode was triggered at some point post-dating the youngest EGRP dates (1.44 Ga). Eventually, relatively homogenous clastic sedimentation began to dominate in the form of Wilbur deposition. The provenance for these rocks is not interpreted from these data since internal reflections appear almost exclusively parallel with the Quincy.

Structural complexity observed at the top of the Quincy (Figure 26, 38) may be due to local plutonic events related to intrusions into the EGRP. Although volcanism may have ceased before Wilbur deposition, occasional and sparse magmatism may have persisted through the end of the Proterozoic based on these data. Hoffman (1989) discussed pulsatory magmatism throughout the Precambrian which may be the mode of uplift exhibited by west-central Indianan pre-Mt. Simon sequences. Post-Wilbur magmatism may have resulted in the broad structural high just west of the MCFZ as well as the complexity of the Quincy apparent on CM-61. Doming below northeastern Owen County (Figure 31) fortifies the interpretation of recurrent post-Wilbur magmatism. Geochronologic evidence, such as Zr dates from midcontinent plutons, may represent late-stage magmatism related to the EGRP. Younger granites and rhyolites have been interpreted to intrude older, similar country rock from exposures in the St. Francois Mountains (Bickford et al., 2015). Lidiak et al. (1993) conclude two distinct phases of EGRP emplacement over an 80 Ma interval. Doming may also be, and is likely, due to the regionally extensive SGRP-related magmatism (1.40-1.34 Ga) or the anomalous 1.27 Ga magmatic episode presented by Bickford et al. (2015). The strong sub-Paleozoic reflection seen throughout the western section of the study area possesses seismic character similar to a volcanic flow or sill (Planke et al., 2000; Magee et al., 2015). This horizon, post-dating pre-Mt. Simon deformation and pre-dating Paleozoic deposition, may be a product of Keweenawan volcanism.

5.2.2 Syn-Middle Run deposition

Seismic similarities between the Wilbur and Middle Run, at its type locality, facilitate the correlation between the two units across Indiana and into Ohio. Moreover, the well-reflective underlying package seen on ODNR-1-88 below the Middle Run resembles the seismic character of the Quincy sequence (Figure 3). Continuity of the Middle Run across southern Indiana, and possibly into central Illinois (Freiburg, 2015), contrasts the localized ECRB model (Shrake et al., 1990, 1991; Drahovzal et al., 1992). Instead, regional distribution of the Wilbur suggests a Grenville foreland basin depositional environment. Hauser (1993) originally suggested the possibility of the Grenville foreland in seismic section below Illinois from COCORP data and the model has since been incorporated from geologic and geophysical evidence from across the region. Deposition of the Quincy sequence in this setting may be similar to the pre-Middle Run scenario discussed in 5.2.1. Quincy origin may be related to widespread clastic deposition across Laurentia following and derived from the

EGRP, along with late-staged rhyolitic volcanism. Geopotential signatures below Cloverdale, Indiana, where the Quincy sequence shallows, and Middletown, Ohio, where the reflective pre-Middle Run unit shallows are similar (Figure 13B, 14B). The broad gravity low below eastern Indiana may indicate a Middle Run thickening, a deepening of the foreland basin, in comparison to gravity anomalies where Quincy reflections shallow. Drahovzal (1997) suggest that the underlying reflective package below the Middle Run in Kentucky may be comprised of Grenville foreland basin deposits.

Santos et al. (2002) argue that, due to Middle Run SHRIMP dates, Grenville provenance is unlikely. Deposition between the Shewinigan and Ottawan phases of the Grenville Orogeny (Moecher et al., 2017; Figure 7) and subsequent deformation (Harris, 1992; Peterman, 2016) point to a foreland basin setting. The poor reflectivity of the Wilbur sequence compares well to the Middle Run below southwestern Ohio (Figure 3) and, thus, may be the lateral equivalent of the pre-Mt. Simon lithic arenite. Dipping, parallel internal reflections within the Wilbur to upper reflections of the Quincy, similar to the relationship of the Middle Run to its underlying reflective sequence in Ohio (Wolfe et al. 1993; Richard et al., 1997), suggests a combination of regional Grenville-related deformation, including magmatism related to either the EGRP or the Ottawan phase (McLelland et al., 2010).

5.3 Pre-Mt. Simon control on Paleozoic depositional systems

The Paleozoic sequence imaged across west-central Indiana, primarily west of the MCFZ, thickens basinward (Figure 17, 27, 30; Appendix, 1, 3, 4). Internal Mt. Simon reflections onlap the Wilbur (Figure 22), suggesting erosion of the sequence prior to the start of Mt. Simon deposition. This paleotopographic surface may have dictated depositional dip along with initial Reelfoot rifting, proto-Illinois Basin genesis, to the west and southwest (Buschbach and Kolata, 1990). CM-59 and 61 display broad, open folds that apparently strike north-south. This compression may have resulted from Paleozoic deformation sourced from the Appalachian Oorogeny, to the east, and Ancestral Rockies, to the west, orogenesis (McBride and Nelson, 1999). Pre-Mt. Simon structural highs do not appear to have influenced drape folding within the Paleozoic sequence especially since post-Wilbur erosion created a basinward ramp for sediments to accumulate. Zones within the Knox, apparent on CM-61, generate higher-amplitude reflectivity above pre-Mt. Simon structural highs (Figure 28). Pre-Mt. Simon control on the overall Paleozoic structural grain is minimal based on these data.

Paleozoic strata are downthrown normally basinward on the west side of the MCFZ (Figure 18, 19A, B). Tanner (1985) and Furer (1996) interpreted this feature as a negative flower structure and these data suggest a true negative nature throughout the fault system. Several antithetic faults significantly offset middle Paleozoic units, such as the New Albany, Eden, and Trenton. Discontinuity persists down through the Mt. Simon and Wilbur into the Quincy where normal offset between a package of upper reflections is apparent. This offset suggests a near vertical, basement-rooted master fault continued movement through, at least, Devonian time. The onset of the MCFZ is not known but may be related to the breakup of Rodinia, post-dating the deposition of the Wilbur sequence. Since reflectivity within the Quincy is relatively discontinuous, the base of the MCFZ may be interpreted in several different styles. Alternative to the vertical interpretation, the apparent localized shallowing and possible structural high of the Quincy west of the MCFZ may have served as a zone of weakness for fault genesis. Chaotic and discontinuous reflection character within this apparent structure, however, contrasts with relative continuity observed within other basement highs imaged on CM-60, -61 and -110. Regional extent of the MCFZ may be inferred from its surface expression (Tanner, 1985). Since there is no indication that the apparent Quincy high seen on CM-59 is a regional feature, and likely is imaged by sideswipe during acquisition, I interpret that the MCFZ is not rooted within the structure.

5.4 Pre-Mt. Simon exploration potential

Structural highs and the Mt. Simon unconformity may provide effective traps for pre-Mt. Simon hydrocarbon accumulation. Although not constrained in these data the pre-Mt. Simon limestone encountered in both western Ohio and eastern Indiana could potentially serve as a productive source for oil and gas generation. Stratigraphic position of this carbonate is not known and may be imaged as an internal reflection within the Wilbur. Welder (2014) interpreted this limestone as an internal reflection within the Middle Run below Jay County, Indiana. Hauser et al. (2000) pose that the lack of potential field anomalies where the pre-Middle Run reflective sequence, potentially the Quincy, below southwestern Ohio subcrobs may relate to the inclusion of this carbonate within the package. Possibilities of overmaturation, therefore, are entirely plausible.

Poor reservoir quality is inferred from generally low porosity throughout the Middle Run (Shrake et al., 1990; Harris, 1992). However, gas shows within the Middle Run of Ohio (Dean and Baranoski, 2002b) may indicate localized tight accumulations across the region. Interbedded shales, commonly associated with the Middle Run, may serve as seals and additional sources. Thickness of the Wilbur, if correlative with the Middle Run, indicates voluminous tight reservoir rock across the eastern U.S. midcontinent. In addition to energy resources, the felsic component(s) of the Quincy sequence may serve as sites for radiogenic decay and subsequent helium (^4He) generation, similar to the Precambrian granitic basement of New Mexico (Broadhead, 2012).

6. CONCLUSIONS

Two distinct, prominent pre-Mt. Simon seismic sequences below west-central Indiana reveal deep structural and stratigraphic complexities. Despite the possibility of both Wilbur and Quincy correlating with the pre-Mt. Simon sequences imaged on ODNR-1-88 I interpret, from these data, that both pre-Mt. Simon sequences imaged below west-central Indiana predate the Middle Run and are instead sedimentary and volcanic units associated with the EGRP. The Quincy may be correlative with pre-Middle Run reflections on ODNR-1-88 as well as the Centralia Sequence first interpreted below Illinois by Pratt et al. (1992). Until a geologic ground truth is available, I caution the loose terminology of all deep reflections below the U.S. midcontinent as the Centralia. Regardless, upper crustal seismic sequences below west-central Indiana provide insight into the composition and crustal evolution of the eastern Illinois Basin and facilitate a polyphase geochronology:

1. Laurentian stability accompanied by recurrent development of volcanic centers and subsequent caldera complexes across the U.S. midcontinent (EGRP; 1.48 - 1.44 Ga)

2. Deposition of clastics and volcaniclastics from volcanic centers and calderas into interspersed basins across the EGRP along with rhyolitic volcanism (Quincy sequence)
3. Deposition of Wilbur sequence into proto-Grenville foreland
4. Igneous intrusions and plutonism related to SGRP magmatism, deforming Quincy and Wilbur sequences (doming) (1.40 Ga – 1.34 Ga); 1.27 Ga magmatic episode resulting in various intrusive rocks of this age may also be responsible, at least in part, for deformation
5. Extrusion of volcanic, possibly associated with Keweenawan volcanism (~1.10 Ga)
6. Middle Run deposition and subsequent deformation related to Grenville orogenesis (1.03 – 0.96 Ga)
7. Erosion and development of angular unconformity of Middle Run, onset of Paleozoic deposition

7. FUTURE WORK

A major caveat of these interpretations, as previously discussed, is the lack of a geologic constraint. Deep wells in Clay, Greene, Lawrence Counties to the west, southwest and south of seismic coverage, respectively, bottom in the Mt. Simon. Sonic and density logs are only available from the Clay and Greene County well though the high-velocity, red arenite member of the Mt. Simon reported from the Lawrence County site may in fact be Middle Run. Regardless, none of these wells penetrates the Quincy sequence. My interpretation of the Quincy is based solely on its geophysical signatures. Drill holes must be developed to fully understand the pre-Mt. Simon basement across the midcontinent. Deep drilling programs, primarily for CO_2 geosequestration, are already underway in the Illinois basin and have recovered pre-Mt. Simon sedimentary rocks (Freiburg, 2015). The dome centered below northeastern Owen County, where the Quincy sequence subcrops, would be an ideal location for deep well to recover and ground truth the pre-Mt. Simon sequences presented here.

3-D seismic coverage over west-central Indiana and surrounding areas would help constrain structure and composition of pre-Mt. Simon seismic stratigraphic units. Acquiring a 3-D reflection volume may resolve the apparent structural high imaged on CM-59 and the true extent of the MCFZ. Deeper structures within or below the Quincy, resolved through re-processing, may provide more insight into its origin. A number of 2-D seismic reflection stacked, migrated sections, donated by CountryMark, will help refine the interpretations posed here in future Wright State University thesis work.

8. REFERENCES

Allmendinger, R.W., Nelson, K.D., Potter, C.J., Barazangi, M., Brown L.D., Oliver, J.E., 1987, Deep seismic reflection characteristics of the continental crust: Geology, v. 15, no. 4, p. 304-310, doi 10.1130/0091-7613

Atekwanna, E.A., Precambrian basement beneath the central Midcontinent United States as interpreted from potential field imagery, in B.A. Van der Pluijm, P. Catacosinos, ed., Basement and basins of eastern North America, Geological Soicety of America Special Paper 308, p. 33-44.

Baranoski, M.T., Dean, S.L., Wicks, J.L., Brown, V.M., 2009, Unconformity-bounded seismic reflection sequences define Grenville-age rift system and foreland basins beneath the Phanerozoic in Ohio: Geosphere, v. 5. No. 2, p. 140-151.

Bear, G.W., Rupp, J.A., Rudman, A.J., 1997, Seismic interpretation of the deep structure of the Wabash Valley Fault System: Seismological Research Letters, v. 68, no. 4, p. 624-640.

Bedle, H., 2008, Studies on the S-velocity structure of the North American upper mantle, Ph.D dissertation, Northwestern University, Chicago, IL, 165 p.

Bickford, M.E., Van Schmus, W.R., 1985, Discovery of two Proterozoic granite-rhyolite terranes in the buried midcontinent basement: the case for shallow drill doles, in C. Barry Raleigh, ed. Observation of the Continental Crust through Drilling I, p. 355-364.

Bickford, M.E., Van Schmus, W.R., Zietz, 1986, Proterozoic history of the midcontinent region of North America: Geology, v. 14, no. 6, p. 492-496, doi 10.1130/0091-7613.

Bickford, M.E., Van Schmus, W.R., Karlstrom, K.E., Mueller, P.A., Kamenov, G.D., 2014, Mesoproterozoic-trans-Laurentian magmatism: A synthesis of continent-wide age distributions, new SIMS U-Pb ages, zircon saturation temperatures, and Hf and Nd compositions: Precambrian Research, v. 265, p. 286-312, doi 10.1016/j.precamres.2014.11.024.

Broadhead, R., 2012, Helium in New Mexico: Origins, uses, economics, geologic distribution and exploration possibilities: Search and Discovery Article #10466.

Buschbach, T.C., Kolata, D.R., 1990, Regional setting of the Illinois basin, in Leighton, M.W., Kolata, D.R., Oltz, D.F., Eidel, J.J., Interior Cratonic Basins: AAPG Memoir 51, p. 29-55.

Cannon, W.F., Lee, M.W., Hinze, W.J., Schulz, K.J., Green, A.G., 1991, Deep crustal structure of Precambrian basement beneath northern Lake Michigan, midcontinent northern Lake Michigan, midcontinent North America, v. 19, no. 3, p. 207-210.

Carter, T.R., Trevail, R.A., Easton, R.M., 1996, Basement controls on some hydrocarbon traps in southern Ontario, Canada in B.A. Van der Pluijm, P. Catacosinos, ed., Basement and basins of eastern North America, Geological Soicety of America Special Paper 308, p. 95-108.

Catacosinos, P.A., Dickas, A.B., Forsyth, D.A., Hinze, W.J., van der Pluijm, B.A., 1996, Basement and basins of eastern North America: A research conference summary: Geological Society of America Special Paper 308, p. 1-6.

Chandler, V.W., 1983, Correlation of magnetic anomalies in east-central Minnesota and northwestern Wisconsin: constraints on magnitude and direction of Keweenawan rifting: Geology, v. 11, no. 3, p. 174-176.

Chew, D.M., Cardona, A., Mišković, A., 2011, Tectonic evolution of western Amazonia from the assembly of Rodinia to its break-up: International Geology Review, v. 53, no. 11-12, p. 1280-1296.

Culotta, R.C., Pratt, T., Oliver, J., 1990, A tale of two sutures: COCORP's deep seismic surveys of the Grenville Province in the eastern U.S. midcontinent: Geology, v. 18, no. 7, p. 646-649.

Dawson, T.A., 1960, Deep test well in Lawrence County, Indiana: drilling techniques and stratigraphic observations: Indiana Department of Conservation, No. 22, 36 p.

Dean, S.L., Baranoski, M.T., 2002a, A look at western Ohio's Precambrian tectonic setting: Oil and Gas Journal, v. 100, no. 29, p. 34-37.

Dean, S.L., Baranoski, M.T., 2002b, Deeper study of Precambrian warranted in western Ohio: Oil and Gas Journal, v. 100, no. 30, p. 37-40.

Denison, R.E., Lidiak, E.G., Bickford, M.E., Kisvarsanyi, E.B., 1984, Geology and Geochronology of Precambrian Rocks in the Central Interior Region of the United States, Geological Survey Professional Survey no. 1241-C.

Drahovzal, J.A., Harris, D.C., Wickstrom, L.H., Walker, D., Baranoski, M.T., Keith, B.D., Furer, L.C., 1992, The East Continent Rift Basin: A new discovery: Cincinnati Arch Consortium, Special Report 52, 25 p.

Drahovzal, J.A., 1997, Proterozoic sequences and their implications for Precambrian and Cambrian geologic evolution of Western Kentucky: evidence from seismic-reflection data: Seisomological Research Letters, v. 68, no. 4, 553-566.

Frieburg, J.T., 2015, The Argenta Formation: a newly recognized Cambrian stratigraphic unit in the Illinois Basin: GSA Abstracts with Programs, v. 47, no. 5, p. 86.

Furer, L.C., 1996, Basement tectonics in the southeastern part of the Illinois basin and its effect on Paleozoic sedimentation, in B.A. van der Pluijm, P. Catacosinos, ed., Basement and basins of eastern North America, Geological Soicety of America Special Paper 308, p. 109-126.

Harris, D.C., 1992, Regional stratigraphy of the Middle Run, in Drahovzal, J.A., Wickstrom, L.H., Keith, B.D., ed., Cincinnati Arch Consortium, the geology and geophysics of the East Continent Rift Basin: Indiana Geological Survey Open-File Report, 337 p., 21 pl.

Harding, T.P., Identification of wrench faults using subsurface structural data: criteria and pitfalls: AAPG Bulletin, v. 74, no. 10, p. 1590-1609.

Hauser, E.C., 1992, Deep crustal sediment study: widespread Precambrian layered rocks (sedimentary?) beneath the U.S. midcontinent, in R.D. Malone, H.D. Shoemaker, C.W. Byrer, eds., Proceedings of the natural gas research and development contractors review meeting, p. 167-188.

Hauser, E.C, 1993, Grenville foreland thrust belt hidden beneath the eastern U.S. midcontinent: Geology, v. 21, p. 61-64.

Hauser, E.C., 1996, Midcontinent rifting in a Grenville embrace, in B.A. van der Pluijm, P. Catacosinos, ed., Basement and basins of eastern North America, Geological Soicety of America Special Paper 308, p. 67-75.

Hauser, E.C., Richard, B.H., Nowak, S., Wolfe, P.J., 2000, Pre-Mt. Simon tectonic basins in western Ohio: Search and Discovery Article #90907.

Heigold, P.C., 1991, Crustal character of the Illinois basin, in Leighton, M.W., Kolata, D.R., Oltz, D.F., Eidel, J.J., Interior Cratonic Basins: AAPG Memoir 51, p. 247-261.

Heigold, P.C., Kolata, D.R., 1993, Proterozoic crustal boundary in the southern part of the Illinois basin: Tectonophysics, v. 217, no. 3-4, p. 307-319.

Hoffman, P.F., 1989, Speculations on Laurentia's first gigayear (2.0 to 1.0 Ga): Geology, v. 17, no. 2, p. 135-138, doi 10.1130/0091-7613.

Kay, R.W., Kay, S.M., 1991, Creation and destruction of lower continental crust: Geologische Rundschau, v. 80, p. 259-278.

Kay, R.W., Kay, S.M., 1993, Delamination and delamination magmatism: Tectonophysics, v. 219, no. 1-3, p. 177-189.

Kisvarsanyi, E.B., 1980, Granitic ring complexes and Precambrian hot-spot activity in the St. Francois Terrane, midcontinent region, United States: Geology, v. 8, no. 1, p. 43-47.

Kolata, D.R., 1991a, Overview of sequences, in Leighton, M.W., Kolata, D.R., Oltz, D.F., Eidel, J.J., Interior Cratonic Basins: AAPG Memoir 51, p. 59-75.

Kolata, D.R., 1991b, Illinois basin geometry, in Leighton, M.W., Kolata, D.R., Oltz, D.F., Eidel, J.J., Interior Cratonic Basins: AAPG Memoir 51, p. 197.

Kolata, D.R., Nelson, W.J., 1991, Tectonic history of the Illinois basin, in Leighton, M.W., Kolata, D.R., Oltz, D.F., Eidel, J.J., Interior Cratonic Basins: AAPG Memoir 51, p. 263-285.

Krogh, T.E., 1994, Precise U-Pb ages for Grenvillian and pre-Grenvillian thrusting of Proterozoic and Archaen metamorphic assemblages

Leighton, M.W., 1996, Interior cratonic basins: A record of regional tectonic influences, in B.A. Van der Pluijm, P. Catacosinos, ed., Basement and basins of eastern North America, Geological Society of America Special Paper 308, p. 77-93.

Lidiak, E.G., Bickford, M.E., Kisvarsanyi, E.B., 1993, Proterozoic Geology of the Midcontinent, in W.R. Van Schmus and M.E., Bickford, eds. Transcontinental Proterozoic provinces, in Reed, J.C. et al., Precambrian: Conterminous U.S.: Boulder, Colorado, Geological Society of America, Geology of North America, v. C-2, p. 260-270.

Lucius, J.E., von Frese, R.R., 1988, Aeromagnetic and gravity anomaly constraints on the crustal geology of Ohio: Geological Society of America Bulletin, v. 100, p. 104-116.

Macke, D.L., 1995, Illinois Basin Province (064) in D.L. Gautier, G.L. Dolton, K.I. Takahashi, and K.L. Varnes, 1995 National assessment of United States oil and gas resources: Results, Methodology, and Supporting Data: USGS Data Series 30.

Magee, C., Maharaj, S.M., Wrona, Jackson, C.A.-L., 2015, Controls on the expression of igneous intrusions in seismic reflection data: Geosphere, v. 11, no. 4, p. 1024-1041.

McBride, J.H., Kolata, D.R., 1999, Upper crust beneath the central Illinois basin, United States: Geological Society of America Bulletin, v. 111, no, 3, p. 375-394, doi 10.1130/0016-7606.

McBride, J.H., Nelson, J.H., 1999, Style and origin of mid-Carboniferous deformation in the Illinois Basin, USA – Ancestral Rockies deformation?: Tectonophysics, v. 305, no. 1-3, p. 249-273.

McBride, J.H., Kolata, D.R., Hildenbrand, T.G., 2003, Geophysical constraints on understanding the origin of the Illinois basin and its underlying crust: Tectonophysics, v. 363, no. 1-2, p. 45-78.

McBride, J.H., Keach II, R.W., Wolfe, E.E., Leetaru, H.E., Chandler, C.K., Greenhaugh, S.R., 2014, Investigating fault continuity associated with carbon storage planning in the Illinois Basin: Interpretation, v. 2, no. 1, p. 151-162.

McBride, J.H., Leetaru, H.E., Keach, R.W., McBride, E.I., 2016, Fine-scale structure of the Precambrian beneath the Illinois Basin: Geosphere, v. 12, no. 2, p. 585-606.

McLelland, J.M., Selleck, B.W., Bickford, M.E., 2010, Review of the Proterozoic evolution of the Grenville Province, its Adirondack outlier, and the Mesoproterozoic inliers of the Appalachians, in Tollo, R.P. ed., From Rodinia to Pangea: The Lithotectonic Record of the Appalachian Region: GSA Memoir 206, p. 21-49.

Mitchum, Jr., R.M., Vail, P.R., Thompson, III, S., 1977, Seismic stratigraphy and global changes of sea level, part 2: the depositional sequence as a basic unit for stratigraphic analysis, in Payton, C.E., ed., Seismic Stratigraphy – Applications to Hydrocarbon Exploration: AAPG Memoir 26, p. 53-62.

Moecher, D.P., Bowersox, J.R., Hickman, J.B., 2017, Is the East Continent Rift Basin really a rift basin, or is it a foreland basin? And did the Grenville orogeny ‘take a breather’ during midcontinent rifting? New evidence from zircon U-Pb geochronology of the Middle Run Fm. And basement orthogneiss in drill core from Kentucky: GSA Abstracts for Programs, v. 49, no. 2.

Nelson, W.J., 1991, Structural styles of the Illinois basin, in Leighton, M.W., Kolata, D.R., Oltz, D.R., Eidel, J.J., 1991, Interior Cratonic Basins: AAPG Memoir 51, p. 209-243.

Okure, M.S., Upper mantle reflectivity beneath and intracratonic basin: insights into the behavior of the mantle beneath the Illinois basin: Brigham Young Univeristy, Provo, UT, 49 p.

Peterman, D.J., Seismic reflection profiling near Middletown, Ohio and interpretation of Precambrian deformational settings, M.S. thesis, Wright State University, Dayton, OH, 85 p.

Planke, S., Symonds, P.A., Alvestad, E., Skogseid, J., 2000, Seismic volcanostratigraphy of large-volume basaltic extrusive complexes on rifted margins: Journal of Geophysical Research, v. 105, B8, p. 19335-19351.

Potter, C.J., Goldhaber, M.B., Heigold, P.C., Drahovzal, J.A., 1995, Structure of the Reelfoot-Rough Creek rift system, Fluorspar area fault complex, and Hicks Dome, southern Illinois and western Kentucky; new constraints from regional seismic reflection data: Geological Survey (U.S.), no. 1538-Q.

Potter, C.J., Drahovzal, J.A., Sargent, M.L., McBride, J.H., 1997, Proterozoic structure, Cambrian rifting, and younger faulting as revealed by a regional seismic reflection network in the southern Illinois Basin: Seisomological Research Letters, v. 68, no. 4, 537-552.

Pratt, T., Culotta, R., Hauser, E., Nelson, D., Brown, L., Kaufman, S., Oliver, J., Hinze, W., 1989, Major Proterozoic basement features of the eastern midcontinent of North America revealed by recent COCORP profiling: Geology, v. 17, no. 6, p. 505-509.

Pratt, T.L., Hauser, E.C., Nelson, K.D., 1992, Widespread buried Precambrian layered sequences in the U.S. mid-continent: evidence for large Proterozoic depositional basins: AAPG Bulletin, v. 76, no. 9, p. 1384-1401.

Prothero, D.R., Schwab, F., 2004, Sedimentary Geology: An Introduction to Sedimentary Rocks and Stratigraphy, New York, W.H. Freeman and Company, 557 p.

Reynolds, J.M., 2011, An Introduction to Applied and Environmental Geophysics, Oxford, Wiley-Blackwell, 696 p.

Richard, B.H., Wolfe, P.J., Potter, P.E., 1997, Pre-Mount Simon basins of western Ohio, in R.W. Ojakangas, A.B. Dickas, J.C. Green ed., Middle Proterozoic to Cambrian Rifting, Central North America, Geological Society of America Special Paper 312, p. 243-252.

Rivers, T., 1997, Lithotectonic elements of the Grenville Province: review and tectonic implications: Precambrian research, v. 86, p. 117-154.

Rivers, T., 2008, Assembly and preservation of lower, mid, and upper orogenic crust in the Grenville Province – Implications for the evolution of large hot long-duration orogons: Precambrian Research, v. 167, no. 3-4, p. 237-259.

Rudman, A.J., Summerson, C.H., Hinze, W.J., 1965, Geology of basement in Midwestern United States: AAPG Bulletin, v. 49, no. 7, p. 894-904.

Santos, J.O.S., Hartmann, L.A., McNaughton, N.J., Easton, R.M., Potter, P.E., 2002, Sensitive high resolution ion microprobe (SHRIMP) detrital zircon geochronology provides new evidence for a hidden Neoproterozoic foreland basin to the Grenville Orogen in the eastern Midwest, U.S.A.: Canadian Journal of Earth Sciences, v. 39, no. 10, p. 1505-1515.

Sargent, M.L., 1993, Structural and tectonic implications of pre-Mt. Simon strata – or a lack of such – in the western part of the Illinois basin: Geological Society Abstracts with Programs, v. 25, no. 3, p. 78.

Sexton, J.L., Braile, L.W., Hinze, W.J., Campbell, M.J., 1986, Seismic reflection profiling studies of a buried Precambrian rift beneath the Wabash Valley fault zone: Geophysics, v. 51, no. 3, p. 640-660.

Sharma, P.V., 1986, Geophysical Methods in Geology (2nd ed.), New York, Elsevier, 442 p.

Shrake, D.L., Wolfe, P.J., Richard, B.H., Swinford, E.M., Wickstrom, L.H., Potter, P.E., Sitler, G.W., 1990, Lithologic and geophysical description of a continuously cored hole in Warren County, Ohio, including description of the Middle Run Formation (Precambrian?) and a seismic profile across the core site: State of Ohio Information Circular no. 56, 11 p.

Shrake, D.L., 1991, The Middle Run Formation: A subsurface stratigraphic unit in southwestern Ohio: The Ohio Journal of Science, v. 91, no. 1, p. 49-55.

Shrake, D.L., Carlton, R.W., Wickstrom, L.H., Potter, P.E., Richard, B.H., Wolfe, P.J., Sitler, B.W., 1991, Pre-Mount Simon basin under the Cinicinnati Arch: Geology, v. 19, no. 2, p. 139-142.

Sides, J.R., Bickford, M.E., Shuster, R.D., Nusbaum, R.L., 1981, Calderas in the Precambrian terrane of the St. Francois Mountains, southeastern Missouri: Journal of Geophysical Research, v. 86, no. B11, p. 10349-10364, doi 10.1029/JB086iB11p10349.

Sloss, L.L., 1963, Sequences in the cratonic interior of North America: Geological Society of America Bulletin, v. 74, p. 93-114.

Stark, T.J., 1997a, The East Continent Rift Complex: evidence and conclusions, in R.W. Ojakangas, A.B. Dickas, J.C. Green ed., Middle Proterozoic to Cambrian Rifting, Central North America, Geological Soicety of America Special Paper 312, p. 253-266.

Stark, T.J., 1997b, The English Graben: A possible Precambrian rift segment of the eastern Midcontinent, in R.W. Ojakangas, A.B. Dickas, J.C. Green ed., Middle Proterozoic to Cambrian Rifting, Central North America, Geological Soicety of America Special Paper 312, p. 267-285.

Tanner, G.F., 1985, The Mt. Carmel fault and associated features in west-central Indiana, M.S. thesis, Indiana University, 66 p.

Thomas, W.A., 2005, Tectonic inheritance at a continental margin: GSA Today, v. 16, no. 2, p. 4-11.

Van Schmus, W.R., Hinze, W.J., 1985, The Midcontinent Rift System: Annual Reviews of Earth Planetary Sciences, v. 13, p. 345-83.

Van Schmus, W.R., Bickford, M.E., Turek A., 1996, Proterozoic geology of the east-central Midcontinent basement, in B.A. Van der Pluijm, P. Catacosinos, ed., Basement and basins of eastern North America, Geological Society of America Special Paper 308, p. 7-32.

United States Geological Survey, 2014, Mineral resources on-line spatial data, http://mrdata.usgs.gov/general/map.html (accessed October 28, 2016).

University of Texas at El Paso, 2013, Regional geospatial service center, http://gis.utep.edu/subpages/CMdata.html (accessed January 30, 2017).

Walker, R., 2015, What's lurking in the basement? Recent insight into basement features in Indiana: Search and Discovery Article #90218.

Welder, J.M., 2014, Seismic interpretation and well log Analysis of Jay County, Indiana, focused on lithologic units below the Mt. Simon Formation, M.S. thesis, Wright State University, Dayton, OH, 54 p.

Windley, B.F., 1992, Proterozoic anorogenic magmatism and its orogenic connections: Journal of the Geological Society, London, v. 150, no. 3, p. 39-50.

Wolfe, P.J., Richard, B.H., Potter, P.E., 1993, Potential seen in Middle Run basins of western Ohio: Oil and Gas Journal, v. 91, no. 14, p. 68-73.

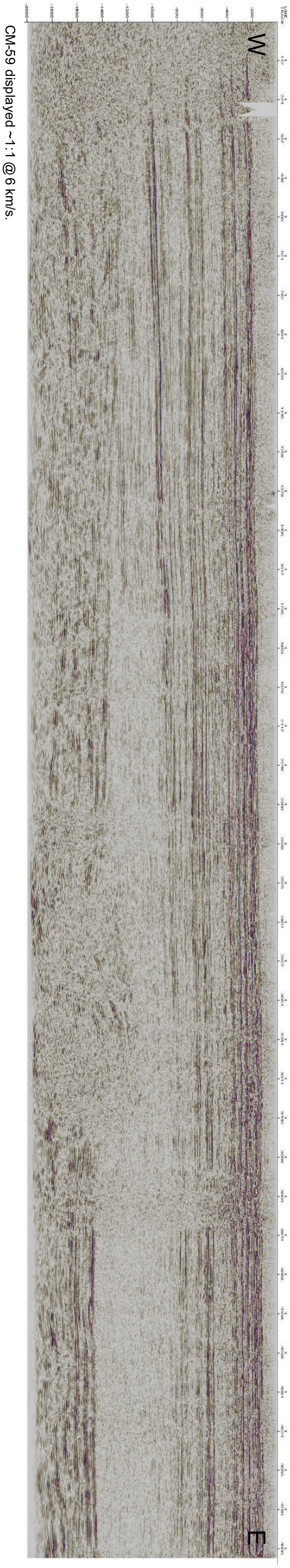

CM-59 displayed ~1:1 @ 6 km/s.

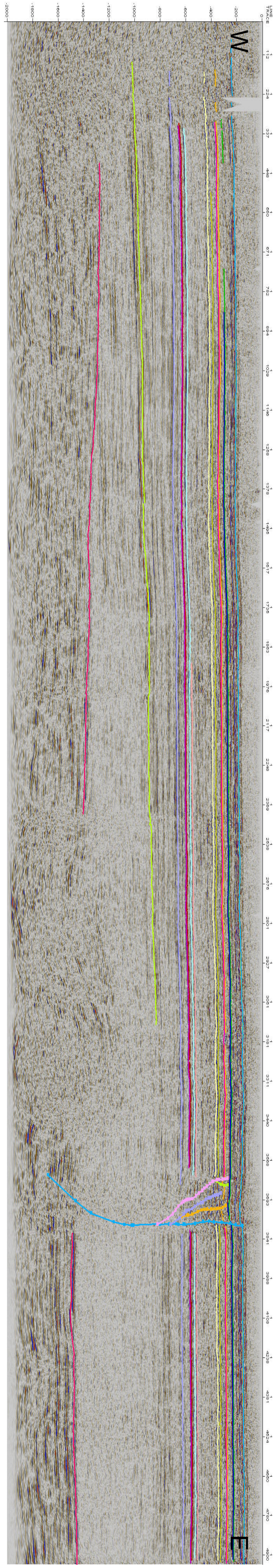

CM-59 displayed ~1:1 @ 6 km/s. New Albany (cyan), Eden (emerald), Trenton (light red), Knox (gold), Eau Claire (maroon), Mt. Simon (violet), poorly reflective pre-Mt. Simon (lime) and well reflection pre-Mt. Simon (red) tops are interpreted here. Other prominent internal reflections are tracked.

APPENDIX II

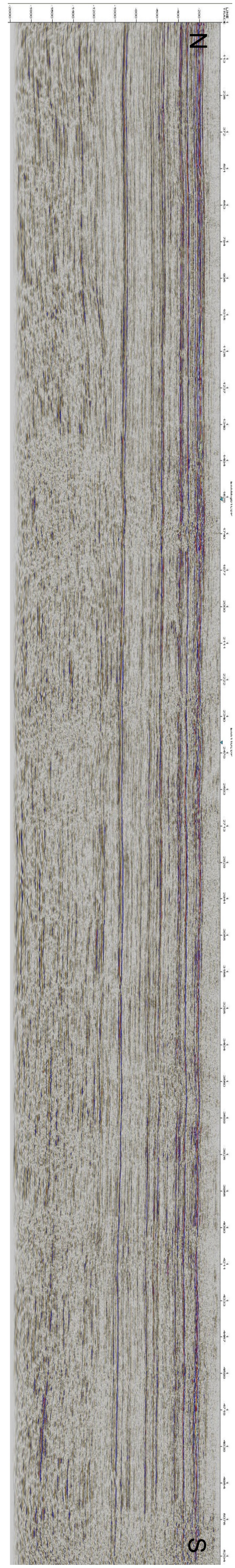

CM-60 displayed ~1:1 @ 6 km/s.

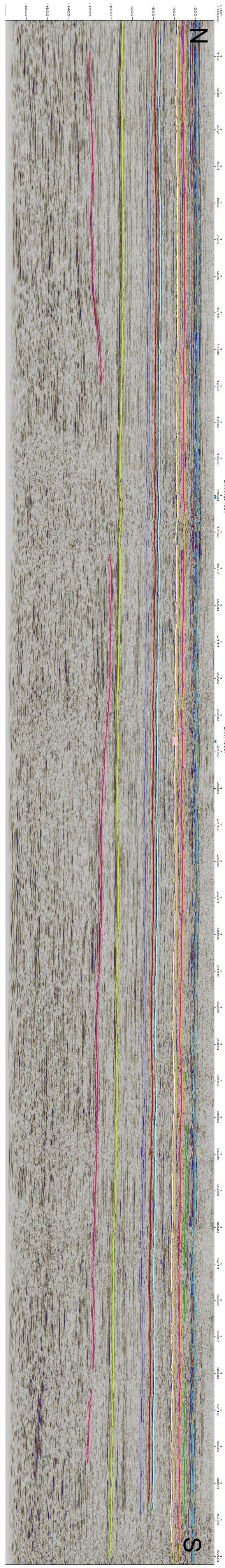

CM-60 displayed ~1:1 @ 6 km/s. New Albany (cyan), Eden (emerald), Trenton (light red), Knox (gold), Eau Claire (maroon), Mt. Simon (violet), poorly reflective pre-Mt. Simon (lime) and well reflection pre-Mt. Simon (red) tops are interpreted here. Other prominent internal reflections are tracked.

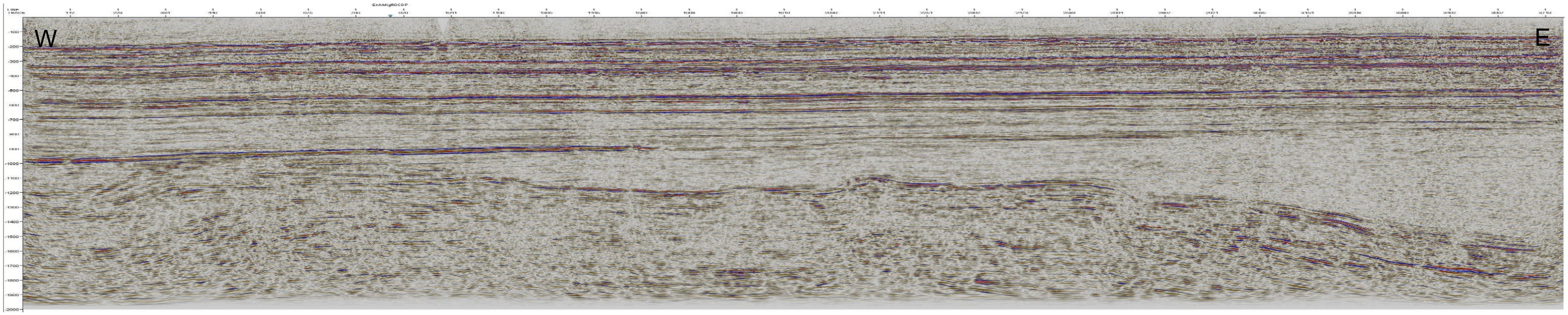

CM-61 displayed ~1:1 @ 6 km/s.

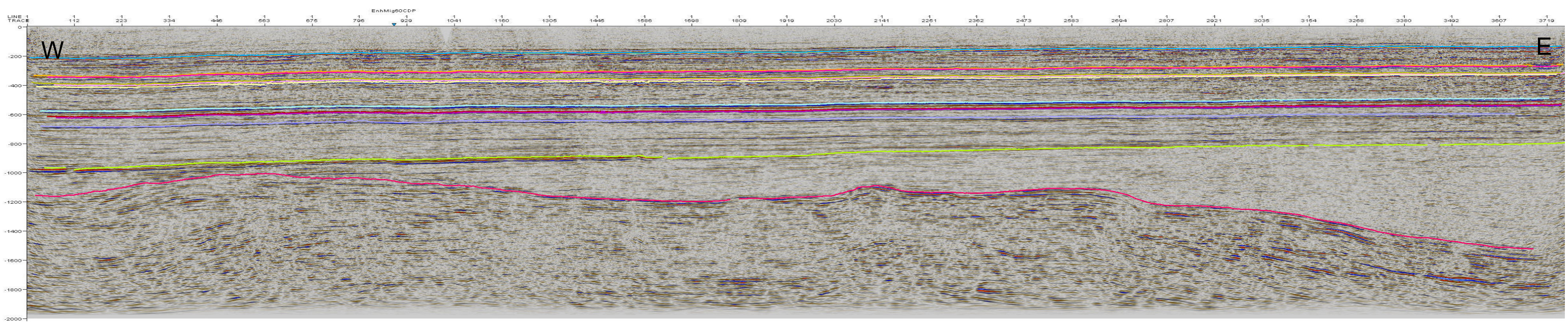

CM-61 displayed ~1:1 @ 6 km/s. New Albany (cyan), Eden (emerald), Trenton (light red), Knox (gold), Eau Claire (maroon), Mt. Simon (violet), poorly reflective pre-Mt. Simon (lime) and well reflection pre-Mt. Simon (red) tops are interpreted here. Other prominent internal reflections are tracked.

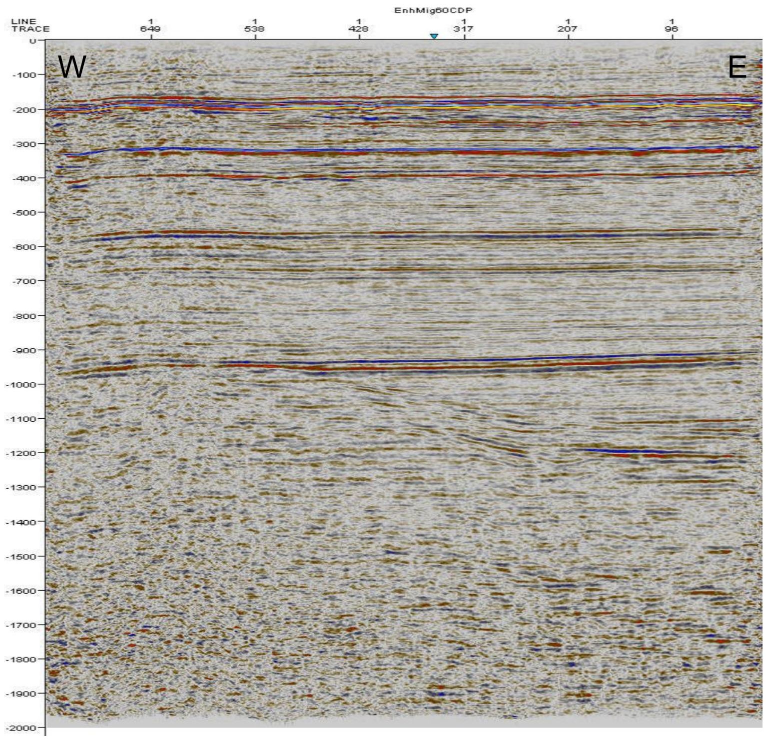

CM-110 displayed ~1:1 @ 6 km/s.

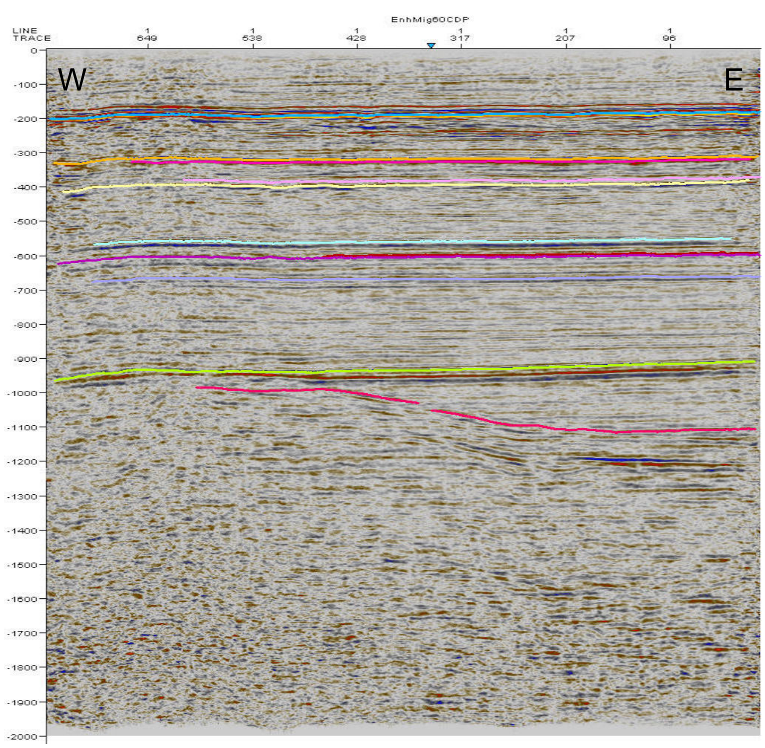

CM-110 displayed ~1:1 @ 6 km/s. New Albany (cyan), Eden (emerald), Trenton (light red), Knox (gold), Eau Claire (maroon), Mt. Simon (violet), poorly reflective pre-Mt. Simon (lime) and well reflection pre-Mt. Simon (red) tops are interpreted here. Other prominent internal reflections are tracked.